

# Quantum geometry and $X$ -wave magnets with $X = p, d, f, g, i$

Motohiko Ezawa<sup>1</sup>

<sup>1</sup>*Department of Applied Physics, The University of Tokyo, 7-3-1 Hongo, Tokyo 113-8656, Japan*  
(Dated: January 29, 2026)

Quantum geometry is a differential geometry based on quantum mechanics. It is related to various transport and optical properties in condensed matter physics. The Zeeman quantum geometry is a generalization of quantum geometry including the spin degrees of freedom. It is related to electromagnetic cross responses. Quantum geometry is generalized to non-Hermitian systems and density matrices. Especially, the latter is quantum information geometry, where the quantum Fisher information naturally arises as quantum metric. We apply these results to the  $X$ -wave magnets, which include  $d$ -wave,  $g$ -wave and  $i$ -wave altermagnets as well as  $p$ -wave and  $f$ -wave magnets. They have universal physics for anomalous Hall conductivity, tunneling magnetoresistance and planar Hall effect. We also study magneto-optical conductivity, magnetic circular dichroism and Friedel oscillations in the  $X$ -wave magnets. Various analytic formulas are derived in the case of two-band Hamiltonians. This paper presents a review of recent progress together with some original results.

## Contents

<b>I. Introduction</b>	2	<b>D. Quantum Fisher information for a pure state and quantum metric</b>	19
<b>II. Quantum geometry</b>	3	<b>E. Fluctuation-dissipation theorem</b>	20
A. Quantum distance and quantum geometric tensor	3	<b>F. Quantum geometry at thermal equilibrium</b>	20
B. Berry connection, Berry curvature and Chern number	4	<b>VII. <math>X</math>-wave magnets</b>	20
C. Wannier function and polarization	5	A. Fermi surface symmetry	20
D. Inequality	5	B. Model Hamiltonian	21
E. Quantum Geometry for two-band systems	6	C. Symmetry	21
F. Analogy of the theory of general relativity	6	1. Spin diagonal case	21
G. Non-Abelian quantum geometry	7	2. Spin nondiagonal case	22
<b>III. Quantum geometry in condensed matter physics</b>	7	D. Quantum geometry of $X$ -wave magnets	23
A. Thouless-Kohmoto-Nightingale-Nijs formula	7	E. Zeeman quantum geometry of $X$ -wave magnets	23
B. Dirac system	8	F. Zeeman quantum geometry induced cross response	24
C. Optical absorption and elliptic dichroism	9	G. Materials	25
D. Sum rule	10	1. $p$ -wave magnet	25
E. Bulk photovoltaic effects	11	2. $d$ -wave altermagnet	25
F. Nonlinear conductivity	11	3. $f$ -wave magnet	25
<b>IV. Zeeman Quantum geometry for momentum and spin</b>	12	4. $g$ -wave altermagnet	25
A. Responses originated from the Zeeman geometry	13	5. $i$ -wave altermagnet	25
B. Zeeman Quantum Geometry for two-band systems	13	<b>VIII. Transport properties of <math>X</math>-wave magnets</b>	25
C. Rashba system	14	A. Without Rashba interaction	25
D. Non-Abelian Zeeman quantum geometry	15	1. Spin current generation	25
<b>V. Quantum geometry for non-Hermitian systems</b>	15	2. Spin Nernst effects	26
A. Open quantum system and non-Hermitian Hamiltonian	15	3. Tunneling magnetoresistance	27
B. Non-Hermitian quantum geometry	16	B. With Rashba interaction	28
C. Two-band systems	16	1. Anomalous Hall effects	28
D. Dirac system with a complex mass	17	2. Planar Hall effects	28
<b>VI. Quantum information geometry</b>	17	<b>IX. Quantum Hall effects</b>	29
A. Uhlmann quantum geometry for density matrix	17	A. Landau levels	29
B. Classical Fisher information	19	1. $p$ -wave magnets and coherent states	29
C. Quantum Cramér-Rao inequality	19	2. $d$ -wave altermagnets and squeezed states	29
		3. $X$ -wave magnets	30
		B. Magneto-optical conductivity	30
		1. $p$ -wave magnets	30
		2. $d$ -wave altermagnets	30
		C. Magnetic circular dichroism	30
		<b>X. Friedel oscillation</b>	31

A. Free electrons	31
B. $p$ -wave magnets	32
C. $d$ -wave altermagnets	32
D. $X$ -wave magnets	32
<b>XI. Summaries, discussions and outlooks</b>	32
<b>Acknowledgements</b>	33
<b>Appendices</b>	33
<b>A. Quantum distance and Abelian quantum geometric tensor</b>	33
<b>B. Quantum distance and non-Abelian quantum geometric tensor</b>	33
<b>C. Hellmann-Feynman theorem</b>	34
<b>D. Bulk photovoltaic effects</b>	35
1. Injection currents	35
2. Shift currents	36
<b>E. Quantum distance and Zeeman quantum geometric tensor</b>	37
<b>F. Zeeman quantum geometry induced intrinsic cross responses</b>	38
1. Hall current and AC Hall current	38
2. Intrinsic gyrotropic magnetic current	38
3. Intrinsic electric field induced spin density	38
4. Intrinsic magnetic field induced spin density	39
<b>G. Zeeman quantum geometry for two-band systems</b>	39
1. Zeeman Berry curvature	39
2. Zeeman quantum metric	39
3. Spin quantum geometry	40
<b>H. Zeeman geometry induced cross responses in <math>X</math>-wave magnets</b>	40
<b>I. Uhlmann geometry</b>	43
1. Positive Operator-Valued Measure	43
2. Quantum Cramér-Rao inequality	43
3. Quantum Fisher information for a pure state	44
<b>References</b>	45

## I. INTRODUCTION

Quantum geometry is a differential geometry based on wave functions of quantum mechanics[1–3]. The key component is the quantum geometric tensor derived from quantum distance under infinitesimal momentum translation. Its real part gives the quantum metric, while its imaginary part gives the Berry curvature. It is well established that the Hall conductivity is related to the integral of the Berry curvature, whose relation is known as the Thouless-Kohmoto-Nightingale-Nijs (TKNN) formula[4, 5]. On the other hand,

quantum metric is related to various observables such as optical absorption[6–19], nonlinear conductivity[20–32] and bulk photovoltaic effects[6, 9, 33, 34]. Quantum geometric tensor is observed experimentally[35, 36]. Recently, quantum geometry is generalized to the Zeeman quantum geometry by introducing spin translation in quantum distance. It is related to electromagnetic responses.

Ferromagnets are useful for magnetic memory and spintronics devices. However, there is a limitation of integration and fast dynamics due to the stray field. On the other hand, there is no such limitation in antiferromagnets. However, it is hard to readout the spin direction of antiferromagnet due to net zero magnetization.  $d$ -wave magnets are antiferromagnets whose electronic band structure has the  $d$ -wave splitting[37–41]. It is prominent that spin current can be generated by applying electric field or thermal gradient without using the spin-orbit interaction[37–41]. The notion of the  $d$ -wave magnets is generalized to altermagnets[42, 43] including  $g$ -wave and  $i$ -wave altermagnets in two and three dimensions. They break time-reversal symmetry. In addition,  $p$ -wave[44, 45] and  $f$ -wave magnets are also recognized, where time-reversal symmetry is preserved. They are summarized in the  $X$ -wave magnets[46] with  $X = p, d, f, g, i$  because they share universal features[47] irrespective of the presence or the absence of time-reversal symmetry.

In this paper, we review recent progress of quantum geometry and the  $X$ -wave magnets. We derive compact analytical formulas of the Zeeman quantum geometry based only on the two-band Hamiltonian without using eigenfunctions. We also generalize the Zeeman quantum geometry to multiband systems. Electromagnetic cross responses of the  $X$ -wave magnet with the Rashba interaction is also studied. We also review quantum geometry defined for non-Hermitian systems and density matrices. We note that there are some recent review articles on quantum geometry[48–51] and altermagnets[43, 52–58].

This paper is composed as follows. In Sec. II, we construct quantum geometry starting from the fidelity of the wave function, which measures the similarity of the two wave functions. The quantum distance is defined based on the fidelity. By expanding the quantum distance with an infinitesimal momentum translation, we obtain the quantum geometric tensor. Its real part gives the quantum metric, while its imaginary part gives the Berry curvature. The integration of the Berry curvature leads to the Chern number, which is an integer characterizing a topological insulator. By making a Fourier transformation of the wave function from the momentum space to the real space, we obtain the Wannier function. It is shown that the quantum metric is related to the fluctuation of the position. We show an equality for the quantum geometry, which gives a lower bound determined by the Chern number. We summarize simple formulas to obtain the quantum metric and the Berry curvature directly from the two-band Hamiltonian without using information about the eigenfunctions. The quantum geometry is generalized to  $N$ -fold degenerate multiband systems.

In Sec. III, the TKNN formula is derived, which relates the Hall conductivity to the Chern number. It explains the quanti-

zation of the Hall conductivity for a topological insulator. We apply these results to the simplest Dirac system in two dimensions. Especially, optical dichroism is shown, where the optical absorption is selectively occurred depending on the chirality of the Dirac system. The sum rule which relates the optical conductivity and the quantum metric is derived. Bulk photovoltaic effects including the injection current and the shift current are related to the quantum metric. In addition, the second-order nonlinear conductivity is shown to be related to the quantum metric.

In Sec. IV, quantum geometry is generalized to include the spin degrees of freedom, which is called Zeemann quantum geometry. The relation between the Zeemann quantum geometry and electromagnetic cross responses are clarified. Simple formulas obtaining the Zeeman quantum geometric tensor for the two-band systems are derived based only on the Hamiltonian without using knowledge of the eigenfunctions. Their results are applied to the Rashba system. The Zeeman quantum geometry is generalized to  $N$ -fold degenerate systems.

In Sec. V, quantum geometry is generalized to non-Hermitian systems. Especially, the quantum metric and the Berry curvature are obtained for the two-band system. They are studied in the Dirac system with a complex mass term.

In Sec. VI, quantum geometry is generalized to density matrices, which is known as the quantum information geometry. Especially, quantum distance is related to quantum Fisher information. The Clamér-Rao inequality is explained, which gives the lower bound of the covariance of the physical observable by the inverse of the quantum Fisher information. It is shown that the quantum Fisher information is reduced to the classical Fisher information for a pure state. Quantum geometry at thermal equilibrium is derived, and it is shown that the Uhlmann curvature is reduced to the Berry curvature at low temperature.

In Sec. VII, the notion of the  $X$ -wave magnets is introduced, which includes the  $d$ -wave,  $g$ -wave and  $i$ -wave altermagnets as well as the  $p$ -wave and  $f$ -wave magnets. Their symmetry properties are summarized. The quantum geometric properties are also calculated.

In Sec. VIII, transport properties of the  $X$ -wave magnets are summarized. The spin current generation by electric field and temperature gradient is analytically studied. It is shown that only the  $d$ -wave altermagnet has a linear response for the spin current. The analytic formula for tunneling magnetoresistance is also studied. Finally, we study a coupled system to the  $X$ -wave magnet and the Rashba system. It is shown that it is impossible to detect the Neel vector of the  $X$ -wave magnet by anomalous Hall conductivity based on the two-band model. Universal formula for the planar Hall conductivity for the  $X$ -wave magnets is presented. Electromagnetic responses of the  $X$ -wave magnets are also studied.

In Sec. IX, we analytically derive Landau levels for the  $p$ -wave magnet by using an analogy of the coherent state and for the  $d$ -wave altermagnet by using an analogy of the squeezed state.

In Sec. X, we analytically derive the Friedel oscillation of the spatial profile of the local density states.

Sec. XI is devoted to summaries, discussions and outlooks.

This paper contains both reviews and original results. Most of the parts are review. The original ones are as follows. Two-band formulas for the Zeeman quantum geometry in Sec. IV.B. Non-Abelian Zeeman quantum geometry in Sec. IV.D. Zeeman quantum geometry induced cross responses in Sec. IV.E and F. Landau levels for the  $p$ -wave magnet in Sec. IX.A. The parts where the results are not original but give some new interpretations are as follows: Spin current generation and spin Nernst effect are derived analytically in Sec. VIII.A. The Landau levels for the  $d$ -wave altermagnet are derived by using the analogy of the coherent state in Sec. IX.A. The Friedel oscillation is discussed for the  $X$ -wave magnet in Sec. X.

## II. QUANTUM GEOMETRY

Quantum geometry is a differential geometry based on the wave functions. The basic notion is the fidelity, which measures the similarity of two wave functions. It acts as the distance in the context of the differential geometry. Starting from the fidelity with an infinitesimal translation in the momentum space, we derive the quantum geometric tensor. Its real part gives the quantum metric, while its imaginary part gives the Berry curvature. The latter is related to the anomalous Hall effect and topological insulators via the Chern number.

### A. Quantum distance and quantum geometric tensor

The fidelity of the wave function  $|\psi_n(\mathbf{k})\rangle$  is defined by

$$F_n(\mathbf{k}, \mathbf{k}') \equiv |\langle \psi_n(\mathbf{k}) | \psi_n(\mathbf{k}') \rangle|, \quad (1)$$

where the wave function is orthonormalized,  $\langle \psi_n(\mathbf{k}) | \psi_n(\mathbf{k}') \rangle = \delta(\mathbf{k}, \mathbf{k}')$ . It satisfies  $0 \leq F_n(\mathbf{k}, \mathbf{k}') \leq 1$ .

The Hilbert-Schmidt distance is defined by

$$s_{\text{HS}}(\mathbf{k}, \mathbf{k}') \equiv \sqrt{1 - F_n(\mathbf{k}, \mathbf{k}')^2}, \quad (2)$$

where  $s_{\text{HS}}(\mathbf{k}, \mathbf{k}') = 0$  when the two wave functions are identical  $|\psi_n(\mathbf{k})\rangle = |\psi_n(\mathbf{k}')\rangle$ , while  $s_{\text{HS}}(\mathbf{k}, \mathbf{k}') = 1$  when they are orthogonal  $\langle \psi_n(\mathbf{k}) | \psi_n(\mathbf{k}') \rangle = 0$ .

The quantum geometric tensor  $\mathcal{F}_n^{\mu\nu}$  is defined as follows. We start with the quantum distance  $ds_{\text{HS}}$  for the infinitesimal translation  $d\mathbf{k}$  of the momentum as [1, 2, 59]

$$ds_{\text{HS}}(\mathbf{k}) \equiv \sqrt{1 - F_n(\mathbf{k}, \mathbf{k} + d\mathbf{k})^2}, \quad (3)$$

with

$$F_n(\mathbf{k}, \mathbf{k} + d\mathbf{k}) = |\langle \psi_n(\mathbf{k}) | U_{d\mathbf{k}} | \psi_n(\mathbf{k}) \rangle|, \quad (4)$$

where

$$U_{d\mathbf{k}} \equiv e^{-i d\mathbf{k} \cdot \mathbf{r}} \quad (5)$$

is the generator of the infinitesimal momentum translation  $d\mathbf{k}$  and  $r_\mu \equiv i\partial/\partial k_\mu$  is the position operator. The quantum distance for the infinitesimal momentum is expanded in terms of

the quantum geometric tensor  $\mathcal{F}_n^{\mu\nu}$  as

$$(ds_{\text{HS}})^2 = \sum_{\mu\nu} \mathcal{F}_n^{\mu\nu} dk_\mu dk_\nu, \quad (6)$$

where  $\mu, \nu$  stand for  $x, y$ , and

$$\mathcal{F}_n^{\mu\nu}(\mathbf{k}) = \langle \partial_{k_\mu} \psi_n(\mathbf{k}) | (1 - |\psi_n(\mathbf{k})\rangle \langle \psi_n(\mathbf{k})|) | \partial_{k_\nu} \psi_n(\mathbf{k}) \rangle, \quad (7)$$

with  $\partial_{k_\mu} \equiv \frac{\partial}{\partial k_\mu}$ . It is called the Fubini-Study metric[60, 61]. It is rewritten as

$$\mathcal{F}_n^{\mu\nu}(\mathbf{k}) = \langle \partial_{k_\mu} \psi_n(\mathbf{k}) | (1 - P_n(\mathbf{k})) | \partial_{k_\nu} \psi_n(\mathbf{k}) \rangle, \quad (8)$$

where we have defined the projection operator,

$$P_n(\mathbf{k}) \equiv |\psi_n(\mathbf{k})\rangle \langle \psi_n(\mathbf{k})|, \quad (9)$$

satisfying the idempotency condition  $P(\mathbf{k})^2 = P(\mathbf{k})$ . The presence of the projection operator is understood as follows.  $|\partial_{k_\nu} \psi_n(\mathbf{k})\rangle$  is generally mapped out of the band  $n$ , where the projection operator restricts  $|\partial_{k_\nu} \psi_n(\mathbf{k})\rangle$  to the band  $n$ .  $\mathcal{F}_n^{\mu\nu}$  is Hermitian,  $(\mathcal{F}_n^{\mu\nu})^* = \mathcal{F}_n^{\nu\mu}$ . The derivation of Eq.(7) is shown in Appendix A.

The quantum metric is the real part of the quantum geometric tensor,

$$g_n^{\mu\nu} \equiv \text{Re} \mathcal{F}_n^{\mu\nu} = \frac{\mathcal{F}_n^{\mu\nu}(\mathbf{k}) + (\mathcal{F}_n^{\mu\nu}(\mathbf{k}))^*}{2}, \quad (10)$$

while the Berry curvature is the imaginary part of the quantum geometric tensor,

$$\Omega_n^{\mu\nu} \equiv 2\text{Im} \mathcal{F}_n^{\mu\nu} = i (\mathcal{F}_n^{\mu\nu}(\mathbf{k}) - (\mathcal{F}_n^{\mu\nu}(\mathbf{k}))^*). \quad (11)$$

There are relations

$$g_n^{\mu\nu} = g_n^{\nu\mu}, \quad \Omega_n^{\mu\nu} = -\Omega_n^{\nu\mu}. \quad (12)$$

With the use of them, the quantum geometric tensor is decomposed into the real and imaginary parts,

$$\mathcal{F}_n^{\mu\nu} = g_n^{\mu\nu} - \frac{i}{2} \Omega_n^{\mu\nu}. \quad (13)$$

The Berry curvature does not contribute to the quantum distance

$$(ds_{\text{HS}})^2 = \sum_{\mu\nu} g_n^{\mu\nu} dk_\mu dk_\nu, \quad (14)$$

because of the symmetry  $dk_\mu dk_\nu = dk_\nu dk_\mu$ .

By introducing the Wilczek-Zee connection[62],

$$a_{nm}^\mu(\mathbf{k}) \equiv i \langle \psi_n(\mathbf{k}) | \partial_{k_\mu} | \psi_m(\mathbf{k}) \rangle, \quad (15)$$

the quantum geometric tensor is rewritten as

$$\begin{aligned} & \mathcal{F}_n^{\mu\nu}(\mathbf{k}) \\ &= \sum_{m \neq n} \langle \partial_{k_\mu} \psi_n(\mathbf{k}) | \psi_m(\mathbf{k}) \rangle \langle \psi_m(\mathbf{k}) | \partial_{k_\nu} \psi_n(\mathbf{k}) \rangle \\ &= \sum_{m \neq n} (i \langle \psi_m(\mathbf{k}) | \partial_{k_\mu} \psi_n(\mathbf{k}) \rangle)^* i \langle \psi_m(\mathbf{k}) | \partial_{k_\nu} \psi_n(\mathbf{k}) \rangle \\ &= \sum_{m \neq n} a_{nm}^{\mu*}(\mathbf{k}) a_{mn}^\nu(\mathbf{k}). \end{aligned} \quad (16)$$

The Wilczek-Zee connection is Hermitian,

$$a_{nm}^{\mu*}(\mathbf{k}) = a_{mn}^\mu(\mathbf{k}), \quad (17)$$

because

$$\begin{aligned} & i \frac{\partial}{\partial k_\mu} \langle \psi_m(\mathbf{k}) | \psi_n(\mathbf{k}) \rangle \\ &= i \langle \partial_{k_\mu} \psi_m(\mathbf{k}) | \psi_n(\mathbf{k}) \rangle + i \langle \psi_m(\mathbf{k}) | \partial_{k_\mu} \psi_n(\mathbf{k}) \rangle \\ &= (-i \langle \psi_n(\mathbf{k}) | \partial_{k_\mu} \psi_m(\mathbf{k}) \rangle)^* + i \langle \psi_m(\mathbf{k}) | \partial_{k_\mu} \psi_n(\mathbf{k}) \rangle \\ &= -a_{nm}^{\mu*}(\mathbf{k}) + a_{mn}^\mu(\mathbf{k}) = 0. \end{aligned} \quad (18)$$

Then, the quantum geometric tensor is rewritten as

$$\mathcal{F}_n^{\mu\nu}(\mathbf{k}) = \sum_{m \neq n} a_{nm}^\mu(\mathbf{k}) a_{mn}^\nu(\mathbf{k}) \quad (19)$$

in terms of the Wilczek-Zee connection.

## B. Berry connection, Berry curvature and Chern number

It follows that  $\Omega_n^{xx}(\mathbf{k}) = \Omega_n^{yy}(\mathbf{k}) = 0$  from the antisymmetric property Eq.(12). Then, the nontrivial contributions are  $\Omega_n^{xy}(\mathbf{k})$  and  $\Omega_n^{yx}(\mathbf{k})$ . The Berry curvature (11) reads

$$\begin{aligned} & \Omega_n^{xy}(\mathbf{k}) \\ &= i \langle \partial_{k_x} \psi_n(\mathbf{k}) | 1 - P(\mathbf{k}) | \partial_{k_y} \psi_n(\mathbf{k}) \rangle \\ & \quad - i \langle \partial_{k_y} \psi_n(\mathbf{k}) | 1 - P(\mathbf{k}) | \partial_{k_x} \psi_n(\mathbf{k}) \rangle \\ &= i \langle \partial_{k_x} \psi_n(\mathbf{k}) | \partial_{k_y} \psi_n(\mathbf{k}) \rangle - i \langle \partial_{k_y} \psi_n(\mathbf{k}) | \partial_{k_x} \psi_n(\mathbf{k}) \rangle \\ & \quad - i \langle \partial_{k_x} \psi_n(\mathbf{k}) | \psi_n(\mathbf{k}) \rangle \langle \psi_n(\mathbf{k}) | \partial_{k_y} \psi_n(\mathbf{k}) \rangle \\ & \quad + i \langle \partial_{k_y} \psi_n(\mathbf{k}) | \psi_n(\mathbf{k}) \rangle \langle \psi_n(\mathbf{k}) | \partial_{k_x} \psi_n(\mathbf{k}) \rangle \\ &= i \langle \partial_{k_x} \psi_n(\mathbf{k}) | \partial_{k_y} \psi_n(\mathbf{k}) \rangle - i \langle \partial_{k_y} \psi_n(\mathbf{k}) | \partial_{k_x} \psi_n(\mathbf{k}) \rangle \\ & \quad + i a_n^{y*}(\mathbf{k}) a_n^x(\mathbf{k}) - i a_n^{x*}(\mathbf{k}) a_n^y(\mathbf{k}), \end{aligned} \quad (20)$$

where we have defined the Berry connection

$$a_n^\mu(\mathbf{k}) \equiv a_{nn}^\mu(\mathbf{k}), \quad (21)$$

which is real,  $a_n^{\mu*}(\mathbf{k}) = a_n^\mu(\mathbf{k})$ .

Then, the Berry curvature (20) is rewritten as

$$\begin{aligned} & \Omega_n^{xy}(\mathbf{k}) \\ &= i \langle \partial_{k_x} \psi_n(\mathbf{k}) | \partial_{k_y} \psi_n(\mathbf{k}) \rangle - i \langle \partial_{k_y} \psi_n(\mathbf{k}) | \partial_{k_x} \psi_n(\mathbf{k}) \rangle \\ &= -2\text{Im} \left\langle \frac{\partial \psi_n(\mathbf{k})}{\partial k_x} \left| \frac{\partial \psi_n(\mathbf{k})}{\partial k_y} \right. \right\rangle \\ &= \frac{\partial a_n^y(\mathbf{k})}{\partial k_x} - \frac{\partial a_n^x(\mathbf{k})}{\partial k_y} = [\nabla \times \mathbf{a}_n(\mathbf{k})]_z. \end{aligned} \quad (22)$$

Its integral over the whole Brillouin zone is quantized

$$\begin{aligned} \frac{1}{2\pi} \int d\mathbf{k} \Omega_n^{xy}(\mathbf{k}) &= \frac{1}{2\pi} \oint dk_\mu \nabla \times \Omega_n^{xy}(\mathbf{k}) \\ &= \frac{1}{2\pi} \oint dk_\mu a_n^\mu(\mathbf{k}) = \mathcal{C}_n, \end{aligned} \quad (23)$$

where  $C_n$  is the Chern number taking an integer.

We go on to prove that  $C_n$  is an integer[63]. The formula (23) is interpreted as the integral of the Berry curvature  $\Omega_n^{xy}(\mathbf{k})$  over the first Brillouin zone, which is the Chern number. Using the Stokes theorem, this can be rewritten as a contour integration along the boundary of the Brillouin zone,

$$C_n = \frac{1}{2\pi} \int d\mathbf{k} \Omega_n^{xy}(\mathbf{k}) = \frac{1}{2\pi} \oint dk_\mu a_n^\mu(\mathbf{k}). \quad (24)$$

Since it is a periodic system, it follows that  $C_n = 0$  if  $a_n^\mu(\mathbf{k})$  is a regular function. However, the gauge potential  $a_n^\mu(\mathbf{k})$  can be singular though the magnetic field  $\Omega_n^{xy}(\mathbf{k})$  is regular. In this case it is necessary to choose the contour integration to avoid these singular points. Then,  $C_n$  counts the number of singularities, following the argument familiar in the theory of Dirac monopoles.

### C. Wannier function and polarization

The Wannier function is defined by

$$|w_n(\mathbf{r})\rangle \equiv \frac{1}{2\pi} \int_{\text{BZ}} d\mathbf{k} e^{-i\mathbf{k}\cdot\mathbf{r}} |\psi_n(\mathbf{k})\rangle, \quad (25)$$

or

$$|\psi_n(\mathbf{k})\rangle = \sum_{\mathbf{r}} e^{i\mathbf{k}\cdot\mathbf{r}} |w_n(\mathbf{r})\rangle. \quad (26)$$

Then, the Berry connection is rewritten as

$$\begin{aligned} a_n^\mu(\mathbf{k}) &\equiv i \langle \psi_n(\mathbf{k}) | \frac{d}{dk_\mu} | \psi_n(\mathbf{k}) \rangle \\ &= \sum_{\mathbf{r}, \mathbf{r}'} \langle w_n(\mathbf{r}') | e^{-i\mathbf{k}\cdot\mathbf{r}'} \frac{d}{dk_\mu} e^{i\mathbf{k}\cdot\mathbf{r}} | w_n(\mathbf{r}) \rangle \\ &= \sum_{\mathbf{r}, \mathbf{r}'} \langle w_n(\mathbf{r}') | e^{i\mathbf{k}\cdot(\mathbf{r}-\mathbf{r}')} r_\mu | w_n(\mathbf{r}) \rangle. \end{aligned} \quad (27)$$

We integrate it over the Brillouin zone and obtain

$$\begin{aligned} &\frac{1}{2\pi} \int_{\text{BZ}} a_n^\mu(\mathbf{k}) d\mathbf{k} \\ &= \sum_{\mathbf{r}, \mathbf{r}'} \langle w_n(\mathbf{r}') | \int_{\text{BZ}} e^{i\mathbf{k}\cdot(\mathbf{r}-\mathbf{r}')} d\mathbf{k} r_\mu | w_n(\mathbf{r}) \rangle \\ &= \sum_{\mathbf{r}, \mathbf{r}'} \langle w_n(\mathbf{r}') | \delta(\mathbf{r}-\mathbf{r}') r_\mu | w_n(\mathbf{r}) \rangle \\ &= \sum_{\mathbf{r}} \langle w_n(\mathbf{r}) | r_\mu | w_n(\mathbf{r}) \rangle = \langle r_\mu \rangle. \end{aligned} \quad (28)$$

It is the expectation value of the position  $r_\mu$ , which represents the polarization.

The quantum metric is related to the fluctuation of the polarization[64],

$$\begin{aligned} &\frac{1}{2\pi} \int_{\text{BZ}} g_n^{\mu\mu}(\mathbf{k}) d\mathbf{k} \\ &= \sum_{\mathbf{r}} \langle w_n(\mathbf{r}) | r_\mu^2 | w_n(\mathbf{r}) \rangle - \langle w_n(\mathbf{r}) | r_\mu | w_n(\mathbf{r}) \rangle^2 \\ &= \langle r_\mu^2 \rangle - \langle r_\mu \rangle^2. \end{aligned} \quad (29)$$

### D. Inequality

There is an inequality for the quantum metric and the Berry curvature in two dimensions[65, 66],

$$\frac{1}{2} \text{Tr} g_n^{\mu\nu}(\mathbf{k}) \geq \sqrt{\det g_n^{\mu\nu}(\mathbf{k})} \geq \frac{|\Omega_n^{xy}(\mathbf{k})|}{2}, \quad (30)$$

where the trace and the determinant are taken over  $\mu$  and  $\nu$ . The first inequality is proved by using the arithmetic geometric mean,

$$\frac{g_+ + g_-}{2} \geq \sqrt{g_+ g_-}, \quad (31)$$

where  $g_\pm$  is the diagonal component of the diagonalized  $g_n^{\mu\nu}(\mathbf{k})$ ,

$$g_n^{\mu\nu}(\mathbf{k}) = \begin{pmatrix} g_+ & 0 \\ 0 & g_- \end{pmatrix} \quad (32)$$

with

$$g_\pm \equiv \frac{g_n^{xx} + g_n^{yy} \pm \sqrt{(g_n^{xx} - g_n^{yy})^2 + 4(g_n^{xy})^2}}{2}. \quad (33)$$

The second inequality is proved by using the non-negativity of  $\mathcal{F}_n^{\mu\nu}(\mathbf{k})$ ,

$$\det \mathcal{F}_n^{\mu\nu}(\mathbf{k}) \geq 0, \quad (34)$$

which is derived from the non-negativity of the quadratic form in Eq.(6). It is equivalent to

$$\det g_n^{\mu\nu}(\mathbf{k}) \geq \left( \frac{\Omega_n^{xy}}{2} \right)^2, \quad (35)$$

where we have used

$$\mathcal{F}_n^{\mu\nu} = \begin{pmatrix} g_n^{xx} & g_n^{xy} - i\Omega_n^{xy}/2 \\ g_n^{xy} + i\Omega_n^{xy}/2 & g_n^{yy} \end{pmatrix}, \quad (36)$$

which is derived from Eqs.(10), (11) and (12).

By integrating the inequality (30) over the whole Brillouin zone, we obtain[65–68]

$$\begin{aligned} &\frac{1}{2\pi} \int d\mathbf{k} \text{Tr} g_n^{\mu\nu}(\mathbf{k}) \\ &\geq 2 \frac{1}{2\pi} \int d\mathbf{k} \sqrt{\det g_n^{\mu\nu}(\mathbf{k})} \\ &\geq \frac{1}{2\pi} \int d\mathbf{k} |\Omega_n^{xy}(\mathbf{k})| \geq \frac{1}{2\pi} \int d\mathbf{k} \Omega_n^{xy}(\mathbf{k}) = C_n. \end{aligned} \quad (37)$$

This gives a lower bound for  $\int d\mathbf{k} \text{Tr} g_n^{\mu\nu}(\mathbf{k})$ , when the system is topological,  $C_n \geq 1$ . There are some applications to this inequality[12, 69, 70].

The quantum volume is defined by the Riemann volume as[67]

$$\text{vol}_g \equiv \frac{1}{2\pi} \int d\mathbf{k} \sqrt{\det g_n^{\mu\nu}(\mathbf{k})}. \quad (38)$$

The quantum weight is defined by[71]

$$K^{\mu\nu} \equiv \frac{1}{2\pi} \int d\mathbf{k} g_n^{\mu\nu}(\mathbf{k}), \quad (39)$$

which measures quantum fluctuation in the center of mass. It is experimentally determined from X-ray scattering.

### E. Quantum Geometry for two-band systems

We consider a two-band system with the index  $n = \pm$ . The Hamiltonian is generally given by

$$H(\mathbf{k}) = h_0(\mathbf{k}) + \boldsymbol{\sigma} \cdot \mathbf{h}(\mathbf{k}), \quad (40)$$

where  $\mathbf{h}(\mathbf{k})$  is parametrized as the normalized vector  $\mathbf{n}(\mathbf{k})$ ,

$$\mathbf{n}(\mathbf{k}) \equiv \mathbf{h}(\mathbf{k}) / |\mathbf{h}(\mathbf{k})| = (\sin \theta \cos \phi, \sin \theta \sin \phi, \cos \theta), \quad (41)$$

and  $\sigma_j$  is the Pauli matrix with  $j = x, y, z$ . In this case, there are simple forms in terms of  $\mathbf{n}(\mathbf{k})$ .

The energy is given by

$$\varepsilon_{\pm} = h_0(\mathbf{k}) \pm |\mathbf{h}(\mathbf{k})|. \quad (42)$$

The eigenfunctions  $\psi_{\pm}(\mathbf{k})$  of the Hamiltonian (40) corresponding to the energy  $\varepsilon_{\pm}$  are given by

$$\psi_{+}(\mathbf{k}) = e^{i\alpha(\mathbf{k})} \begin{pmatrix} e^{-i\phi(\mathbf{k})} \cos \frac{\theta(\mathbf{k})}{2} \\ \sin \frac{\theta(\mathbf{k})}{2} \end{pmatrix}, \quad (43)$$

$$\psi_{-}(\mathbf{k}) = e^{i\alpha(\mathbf{k})} \begin{pmatrix} -e^{-i\phi(\mathbf{k})} \sin \frac{\theta(\mathbf{k})}{2} \\ \cos \frac{\theta(\mathbf{k})}{2} \end{pmatrix}, \quad (44)$$

where  $\alpha(\mathbf{k})$  is a real function representing a gauge degrees of freedom. Then, the Wilczek-Zee connection (15) is calculated as

$$\begin{aligned} a_{+-}^{\mu}(\mathbf{k}) &= -i \langle \psi_{+}(\mathbf{k}) | \partial_{k_{\mu}} \psi_{-}(\mathbf{k}) \rangle \\ &= i \frac{\partial_{k_{\mu}} \theta}{2} + \frac{\partial_{k_{\mu}} \phi}{2} \sin \theta, \end{aligned} \quad (45)$$

and

$$\begin{aligned} a_{-+}^{\mu}(\mathbf{k}) &= -i \langle \psi_{-}(\mathbf{k}) | \partial_{k_{\mu}} \psi_{+}(\mathbf{k}) \rangle \\ &= -i \frac{\partial_{k_{\mu}} \theta}{2} + \frac{\partial_{k_{\mu}} \phi}{2} \sin \theta, \end{aligned} \quad (46)$$

irrespective of  $\alpha$ .

The quantum metric is explicitly given by[12, 15, 17, 18, 72–75]

$$\begin{aligned} g_{\pm}^{\mu\nu}(\mathbf{k}) &= \pm \frac{1}{2} (\partial_{k_{\mu}} \mathbf{n}) \cdot (\partial_{k_{\nu}} \mathbf{n}) \\ &= \pm \frac{1}{4} (\partial_{k_{\mu}} \theta \partial_{k_{\nu}} \theta + \sin^2 \theta \partial_{k_{\mu}} \phi \partial_{k_{\nu}} \phi) \end{aligned} \quad (47)$$

with the normalized vector (41). Two or three components of  $\mathbf{n}$  should be nonzero for nonzero  $g^{\mu\nu}$ . It is understood as follows: If only one component  $n_z(\mathbf{k})$  is nonzero, it is given by  $n_z(\mathbf{k}) = h_z(\mathbf{k}) / |h_z(\mathbf{k})|$ , whose derivative  $\partial_{k_{\mu}} \mathbf{n}$  is singular.

The Berry curvature is explicitly given by[73, 75, 79–81]

$$\begin{aligned} \Omega_{\pm}^{xy}(\mathbf{k}) &= \mp \frac{1}{2} \mathbf{n} \cdot (\partial_{k_x} \mathbf{n} \times \partial_{k_y} \mathbf{n}) \\ &= \pm \frac{1}{2} \sin \theta (\partial_{k_x} \phi \partial_{k_y} \theta - \partial_{k_x} \theta \partial_{k_y} \phi). \end{aligned} \quad (48)$$

It is a solid angle of the vector  $\mathbf{n}$ . Hence, three components of  $\mathbf{n}$  should be nonzero for nonzero  $\Omega_{\pm}^{xy}$ .

### F. Analogy of the theory of general relativity

The quantum metric and the Berry curvature are mainly studied in the current stage. In addition to them, there are following quantities that can be defined in the analogy of the theory of general relativity[15, 76]. They are the Christoffel symbol

$$\Gamma_{\mu\nu}^{\lambda} \equiv \frac{1}{2} g_{\lambda\sigma} (\partial_{\mu} g_{\nu\sigma} + \partial_{\nu} g_{\sigma\mu} - \partial_{\sigma} g_{\mu\nu}), \quad (49)$$

the Riemann tensor

$$R_{\sigma\mu\nu}^{\rho} \equiv \partial_{\mu} \Gamma_{\nu\sigma}^{\rho} - \partial_{\nu} \Gamma_{\mu\sigma}^{\rho} + \Gamma_{\mu\lambda}^{\rho} \Gamma_{\nu\sigma}^{\lambda} - \Gamma_{\nu\lambda}^{\rho} \Gamma_{\mu\sigma}^{\lambda}, \quad (50)$$

the Ricci tensor

$$R_{\mu\nu} \equiv R_{\mu\lambda\nu}^{\lambda}, \quad (51)$$

the Ricci scalar

$$R \equiv g^{\mu\nu} R_{\mu\nu}, \quad (52)$$

and the Einstein tensor

$$G_{\mu\nu} \equiv R_{\mu\nu} - \frac{1}{2} R g_{\mu\nu}. \quad (53)$$

Especially, the Christoffel symbol is given by

$$\Gamma_{\mu\nu}^{\lambda} = \frac{1}{4} \partial_{\lambda} \mathbf{n} \cdot \partial_{\mu} \partial_{\nu} \mathbf{n} \quad (54)$$

for the two-band system[77]. Furthermore, the Riemann tensor reads

$$\begin{aligned} R_{\sigma\mu\nu}^{\rho} &= \frac{1}{4} [\partial_{\mu} \partial_{\rho} \mathbf{n} \cdot \partial_{\nu} \partial_{\sigma} \mathbf{n} + \partial_{\rho} \mathbf{n} \cdot \partial_{\mu} \partial_{\nu} \partial_{\sigma} \mathbf{n} \\ &\quad - \partial_{\nu} \partial_{\rho} \mathbf{n} \cdot \partial_{\mu} \partial_{\sigma} \mathbf{n} - \partial_{\rho} \mathbf{n} \cdot \partial_{\mu} \partial_{\nu} \partial_{\sigma} \mathbf{n}] \\ &\quad + \frac{1}{16} (\partial_{\rho} \mathbf{n} \cdot \partial_{\mu} \partial_{\lambda} \mathbf{n}) (\partial_{\lambda} \mathbf{n} \cdot \partial_{\nu} \partial_{\sigma} \mathbf{n}) \\ &\quad - \frac{1}{16} (\partial_{\rho} \mathbf{n} \cdot \partial_{\nu} \partial_{\lambda} \mathbf{n}) (\partial_{\lambda} \mathbf{n} \cdot \partial_{\mu} \partial_{\sigma} \mathbf{n}), \end{aligned} \quad (55)$$

and the Ricci tensor reads

$$\begin{aligned} R_{\mu\nu} &= \frac{1}{4} [\partial_{\lambda} \partial_{\lambda} \mathbf{n} \cdot \partial_{\nu} \partial_{\mu} \mathbf{n} - \partial_{\nu} \partial_{\lambda} \mathbf{n} \cdot \partial_{\lambda} \partial_{\mu} \mathbf{n}] \\ &\quad + \frac{1}{16} (\partial_{\lambda} \mathbf{n} \cdot \partial_{\lambda} \partial_{\lambda} \mathbf{n}) (\partial_{\lambda} \mathbf{n} \cdot \partial_{\nu} \partial_{\mu} \mathbf{n}) \\ &\quad - \frac{1}{16} (\partial_{\lambda} \mathbf{n} \cdot \partial_{\nu} \partial_{\lambda} \mathbf{n}) (\partial_{\lambda} \mathbf{n} \cdot \partial_{\lambda} \partial_{\mu} \mathbf{n}). \end{aligned} \quad (56)$$

### G. Non-Abelian quantum geometry

So far, we have studied the case where the target band is a single band. If the target bands are  $N$ -fold degenerate, we consider the  $N$ -fold degenerate wave function,

$$|\psi(\mathbf{k})\rangle = \sum_{n=1}^N c_n |\psi_n(\mathbf{k})\rangle, \quad (57)$$

satisfying the normalization condition,  $\sum_{n=1}^N |c_n|^2 = 1$ . It is necessary to generalize quantum geometry to the non-Abelian quantum geometry[3]. The fidelity of the wave functions  $|\psi(\mathbf{k})\rangle$  and  $|\psi(\mathbf{k} + d\mathbf{k})\rangle$  is defined by

$$F(\mathbf{k}, \mathbf{k} + d\mathbf{k}) \equiv |\langle \psi(\mathbf{k}) | U_{d\mathbf{k}} | \psi(\mathbf{k}) \rangle| \quad (58)$$

with  $U_{d\mathbf{k}}$  given by Eq.(5). The quantum distance is

$$d_{\text{HS}} \equiv \sqrt{1 - F(\mathbf{k}, \mathbf{k} + d\mathbf{k})^2} \quad (59)$$

The non-Abelian quantum geometric tensor is given by

$$(d_{\text{HS}})^2 \equiv \sum_{\mu\nu} \sum_{nm} \mathcal{F}_{nm}^{\mu\nu} dk_\mu dk_\nu \quad (60)$$

with

$$\mathcal{F}_{nm}^{\mu\nu} = \langle \partial_{k_\mu} \psi_n(\mathbf{k}) | (1 - P(\mathbf{k})) | \partial_{k_\nu} \psi_m(\mathbf{k}) \rangle \quad (61)$$

where  $P(\mathbf{k})$  is the projection operator onto the target bands,

$$P(\mathbf{k}) \equiv \sum_{n=1}^N |\psi_n(\mathbf{k})\rangle \langle \psi_n(\mathbf{k})|, \quad (62)$$

which satisfies the idempotence relation  $P(\mathbf{k})^2 = P(\mathbf{k})$ . The derivation is shown in Appendix B.

The quantum metric is the real part of the quantum geometric tensor,

$$g_{nm}^{\mu\nu} \equiv \text{Re} \mathcal{F}_{nm}^{\mu\nu} = \frac{\mathcal{F}_{mn}^{\mu\nu}(\mathbf{k}) + (\mathcal{F}_{mn}^{\mu\nu}(\mathbf{k}))^*}{2}, \quad (63)$$

while the Berry curvature is the imaginary part of the quantum geometric tensor,

$$\Omega_{nm}^{\mu\nu} \equiv 2\text{Im} \mathcal{F}_{nm}^{\mu\nu} = i (\mathcal{F}_{mn}^{\mu\nu}(\mathbf{k}) - (\mathcal{F}_{mn}^{\mu\nu}(\mathbf{k}))^*). \quad (64)$$

It is further calculated as

$$\begin{aligned} \Omega_{nm}^{\mu\nu} &= i \langle \partial_{k_\mu} \psi_n(\mathbf{k}) | 1 - P(\mathbf{k}) | \partial_{k_\nu} \psi_m(\mathbf{k}) \rangle \\ &\quad - i \langle \partial_{k_\nu} \psi_m(\mathbf{k}) | 1 - P(\mathbf{k}) | \partial_{k_\mu} \psi_n(\mathbf{k}) \rangle \\ &= i \langle \partial_{k_\mu} \psi_n(\mathbf{k}) | \partial_{k_\nu} \psi_m(\mathbf{k}) \rangle - i \langle \partial_{k_\nu} \psi_m(\mathbf{k}) | \partial_{k_\mu} \psi_n(\mathbf{k}) \rangle \\ &\quad - i \sum_{n' \neq n, m} \langle \partial_{k_\mu} \psi_n(\mathbf{k}) | \psi_{n'}(\mathbf{k}) \rangle \langle \psi_{n'}(\mathbf{k}) | \partial_{k_\nu} \psi_m(\mathbf{k}) \rangle \\ &\quad + i \sum_{n' \neq n, m} \langle \partial_{k_\nu} \psi_m(\mathbf{k}) | \psi_{n'}(\mathbf{k}) \rangle \langle \psi_{n'}(\mathbf{k}) | \partial_{k_\mu} \psi_n(\mathbf{k}) \rangle \\ &= i \langle \partial_{k_\mu} \psi_n(\mathbf{k}) | \partial_{k_\nu} \psi_m(\mathbf{k}) \rangle - i \langle \partial_{k_\nu} \psi_m(\mathbf{k}) | \partial_{k_\mu} \psi_n(\mathbf{k}) \rangle \\ &\quad + \sum_{n' \neq n, m} i a_{n'n}^{\mu*} a_{n'm}^\nu - i a_{n'm}^{\nu*} a_{n'n}^\mu. \end{aligned} \quad (65)$$

With the use of the Hermiticity condition of the Berry connection (17), we have

$$\begin{aligned} \Omega_{nm}^{\mu\nu} &= i \langle \partial_{k_\mu} \psi_n(\mathbf{k}) | \partial_{k_\nu} \psi_m(\mathbf{k}) \rangle \\ &\quad - i \langle \partial_{k_\nu} \psi_m(\mathbf{k}) | \partial_{k_\mu} \psi_n(\mathbf{k}) \rangle \\ &\quad - \sum_{n' \neq n, m} i a_{nn'}^\mu a_{n'm}^\nu + \sum_{n' \neq n, m} i a_{mn'}^\nu a_{n'n}^\mu \\ &= \nabla \times a_{nm}^\mu - \sum_{n' \neq n, m} i [a_{nn'}^\mu, a_{n'm}^\nu]. \end{aligned} \quad (66)$$

There is an additional term  $-i [a_{nn'}^\mu, a_{n'm}^\nu]$  in the Wilczek-Zee connection comparing with the Berry connection.

### III. QUANTUM GEOMETRY IN CONDENSED MATTER PHYSICS

Quantum geometric properties are observable in condensed matter physics. First, we review that the Berry curvature is observable by the Hall conductance. The Hall conductance is quantized for an insulator, which is well described by the Chern number. On the other hand, the quantum metric appears in the optical absorption, the bulk photovoltaic effect and nonlinear conductivities.

#### A. Thouless-Kohmoto-Nightingale-Nijs formula

The Berry curvature is related to the Hall conductivity. Especially, the Hall conductivity is quantized in an insulator and is proportional to the Chern number, which is known as the TKNN formula[4].

According to the Kubo formula, the Hall conductance is given by

$$\begin{aligned} \sigma_{xy} &= -i\hbar e^2 \int d\mathbf{k} \sum_{n \neq m} \frac{f(\varepsilon_n(\mathbf{k}))}{(\varepsilon_n(\mathbf{k}) - \varepsilon_m(\mathbf{k}))^2} \\ &\quad \times [\langle \psi_n(\mathbf{k}) | v_x | \psi_m(\mathbf{k}) \rangle \langle \psi_m(\mathbf{k}) | v_y | \psi_n(\mathbf{k}) \rangle \\ &\quad - \langle \psi_n(\mathbf{k}) | v_y | \psi_m(\mathbf{k}) \rangle \langle \psi_m(\mathbf{k}) | v_x | \psi_n(\mathbf{k}) \rangle], \end{aligned} \quad (67)$$

where  $f(\varepsilon_n(\mathbf{k})) = 1/(\exp[(\varepsilon_n(\mathbf{k}) - \mu)/(k_B T) + 1])$  is the Fermi distribution function and  $\mu$  is the chemical potential. By using the Hellmann-Feynman theorem

$$\begin{aligned} &\langle \psi_m(\mathbf{k}) | v_\mu | \psi_n(\mathbf{k}) \rangle \\ &= \frac{1}{\hbar} \partial_{k_\mu} \varepsilon_n(\mathbf{k}) \langle \psi_m(\mathbf{k}) | \psi_n(\mathbf{k}) \rangle \\ &\quad + \frac{1}{\hbar} (\varepsilon_n(\mathbf{k}) - \varepsilon_m(\mathbf{k})) \langle \psi_m(\mathbf{k}) | \partial_{k_\mu} | \psi_n(\mathbf{k}) \rangle \end{aligned} \quad (68)$$

for the states subject to the orthonormalization condition,  $\langle \psi_m(\mathbf{k}) | \psi_n(\mathbf{k}) \rangle = \delta_{mn}$ , the Hall conductance is rewritten

as

$$\begin{aligned} \sigma_{xy} = & -\frac{ie^2}{\hbar} \int d\mathbf{k} \sum_{n,m} f(\varepsilon_n(\mathbf{k})) \\ & \times [\langle \psi_n(\mathbf{k}) | \partial_{k_x} \psi_m(\mathbf{k}) \rangle \langle \psi_m(\mathbf{k}) | \partial_{k_y} \psi_n(\mathbf{k}) \rangle \\ & - \langle \psi_n(\mathbf{k}) | \partial_{k_y} \psi_m(\mathbf{k}) \rangle \langle \psi_m(\mathbf{k}) | \partial_{k_x} \psi_n(\mathbf{k}) \rangle]. \end{aligned} \quad (69)$$

It should be noticed that the sum can be extended to include the states with  $n = m$  in this formula, since

$$\begin{aligned} & \langle \psi_n(\mathbf{k}) | \partial_{k_x} \psi_n(\mathbf{k}) \rangle \langle \psi_n(\mathbf{k}) | \partial_{k_y} \psi_n(\mathbf{k}) \rangle \\ & = \langle \psi_n(\mathbf{k}) | \partial_{k_y} \psi_n(\mathbf{k}) \rangle \langle \psi_n(\mathbf{k}) | \partial_{k_x} \psi_n(\mathbf{k}) \rangle. \end{aligned} \quad (70)$$

The proof of the Hellmann-Feynman theorem is shown in Appendix C.

Making the use of the relation

$$\begin{aligned} & \langle \psi_n(\mathbf{k}) | \partial_{k_x} \psi_m(\mathbf{k}) \rangle + \langle \partial_{k_x} \psi_n(\mathbf{k}) | \psi_m(\mathbf{k}) \rangle \\ & = \partial_{k_x} \langle \psi_m(\mathbf{k}) | \psi_n(\mathbf{k}) \rangle = 0, \end{aligned} \quad (71)$$

the Hall conductance is rewritten as

$$\begin{aligned} \sigma_{xy} = & -\frac{ie^2}{\hbar} \int d\mathbf{k} \sum_{n,m} f(\varepsilon(\mathbf{k})) \\ & \times [\langle \partial_{k_x} \psi_n(\mathbf{k}) | \psi_m(\mathbf{k}) \rangle \langle \psi_m(\mathbf{k}) | \partial_{k_y} \psi_n(\mathbf{k}) \rangle \\ & - \langle \partial_{k_y} \psi_n(\mathbf{k}) | \psi_m(\mathbf{k}) \rangle \langle \psi_m(\mathbf{k}) | \partial_{k_x} \psi_n(\mathbf{k}) \rangle]. \end{aligned} \quad (72)$$

Using the completeness condition  $\sum_m |\psi_m(\mathbf{k})\rangle \langle \psi_m(\mathbf{k})| = 1$ , we obtain

$$\begin{aligned} \sigma_{xy} = & \frac{ie^2}{\hbar} \int d\mathbf{k} \sum_n f(\varepsilon_n(\mathbf{k})) [\langle \partial_{k_x} \psi_n(\mathbf{k}) | \partial_{k_y} \psi_n(\mathbf{k}) \rangle \\ & - \langle \partial_{k_y} \psi_n(\mathbf{k}) | \partial_{k_x} \psi_n(\mathbf{k}) \rangle]. \end{aligned} \quad (73)$$

It is rewritten as

$$\sigma_{xy} = \frac{e^2}{2\pi\hbar} \sum_n \int d\mathbf{k} f(\varepsilon_n(\mathbf{k})) \Omega_n^{xy}(\mathbf{k}), \quad (74)$$

where

$$\Omega_n^{xy}(\mathbf{k}) = i [\langle \partial_{k_x} \psi_n(\mathbf{k}) | \partial_{k_y} \psi_n(\mathbf{k}) \rangle - \langle \partial_{k_y} \psi_n(\mathbf{k}) | \partial_{k_x} \psi_n(\mathbf{k}) \rangle]. \quad (75)$$

The conductance is the sum of the contributions from various bands indexed by  $n$ . It is convenient to define a "gauge potential" in the momentum space for each band index  $n$  by

$$a_n^\mu(\mathbf{k}) = -i \langle \psi_n(\mathbf{k}) | \partial_{k_\mu} \psi_n(\mathbf{k}) \rangle, \quad (76)$$

which is the Berry connection. We may rewrite (75) as

$$\Omega_n^{xy}(\mathbf{k}) = \partial_{k_x} a_n^y(\mathbf{k}) - \partial_{k_y} a_n^x(\mathbf{k}). \quad (77)$$

This is the "magnetic field", which is the Berry curvature.

We consider the zero-temperature limit, where the Fermi distribution function becomes a step function,  $f(\varepsilon_n(\mathbf{k})) = \theta(\mu - \varepsilon_n)$ . The conductance (74) is simplified as

$$\sigma_{xy} = \frac{e^2}{h} \sum_{n=1}^N \mathcal{C}_n, \quad (78)$$

because the integration is taken below the Fermi energy.

## B. Dirac system

We apply the above formula to the Dirac Hamiltonian[? ],

$$H^\xi = \hbar v_F (\xi k_x \sigma_x + k_y \sigma_y) + m \sigma_z, \quad (79)$$

where  $\xi = \pm 1$  is the valley degrees of freedom. It describes the low-energy theory of graphene. It is expressed as  $H^\xi = \mathbf{h} \cdot \boldsymbol{\sigma}$  with

$$\mathbf{n}(\mathbf{k}) = \frac{1}{\sqrt{(\hbar v_F k)^2 + m^2}} (\xi \hbar v_F k_x, \hbar v_F k_y, m) \quad (80)$$

in the polar coordinate  $\mathbf{k} = (k, \phi)$ .

The quantum metrics are calculated as

$$g_{\pm}^{xx}(\mathbf{k}) = \mp \frac{(\hbar v_F)^2 \left( (\hbar v_F k_y)^2 + m^2 \right)}{\left( (\hbar v_F k)^2 + m^2 \right)^2}, \quad (81)$$

$$g_{\pm}^{yy}(\mathbf{k}) = \mp \frac{(\hbar v_F)^2 \left( (\hbar v_F k_x)^2 + m^2 \right)}{\left( (\hbar v_F k)^2 + m^2 \right)^2}, \quad (82)$$

$$g_{\pm}^{xy}(\mathbf{k}) = \pm \frac{(\hbar v_F)^2 (\hbar v_F k_x) (\hbar v_F k_y)}{\left( (\hbar v_F k)^2 + m^2 \right)^2}, \quad (83)$$

while the Berry curvature is calculated as

$$\Omega_{\pm}^{xy}(\mathbf{k}) = \pm \xi \frac{m (\hbar v_F)^2}{\left( (\hbar v_F k)^2 + m^2 \right)^{3/2}}. \quad (84)$$

When the chemical potential is within the gap  $\mu < |m|$ , we may calculate the Chern number explicitly as

$$\begin{aligned} \mathcal{C}^\xi = & \frac{1}{2\pi} \int_0^\infty 2\pi k dk \Omega_{\pm}^{xy}(\mathbf{k}) \\ = & -\frac{\xi}{2} \frac{m}{|m|^3} \int_0^\infty d\mathbf{k} \frac{(\hbar v_F)^2}{2 \left( (\hbar v_F/m)^2 k^2 + 1 \right)^{3/2}} \\ = & -\frac{\xi}{4} \frac{m}{|m|} \int_0^\infty dx \frac{1}{(x+1)^{3/2}} \\ = & -\frac{\xi}{4} \frac{m}{|m|} \int_1^\infty dy y^{-\frac{3}{2}} \\ = & \frac{\xi}{2} \frac{m}{|m|} y^{-\frac{1}{2}} \Big|_1^\infty = -\frac{\xi}{2} \text{sgn}(m). \end{aligned} \quad (85)$$

When the chemical potential is among the gap,  $|\mu| < |m|$ , the Chern number is already calculated as in (85). When the chemical potential is below or above the gap,  $|\mu| > |m|$ , the integration is taken in the region for  $k > k_F$  with

$$k_F = \frac{1}{\hbar v_F} \sqrt{\mu^2 - m^2}, \quad (86)$$



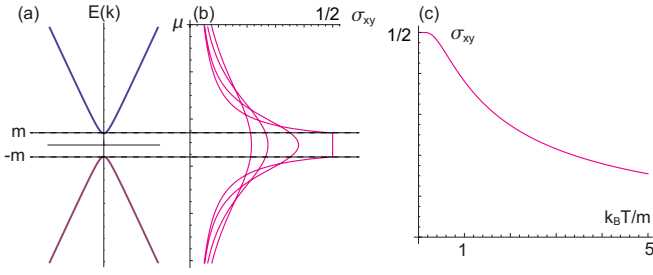


FIG. 1: (a) The energy spectrum of the massive Dirac fermion with the mass  $m$ . (b) Hall conductance as a function of the chemical potential for the massive Dirac Hamiltonian. (c) The temperature dependence of the Hall conductance at the Fermi energy  $\mu = 0$ .

which is the solution of  $\varepsilon(\mathbf{k}) = \mu$ . The Hall conductivity is calculated as

$$\begin{aligned}
 \frac{\sigma_{xy}^\xi}{e^2/h} &= \frac{1}{2\pi} \int_{k_F}^{\infty} 2\pi k dk \Omega^\xi(\mathbf{k}) \\
 &= -\frac{\xi}{2} \frac{m}{|m|^3} \int_{k_F^2}^{\infty} d^2k \frac{(\hbar v_F)^2}{2 \left( (\hbar v_F/m)^2 k^2 + 1 \right)^{3/2}} \\
 &= -\frac{\xi}{2} \frac{m}{|m|} \int_{\mu^2/m^2-1}^{\infty} dx \frac{1}{2(x+1)^{3/2}} \\
 &= -\frac{\xi}{4} \frac{m}{|m|} \int_{\mu^2/m^2}^{\infty} dy y^{-3/2} \\
 &= \frac{\xi}{2} \frac{m}{|m|} y^{-1/2} \Big|_{\mu^2/m^2}^{\infty} = -\frac{\xi}{2} \frac{|m|}{|\mu|} \text{sgn}(m). \quad (87)
 \end{aligned}$$

The TKNN formula dictates that the Hall conductance is proportional to the Chern number. The Hall conductance is given by  $\sigma_{xy} = \sum_{\xi} \sigma_{xy}^{\xi}$  with

$$\sigma_{xy}^{\xi} = \begin{cases} -\frac{\xi}{2} \frac{e^2}{h} \text{sgn}(m) & \text{for } |\mu| < |m| \\ -\frac{\xi}{2} \frac{|m|}{|\mu|} \frac{e^2}{h} \text{sgn}(m) & \text{for } |\mu| > |m| \end{cases} \quad (88)$$

as a function of the chemical potential. It is quantized between the bulk band gap,  $|\mu| < |m|$ , which is known as the quantum anomalous Hall effect. On the other hand, the Hall conductance is anti-proportional to the chemical potential outside the band gap,  $|\mu| > |m|$ . Eq.(88) is shown in Fig.1.

We have

$$\text{Tr} g_n^{\mu\nu}(\mathbf{k}) = (\hbar v_F)^2 \frac{2m^2 + (\hbar v_F k)^2}{2 \left( (\hbar v_F k)^2 + m^2 \right)^2}, \quad (89)$$

and

$$\sqrt{\det g_n^{\mu\nu}(\mathbf{k})} = \frac{|m| (\hbar v_F)^2}{2 \left( (\hbar v_F k)^2 + m^2 \right)^{3/2}}. \quad (90)$$

Especially, there is a relation

$$2\sqrt{\det g_n^{\mu\nu}(\mathbf{k})} = \left| \Omega_{\pm}^{xy}(\mathbf{k}) \right|. \quad (91)$$

We can check the inequality (30) is satisfied. The quantum volume is calculated as

$$\int d\mathbf{k} \sqrt{\det g_n^{\mu\nu}(\mathbf{k})} = \frac{1}{8} \left( \frac{\hbar v_F}{m} \right)^2. \quad (92)$$

A comment is in order. The Dirac system gives a half-integer of the Chern number, which may contradict the fact that the Chern number is an integer. This problem is solved by the Nielsen-Ninomiya theorem, which shows that the number of Dirac cones must be even for the system defined for the Brillouin zone. Then, the total Chern number is always an integer, which is relevant in realistic materials.

### C. Optical absorption and elliptic dichroism

We study optical inter-band transitions from the state  $|\psi_{-}(\mathbf{k})\rangle$  in the valence band to the state  $|\psi_{+}(\mathbf{k})\rangle$  in the conduction band. We apply a beam of elliptical polarized light perpendicular onto the sample, where the corresponding electromagnetic potential is given by  $\mathbf{A}(t) = (A_x \sin \omega t, A_y \cos \omega t)$ . The electromagnetic potential is introduced into the Hamiltonian by way of the minimal substitution, that is, by replacing the momentum  $k_j$  with the covariant momentum  $P_j \equiv \hbar k_j + eA_j$ .

Optical absorption is given by the optical conductivity

$$\begin{aligned}
 \sigma(\omega; \vartheta) &= \sigma_0 \int d\mathbf{k} \frac{f_{-}(\mathbf{k}) - f_{+}(\mathbf{k})}{\varepsilon_{-} - \varepsilon_{+}} |P_{\vartheta}(\mathbf{k})|^2 \\
 &\quad \times \delta[\varepsilon_{+}(\mathbf{k}) - \varepsilon_{-}(\mathbf{k}) - \hbar\omega], \quad (93)
 \end{aligned}$$

where we have set

$$\sigma_0 \equiv \frac{\pi e^2}{(2\pi)^2}. \quad (94)$$

We start with the optical matrix element between the initial and final states in the photo-emission process given by [19, 82–86]

$$P_i(\mathbf{k}) \equiv \hbar \langle \psi_{+}(\mathbf{k}) | v_{\mu} | \psi_{-}(\mathbf{k}) \rangle, \quad (95)$$

with the velocity

$$v_{\mu} = \frac{1}{\hbar} \frac{\partial H(\mathbf{k})}{\partial k_{\mu}}. \quad (96)$$

The optical matrix element of the elliptic polarization is given by

$$P_{\vartheta}(\mathbf{k}) = P_x(\mathbf{k}) \cos \vartheta + iP_y(\mathbf{k}) \sin \vartheta, \quad (97)$$

where  $\vartheta$  is the ellipticity of the injected beam, with  $0 < \vartheta < \pi$  for the right polarization and  $-\pi < \vartheta < 0$  for the left polarization.  $P_{\pi/4}(\mathbf{k})$  corresponds to the right circularly polarized light, and  $P_{-\pi/4}(\mathbf{k})$  corresponds to the left circularly polarized light.

In the following, we assume that the temperature is absolutely zero. The optical matrix element for the elliptic polarized light is expanded as

$$\begin{aligned} & |P_\vartheta(\mathbf{k})|^2 \\ &= |P_x(\mathbf{k})|^2 \cos^2 \vartheta + |P_y(\mathbf{k})|^2 \sin^2 \vartheta \\ &+ i [P_x^*(\mathbf{k})P_y(\mathbf{k}) - P_y^*(\mathbf{k})P_x(\mathbf{k})] \sin \vartheta \cos \vartheta. \end{aligned} \quad (98)$$

By using the Hellmann-Feynman theorem

$$\begin{aligned} & \langle \psi_m(\mathbf{k}) | v_\mu | \psi_n(\mathbf{k}) \rangle \\ &= \frac{1}{\hbar} (\varepsilon_n(\mathbf{k}) - \varepsilon_m(\mathbf{k})) \langle \psi_m(\mathbf{k}) | \partial_{k_\mu} | \psi_n(\mathbf{k}) \rangle \end{aligned} \quad (99)$$

for  $m \neq n$ , we have

$$\begin{aligned} & \frac{|P_\mu(\mathbf{k})|^2}{(\varepsilon_n(\mathbf{k}) - \varepsilon_m(\mathbf{k}))^2} \\ &= \hbar^2 \langle \psi_-(\mathbf{k}) | v_\mu | \psi_+(\mathbf{k}) \rangle \langle \psi_+(\mathbf{k}) | v_\mu | \psi_-(\mathbf{k}) \rangle \\ &= -\Delta^2(\mathbf{k}) \langle \partial_{k_\mu} \psi_-(\mathbf{k}) | \psi_+(\mathbf{k}) \rangle \langle \psi_+(\mathbf{k}) | \partial_{k_\mu} \psi_-(\mathbf{k}) \rangle \\ &= -\Delta^2(\mathbf{k}) g_-^{\mu\mu}(\mathbf{k}), \end{aligned} \quad (100)$$

with  $\mu = x, y$ , and

$$\begin{aligned} & i \frac{[P_y^*(\mathbf{k})P_x(\mathbf{k}) - P_x^*(\mathbf{k})P_y(\mathbf{k})]}{(\varepsilon_n(\mathbf{k}) - \varepsilon_m(\mathbf{k}))^2} \\ &= i\Delta^2(\mathbf{k}) [\langle \psi_-(\mathbf{k}) | v_y | \psi_+(\mathbf{k}) \rangle \langle \psi_+(\mathbf{k}) | v_x | \psi_-(\mathbf{k}) \rangle \\ &\quad - \langle \psi_-(\mathbf{k}) | v_x | \psi_+(\mathbf{k}) \rangle \langle \psi_+(\mathbf{k}) | v_y | \psi_-(\mathbf{k}) \rangle] \\ &= i\Delta^2(\mathbf{k}) [\mathcal{F}_{-+}^{xy}(\mathbf{k}) - \mathcal{F}_{+-}^{yx}(\mathbf{k})] = \Delta^2(\mathbf{k}) \Omega_-^{xy}(\mathbf{k}). \end{aligned} \quad (101)$$

Then, the optical conductivity is rewritten by using the components of the quantum geometric tensor[19] as

$$\sigma(\omega; \vartheta) = \hbar\omega\sigma_0 \int d\mathbf{k} f(\mathbf{k}) G(\mathbf{k}; \vartheta) \delta[\varepsilon_+(\mathbf{k}) - \varepsilon_-(\mathbf{k}) - \hbar\omega], \quad (102)$$

with

$$G(\mathbf{k}; \vartheta) \equiv g_-^{xx}(\mathbf{k}) \cos^2 \vartheta + g_-^{yy}(\mathbf{k}) \sin^2 \vartheta + \Omega_-^{xy}(\mathbf{k}) \sin \vartheta \cos \vartheta. \quad (103)$$

We study the optical absorption of the Dirac Hamiltonian (79) at the band edge  $\hbar\omega = \varepsilon_+(\mathbf{0}) - \varepsilon_-(\mathbf{0})$ . It is simply given by

$$\begin{aligned} \frac{\sigma(\omega; \vartheta)}{\hbar\omega\sigma_0} &= G(\mathbf{0}; \vartheta) \\ &= g_-^{xx}(\mathbf{0}) \cos^2 \vartheta + g_-^{yy}(\mathbf{0}) \sin^2 \vartheta + \Omega_-^{xy}(\mathbf{0}) \sin \vartheta \cos \vartheta \\ &= \frac{(\hbar v_F)^2}{m^2} \left( 1 - \frac{\xi}{2} \sin 2\vartheta \right), \end{aligned} \quad (104)$$

where we have used quantum metrics

$$g_-^{xx}(\mathbf{0}) = g_-^{yy}(\mathbf{0}) = \frac{(\hbar v_F)^2}{m^2}, \quad (105)$$

and the Berry curvature

$$\Omega_-^{xy}(\mathbf{0}) = -\xi \frac{(\hbar v_F)^2}{m^2}. \quad (106)$$

It shows elliptic dichroism, where there is no absorption

$$\sigma(\omega; \vartheta) = 0 \quad (107)$$

for  $\vartheta = \xi\pi/4$ . Namely, the right or left circularly polarized light is selectively absorbed depending on  $\xi$ .

#### D. Sum rule

The optical conductivity is given by

$$\begin{aligned} \sigma_D^{\mu\nu}(\omega; \vartheta) &= \sigma_0 \int d\mathbf{k} \frac{f_-(\mathbf{k}) - f_+(\mathbf{k})}{\varepsilon_- - \varepsilon_+} \\ &\quad \times \langle \psi_-(\mathbf{k}) | v_\mu | \psi_+(\mathbf{k}) \rangle \langle \psi_+(\mathbf{k}) | v_\nu | \psi_-(\mathbf{k}) \rangle \\ &\quad \times \delta[\varepsilon_+(\mathbf{k}) - \varepsilon_-(\mathbf{k}) - \hbar\omega]. \end{aligned} \quad (108)$$

By using the Hellmann-Feynman theorem, it is rewritten as

$$\begin{aligned} \sigma_D^{\mu\nu}(\omega; \vartheta) &= \omega\sigma_0 \int d\mathbf{k} f_{-+}(\mathbf{k}) a_{-+}^{\mu}(\mathbf{k}) a_{+-}^{\nu}(\mathbf{k}) \\ &\quad \times \delta[\varepsilon_+(\mathbf{k}) - \varepsilon_-(\mathbf{k}) - \hbar\omega], \end{aligned} \quad (109)$$

where  $f_{-+}(\mathbf{k}) \equiv f_-(\mathbf{k}) - f_+(\mathbf{k})$ . With the use of Eq.(19), the optical conductivity is related to the quantum geometric tensor,

$$\begin{aligned} \sigma_D^{\mu\nu}(\omega; \vartheta) &= \frac{\omega}{\hbar} \sigma_0 \int d\mathbf{k} f_{-+}(\mathbf{k}) \mathcal{F}_{-+}^{\mu\nu} \\ &\quad \times \delta[\varepsilon_+(\mathbf{k}) - \varepsilon_-(\mathbf{k}) - \hbar\omega]. \end{aligned} \quad (110)$$

Then, we arrive at a relation between the quantum geometric tensor and the conductivity[10, 12]

$$\int_0^\infty \frac{d\omega}{\omega} \sigma_D^{\mu\nu}(\omega) = \frac{\pi e^2}{\hbar(2\pi)^2} \int \mathcal{F}_{-+}^{\mu\nu} d\mathbf{k}, \quad (111)$$

where  $\sigma_D^{\mu\nu}(\omega)$  denotes the dissipative (absorptive) component of the optical conductivity.

The real part reads[10]

$$\int_0^\infty \frac{d\omega}{\omega} \text{Re} \sigma_D^{\mu\nu}(\omega) = \frac{\pi e^2}{\hbar(2\pi)^2} \int g_{-+}^{\mu\nu} d\mathbf{k}. \quad (112)$$

The imaginary part is related to the Chern number,

$$\int_0^\infty \frac{d\omega}{\omega} \text{Im} \sigma_D^{\mu\nu}(\omega) = \frac{\pi e^2}{\hbar(2\pi)^2} \int \frac{\Omega_-^{xy}}{2} d\mathbf{k} = \frac{e^2}{2\hbar} \mathcal{C}_-, \quad (113)$$

where we have used the TKNN formula

$$\sigma_D^{xy}(0) \equiv \sigma_{xy} = \frac{e^2}{\hbar} \mathcal{C}_-, \quad (114)$$

and the Kramers-Kronig relation. This relates the real and imaginary parts of the optical Hall conductivity

$$\int_0^\infty \frac{d\omega}{\omega} \text{Im} \sigma_D^{\mu\nu}(\omega) = \frac{\pi}{2} \sigma_{xy}(0). \quad (115)$$

## E. Bulk photovoltaic effects

Photovoltaic currents are generated under photo-irradiation, which will be useful for solar cell technologies. A  $p$ - $n$  junction presents a conventional way to generate photocurrent. On the other hand, the bulk photovoltaic photocurrent generation presents another way without using a junction[87–91]. The injection current[6, 9, 33, 89, 90, 92–95] and the shift current[6, 9, 33, 88–90, 92–94, 96–101] are prominent, which are second order bulk photovoltaic currents.

The current density  $J^\mu$  along the  $\mu$  direction induced by the applied electric field  $E_x$  along the  $x$  direction is expanded in a power series of  $E_x$  as

$$J^\mu = \sum_{\ell=1}^{\infty} \sigma^{\mu;x^\ell} E_x^\ell \equiv \sum_{\ell=1}^{\infty} J^{\mu;x^\ell}, \quad (116)$$

where  $\mu = x, y, z$ . We refer to  $J^{\mu;x^\ell} \equiv \sigma^{\mu;x^\ell} E_x^\ell$  as the  $\ell$ -th order current, where  $\sigma^{\mu;x^\ell}$  is the  $\ell$ -th order conductivity. If there is inversion symmetry in the system, the even order conductivities with even  $\ell$  are prohibited, because

$$J^\mu \mapsto -J^\mu, \quad E_x \mapsto -E_x \quad (117)$$

under inversion symmetry.

The second order response has a form

$$J^{\mu;x^2}(\omega_1 + \omega_2) = \sigma^{\mu;x^2}(\omega_1 + \omega_2; \omega_1, \omega_2) E_x(\omega_1) E_x(\omega_2). \quad (118)$$

We investigate the direct current generation,

$$J^{\mu;x^2}(0) = \sigma^{\mu;x^2}(0; \omega, -\omega) E_x(\omega) E_x(-\omega). \quad (119)$$

In the following, we use the abbreviation  $J^{\mu;x^2} \equiv J^{\mu;x^2}(0)$  and  $\sigma^{\mu;x^2}(\omega) \equiv \sigma^{\mu;x^2}(0; \omega, -\omega)$ .

The conductivity of the injection current is in general given by the formula[6, 9, 33, 89, 90, 92–95]

$$\sigma_{\text{inject}}^{\mu;x^2} = -\tau \frac{2\pi e^3}{\hbar^2} \sum_{n,m} \int d\mathbf{k} f_{nm} \Delta_{mn}^\mu a_{nm}^x a_{mn}^x \delta(\omega_{mn} - \omega), \quad (120)$$

where  $\tau$  is the relaxation time,  $f_{nm} = f_n - f_m$  with the Fermi distribution function  $f_n$  for the band  $n$ ,  $a_{nm}^x$  is the Wilczek-Zee connection,  $\omega_{nm} \equiv (\varepsilon_n - \varepsilon_m)/\hbar$ , and

$$\Delta_{mn}^\mu = v_m^\mu - v_n^\mu \quad (121)$$

is the difference of the velocities defined by

$$v_m^\mu = \frac{1}{\hbar} \langle m | \partial_{k_\mu} H | m \rangle \quad (122)$$

with the Hamiltonian  $H$ . The injection current is induced when the velocities are different ( $\Delta_{mn}^\mu \neq 0$ ) between the conduction band  $n$  and the valence band  $m$  along the  $\mu$  direction. The derivation is shown in Appendix D 1.

The shift current is in general given by the formula[6, 9, 33, 89, 90, 92–94, 96–101]

$$\sigma_{\text{shift}}^{\mu;x^2} = -\frac{\pi e^3}{\hbar^2} \sum_{n,m} \int d\mathbf{k} f_{nm} R_{mn}^{\mu,x} a_{nm}^x a_{mn}^x \delta(\omega_{mn} - \omega), \quad (123)$$

where

$$R_{mn}^{\mu,x} = a_{mm}^x - a_{nn}^x + i\partial_{k_\mu} \log a_{mn}^x \quad (124)$$

is the shift vector[90]. The shift vector is gauge invariant although the Wilczek-Zee connection is not gauge invariant. The shift vector describes the difference of the mean position of the Wannier function between two bands  $m$  and  $n$ . The integrand in Eq.(124) is rewritten as

$$R_{mn}^{\mu,x} a_{nm}^x a_{mn}^x = i a_{mn}^x a_{nm,\mu}^x, \quad (125)$$

where we have defined the covariant derivative,

$$\nabla_{k_\mu} a_{nm}^x \equiv a_{nm,\mu}^x \equiv \frac{\partial a_{nm}^x}{\partial k_\mu} - i a_{nm}^x (a_{nn}^x - a_{mm}^x). \quad (126)$$

The shift current is induced when the mean positions are different ( $R_{mn}^{\mu,x} \neq 0$ ) between the conduction band  $n$  and the valence band  $m$ . The derivation is shown in Appendix D 2.

In the following, we concentrate on the longitudinal conductivities by setting  $\mu = x$ .

The injection current is rewritten in terms of the quantum metric[6, 9, 34] as

$$\sigma_{\text{inject}}^{x;x^2} = -\tau \frac{2\pi e^3}{\hbar^2} \int d\mathbf{k} f_{-+} \Delta_{+-}^x g_{-+}^{xx} \delta(\omega_{+-} - \omega). \quad (127)$$

while the shift current is rewritten in terms of the quantum metric[33, 34] as

$$\sigma_{\text{shift}}^{x;x^2} = -\frac{\pi e^3}{\hbar^2 V} \int d\mathbf{k} f_{-+} R_{+-}^{x,x} g_{-+}^{xx} \delta(\omega_{+-} - \omega). \quad (128)$$

## F. Nonlinear conductivity

The second-order nonlinear conductivity  $\sigma^{\mu\nu;\rho}$  is expanded in terms of the electron relaxation time  $\tau$  as[27]

$$\sigma^{\mu\nu;\rho} = \sigma_{\text{NLDrude}}^{\mu\nu;\rho} + \sigma_{\text{Dipole}}^{\mu\nu;\rho} + \sigma_{\text{Metric}}^{\mu\nu;\rho}, \quad (129)$$

where

$$\sigma_{\text{Metric}}^{\mu\nu;\rho} \propto \tau^0, \quad \sigma_{\text{Dipole}}^{\mu\nu;\rho} \propto \tau, \quad \sigma_{\text{NLDrude}}^{\mu\nu;\rho} \propto \tau^2. \quad (130)$$

First,  $\sigma_{\text{NLDrude}}^{\mu\nu;\rho}$  is the nonlinear Drude conductivity[102, 103],

$$\sigma_{\text{NLDrude}}^{\mu\nu;\rho} = -\frac{e^3 \tau^2}{\hbar^3} \sum_n \int d\mathbf{k} f_n \frac{\partial^3 \varepsilon_n}{\partial k_\mu \partial k_\nu \partial k_\rho}. \quad (131)$$

It is also an extrinsic nonlinear conductivity.

Second,  $\sigma_{\text{Dipole}}^{\mu\nu;\rho}$  is the nonlinear transverse conductivity induced by the Berry curvature dipole (BCD)[20],

$$\sigma_{\text{Dipole}}^{\mu\nu;\rho} = -\frac{e^3\tau}{\hbar^2} \sum_n \int d\mathbf{k} f_n \left( \frac{\partial \Omega_n^{\nu\rho}}{\partial k_\mu} + \frac{\partial \Omega_n^{\mu\rho}}{\partial k_\nu} \right). \quad (132)$$

It is an extrinsic nonlinear conductivity, since it vanishes as  $\tau \rightarrow 0$ .

Third, only the term  $\sigma_{\text{Metric}}^{\mu\nu;\rho}$  survives in the dirty limit  $\tau \rightarrow 0$ , which is the intrinsic nonlinear conductivity. It is the quantum-metric induced nonlinear conductivity. There are still debates[104, 105] on the coefficients of the quantum-metric induced nonlinear conductivity.

(i) The Luttinger-Kohn approach[27] gives

$$\begin{aligned} & \sigma_{\text{Metric}}^{\mu\nu;\rho} \\ &= -\frac{e^3}{\hbar} \sum_n \int d\mathbf{k} f_n \left( 2 \frac{\partial G_n^{\mu\nu}}{\partial k_\rho} - \frac{1}{2} \left( \frac{\partial G_n^{\nu\rho}}{\partial k_\mu} + \frac{\partial G_n^{\mu\rho}}{\partial k_\nu} \right) \right), \end{aligned} \quad (133)$$

where  $G_n^{ab}$  is the band-energy normalized quantum metric or the Berry connection polarizability. It is given as[22, 24, 27, 106–108]

$$G_n^{\mu\nu} = 2\text{Re} \sum_{m \neq n} \frac{a_{nm}^\mu(\mathbf{k}) a_{mn}^\nu(\mathbf{k})}{\varepsilon_n(\mathbf{k}) - \varepsilon_m(\mathbf{k})}. \quad (134)$$

(ii) The wave packet dynamics approach[107] gives

$$\begin{aligned} & \sigma_{\text{Metric}}^{\mu\nu;\rho} \\ &= -\frac{e^3}{\hbar} \sum_n \int d\mathbf{k} f_n \left( \frac{\partial G_n^{\mu\nu}}{\partial k_\rho} - \frac{1}{2} \left( \frac{\partial G_n^{\nu\rho}}{\partial k_\mu} + \frac{\partial G_n^{\mu\rho}}{\partial k_\nu} \right) \right). \end{aligned} \quad (135)$$

(iii) The quantum kinetics approach[24] gives

$$\begin{aligned} & \sigma_{\text{Metric}}^{\mu\nu;\rho} \\ &= -\frac{e^3}{\hbar} \sum_n \int d\mathbf{k} f_n \left( \frac{1}{2} \frac{\partial G_n^{\mu\nu}}{\partial k_\rho} - \left( \frac{\partial G_n^{\nu\rho}}{\partial k_\mu} + \frac{\partial G_n^{\mu\rho}}{\partial k_\nu} \right) \right). \end{aligned} \quad (136)$$

(iv) The intrinsic Ohmic conductivity[109] gives

$$\begin{aligned} & \sigma_{\text{Metric}}^{\mu\nu;\rho} \\ &= \frac{e^3}{\hbar} \sum_n \int d\mathbf{k} f_n \left( \frac{\partial G_n^{\mu\nu}}{\partial k_\rho} + \frac{\partial G_n^{\nu\rho}}{\partial k_\mu} + \frac{\partial G_n^{\mu\rho}}{\partial k_\nu} \right). \end{aligned} \quad (137)$$

#### IV. ZEEMAN QUANTUM GEOMETRY FOR MOMENTUM AND SPIN

So far, we have considered quantum geometry for momentum translation. However, there is also a spin degree of freedom for electrons. It is important to study the effect of spin rotation in the context of spintronics. This is

achieved by generalizing quantum geometry to Zeeman quantum geometry[110–113], where local spin rotation between two adjacent wave functions is also taken into account.

The Zeeman quantum geometric tensor  $g_{nm}^{\mu\nu}$  is defined by the quantum distance  $ds_{\text{HS}}$  for the infinitesimal translation  $d\mathbf{k}$  of the momentum and infinitesimal spin rotation  $d\theta$  as[110–113]

$$ds_{\text{HS}}(\mathbf{k}) \equiv \sqrt{1 - |\langle \psi_n(\mathbf{k}) | U_{d\theta} U_{d\mathbf{k}} | \psi_n(\mathbf{k}) \rangle|^2}, \quad (138)$$

where

$$U_{d\theta} \equiv e^{-\frac{i}{2}d\theta \cdot \sigma}, \quad U_{d\mathbf{k}} \equiv e^{-id\mathbf{k} \cdot \mathbf{r}} \quad (139)$$

are the generators of the spin angular momentum  $d\theta$  and the momentum  $d\mathbf{k}$ . The Zeeman quantum geometric tensor  $z_{nm}^{\mu\nu}$  and the spin quantum geometric tensor  $s_{nm}^{\mu\nu}$  are given by

$$\begin{aligned} (ds_{\text{HS}})^2 &= \sum_{\mu\nu} \sum_{n \neq m} (\mathcal{F}_{nm}^{\mu\nu} dk_\mu dk_\nu + \frac{s_{nm}^{\mu\nu}}{4} d\theta_\mu d\theta_\nu \\ &+ \frac{z_{nm}^{\mu\nu} + z_{mn}^{\mu\nu}}{2} dk_\mu d\theta_\nu), \end{aligned} \quad (140)$$

where

$$\mathcal{F}_{nm}^{\mu\nu} \equiv a_{nm}^\mu a_{mn}^\nu \quad (141)$$

is the quantum geometric tensor,

$$s_{nm}^{\mu\nu} \equiv s_{nm}^\mu s_{mn}^\nu \quad (142)$$

is the spin quantum geometric tensor, and

$$z_{nm}^{\mu\nu} \equiv a_{nm}^\mu s_{mn}^\nu \quad (143)$$

is the Zeeman quantum geometric tensor, where we have defined the expectation value of the spin operator,

$$s_{nm}^\mu \equiv \langle \psi_n(\mathbf{k}) | \sigma_\mu | \psi_n(\mathbf{k}) \rangle. \quad (144)$$

The derivation from Eq.(140)~Eq.(143) is shown in Appendix E.

As in the case of the quantum metric and the Berry curvature, the Zeeman quantum metric  $Q_{nm}^{\mu\nu}$  is defined by the real part of the Zeeman quantum geometric tensor,

$$Q_{nm}^{\mu\nu} \equiv \text{Re} z_{nm}^{\mu\nu} = (a_{nm}^\mu s_{mn}^\nu + a_{mn}^\mu s_{nm}^\nu) / 2, \quad (145)$$

and the Zeeman Berry curvature  $\mathcal{Z}_{nm}^{\mu\nu}$  by the imaginary part of the Zeeman quantum geometric tensor,

$$\mathcal{Z}_{nm}^{\mu\nu} \equiv 2\text{Im} z_{nm}^{\mu\nu} = i(a_{nm}^\mu s_{mn}^\nu - a_{mn}^\mu s_{nm}^\nu). \quad (146)$$

We also define the spin quantum metric  $S_{nm}^{\mu\nu}$  by the real part of the spin quantum geometric tensor,

$$S_{nm}^{\mu\nu} \equiv \text{Re} s_{nm}^{\mu\nu} \equiv (s_{nm}^\mu s_{mn}^\nu + s_{mn}^\mu s_{nm}^\nu) / 2, \quad (147)$$

and the spin Berry curvature  $\mathcal{A}_{nm}^{\mu\nu}$  by

$$\mathcal{A}_{nm}^{\mu\nu} \equiv 2\text{Im} s_{nm}^{\mu\nu} \equiv i(s_{nm}^\mu s_{mn}^\nu - s_{mn}^\mu s_{nm}^\nu). \quad (148)$$

### A. Responses originated from the Zeeman geometry

In the linear response theory, we obtain the response of the current  $J^{\mu;\nu}$  or the spin polarization  $S^{\mu;\nu}$  by applying electric field  $E^\nu$  or magnetic field  $B^\nu$ .

We apply alternating electric field  $E^\nu(t)$  and alternating magnetic field  $B^\nu(t)$ ,

$$E^\nu(t) = \frac{1}{2} E^\nu \sum_{\omega_1=\pm\omega} e^{-i\omega_1 t}, \quad (149)$$

$$B^\nu(t) = \frac{1}{2} B^\nu \sum_{\omega_1=\pm\omega} e^{-i\omega_1 t}. \quad (150)$$

The Hamiltonian for the external fields is given by

$$H_1 = E^\nu(t) a^\nu - g\mu_B B^\nu(t) \sigma^\nu. \quad (151)$$

We solve the quantum Liouville equation

$$i\frac{\partial \rho}{\partial t} = [H', \rho] \quad (152)$$

with  $H' = H + H_1$ , where  $H$  is the non-perturbed Hamiltonian.

The first-order solution of the density matrix is given by[111]

$$\begin{aligned} \rho_{mn}^{\mu\nu} = & \frac{1}{2} \sum_{\omega_1=\pm\omega} [i\delta_{mn}\partial_{k_\mu} f_m + f_{nm} a_{mn}^\mu] \frac{E^\nu e^{-i\omega_1 t}}{\hbar\omega_1 - \varepsilon_{mn} + i\eta} \\ & - \frac{g\mu_B}{2} \sum_{\omega_1=\pm\omega} \frac{f_{nm} s_{mn}^\mu B^\nu e^{-i\omega_1 t}}{\hbar\omega_1 - \varepsilon_{mn} + i\eta}, \end{aligned} \quad (153)$$

where  $f_{nm} \equiv f_n - f_m$  and  $\varepsilon_{mn} \equiv \varepsilon_m - \varepsilon_n$ .

In the linear response theory, the current  $J^{\mu;\nu}$  is given by

$$J^{\mu;\nu} = \sum_{nm} \int d\mathbf{k} v_{nm}^\mu \rho_{mn}^{\mu\nu}, \quad (154)$$

where  $v_{nm}^\mu$  is the velocity operator. By using the Hellmann–Feynman theorem, it is rewritten as

$$v_{nm}^\mu = i\varepsilon_{nm} a_{nm}^\mu. \quad (155)$$

On the other hand, the spin  $S^{\mu;\nu}$  polarization is given by

$$S^{\mu;\nu} = \sum_{nm} \int d\mathbf{k} s_{nm}^\mu \rho_{mn}^{\mu\nu}. \quad (156)$$

There are four types of responses,  $J^{\mu;\nu}/E^\nu$ ,  $J^{\mu;\nu}/B^\nu$ ,  $S^{\mu;\nu}/E^\nu$  and  $S^{\mu;\nu}/B^\nu$ , where  $J^{\mu;\nu}/E^\nu$  and  $S^{\mu;\nu}/B^\nu$  are direct responses, while  $J^{\mu;\nu}/B^\nu$  and  $S^{\mu;\nu}/E^\nu$  are cross responses.

(i) The current  $J^{\mu;\nu}$  is induced by electric field  $E^\nu$  as[110]

$$\begin{aligned} & \frac{J^{\mu;\nu}}{E^\nu} \\ & = \int d\mathbf{k} \sum_{n>m} f_{nm} \left[ \Omega_{nm}^{\mu\nu} \cos \omega t + 2g_{nm}^{\mu\nu} \frac{\omega \sin \omega t}{\varepsilon_{mn}} \right]. \end{aligned} \quad (157)$$

The first term represents the Hall current generated by the Berry curvature  $\Omega_{nm}^{\mu\nu}$ . The quantum metric  $g_{nm}^{\mu\nu}$  in the second term appears as an oscillating response[114].

(ii) The current  $J^{\mu;\nu}$  is induced by magnetic field  $B^\nu$  as[111]

$$\begin{aligned} & \frac{J^{\mu;\nu}}{B^\nu} \\ & = g\mu_B \int d\mathbf{k} \sum_{n>m} f_{nm} \left[ \mathcal{Z}_{nm}^{\mu\nu} \cos \omega t + 2Q_{nm}^{\mu\nu} \frac{\omega \sin \omega t}{\varepsilon_{mn}} \right]. \end{aligned} \quad (158)$$

The Zeeman quantum geometric tensor  $\mathcal{Z}_{nm}^{\mu\nu}$  contributes to the cross response between the magnetic field  $B^\nu$  and the current  $J^{\mu;\nu}$ , where  $J^{\mu;\nu}$  is called the intrinsic gyrotropic magnetic current  $J^{\mu;\nu}$ . The Zeeman quantum metric  $Q_{nm}^{\mu\nu}$  in the second term appears as an oscillating response.

(iii) Spin polarization  $S^{\mu;\nu}$  is induced by electric field  $E^\nu$  as[110]

$$\begin{aligned} & \frac{S^{\mu;\nu}}{E^\nu} \\ & = - \int d\mathbf{k} \sum_{n>m} f_{nm} \left[ \frac{2Q_{nm}^{\mu\nu}}{\varepsilon_{mn}} \cos \omega t + \mathcal{Z}_{nm}^{\mu\nu} \frac{\omega \sin \omega t}{\varepsilon_{mn}^2} \right]. \end{aligned} \quad (159)$$

The Zeeman quantum metric  $Q_{nm}^{\mu\nu}$  contributes to the cross response between the electric field  $E^\nu$  and the spin polarization  $S^{\mu;\nu}$ . The Zeeman quantum geometric tensor  $\mathcal{Z}_{nm}^{\mu\nu}$  in the second term appears as an oscillating response.

(iv) Spin polarization  $S^{\mu;\nu}$  is also induced by magnetic field  $B^\nu$  as

$$\begin{aligned} & \frac{S^{\mu;\nu}}{B^\nu} \\ & = g\mu_B \int d\mathbf{k} \sum_{n>m} f_{nm} \left[ \frac{\mathcal{S}_{nm}^{\mu\nu}}{\varepsilon_{mn}} \cos \omega t + 2\mathcal{A}_{nm}^{\mu\nu} \frac{\omega \sin \omega t}{\varepsilon_{mn}^2} \right]. \end{aligned} \quad (160)$$

It is interesting that there may be off-diagonal response if  $\mathcal{S}_{nm}^{\mu\nu}$  or  $\mathcal{A}_{nm}^{\mu\nu}$  has off-diagonal components. Detailed derivations of Eqs.(157), (158), (159) and (160) are given in Appendix F.

We may call the first terms in Eqs.(157), (158), (159) and (160) the static terms and the second terms the dynamic terms, because the second terms vanish for  $\omega = 0$ .

### B. Zeeman Quantum Geometry for two-band systems

We consider the two-band system (40) with the index  $n = \pm$ . The simple relations for the Zeeman quantum metric are derived as

$$\mathcal{Z}_{+-}^{\mu\nu} = -\mathcal{Z}_{-+}^{\mu\nu} = \frac{\partial n_\nu}{\partial k_\mu}. \quad (161)$$

Two or three components of  $\mathbf{n}$  should be nonzero for nonzero  $\mathcal{Z}_{+-}^{\mu\nu}$ . In general, we have  $\mathcal{Z}_{+-}^{\mu\nu} \neq \mathcal{Z}_{+-}^{\nu\mu}$ .

The Zeeman Berry curvature is derived as

$$\mathcal{Q}_{+-}^{\mu\nu} = \frac{1}{2} \sum_{\rho\sigma} \varepsilon_{\nu\rho\sigma} n_\rho \frac{\partial n_\sigma}{\partial k_\mu}, \quad (162)$$

Two or three components of  $\mathbf{n}$  should be nonzero for nonzero  $\mathcal{Q}_{+-}^{\mu\nu}$ .

The spin quantum metric is

$$\mathcal{S}_{+-}^{\mu\nu} = \delta_{\mu\nu} - n_\mu n_\nu, \quad (163)$$

while the spin Berry curvature is

$$\mathcal{A}_{+-}^{\mu\nu} = -2 \sum_{\rho} \varepsilon_{\mu\nu\rho} n_\rho. \quad (164)$$

They are defined even when only a single component of  $\mathbf{n}$  is nonzero.

### C. Rashba system

As an example of the two-band system, we consider the Rashba system described by

$$H(\mathbf{k}) = \frac{\hbar^2 \mathbf{k}^2}{2m} + \lambda (\mathbf{k} \times \boldsymbol{\sigma})_z + B \sigma_z, \quad (165)$$

where  $\lambda$  is the strength of the Rashba interaction and  $B$  is static magnetic field applied perpendicularly to the plane.

The energy is given by

$$E_\chi = \frac{\hbar^2 k^2}{2m} + \chi \sqrt{\lambda^2 k^2 + B^2} \quad (166)$$

for the lower band with  $\chi = -1$  and for the upper band with  $\chi = 1$ . The Fermi surface is given by

$$k_\eta^\chi = \sqrt{m} \sqrt{\mu + m\lambda^2 + \eta \sqrt{m^2 \lambda^4 + 2\mu m \lambda^2 + B^2}}, \quad (167)$$

where  $\eta = -1$  describes the inner Fermi surface and  $\eta = 1$  describes the outer Fermi surface.

The Berry curvature is given by

$$\Omega^{xy} = -\frac{B\lambda^2}{2(\lambda^2 k^2 + B^2)^{3/2}}, \quad (168)$$

while the quantum metrics are given by

$$g_{+-}^{xx} = \frac{\lambda^2 (\lambda^2 k_y^2 + B^2)}{2(\lambda^2 k^2 + B^2)^2}, \quad (169)$$

$$g_{+-}^{xy} = g_{+-}^{yx} = \frac{-\lambda^4 k_x k_y}{2(\lambda^2 k^2 + B^2)^2}, \quad (170)$$

$$g_{+-}^{yy} = \frac{\lambda^2 (\lambda^2 k_x^2 + B^2)}{2(\lambda^2 k^2 + B^2)^2}. \quad (171)$$

There is no contribution from the quantum metric  $g_{+-}^{xy}$  in the Hall current (157) because  $g_{+-}^{xy} \propto \sin 2\phi$  leads to  $\int g_{+-}^{xy} d\phi = 0$ .

The Zeeman Berry curvatures are calculated as

$$\mathcal{Z}_{+-}^{xx} = \frac{\partial n_x}{\partial k_x} = \frac{\lambda^3 k_x k_y}{(\lambda^2 k^2 + B^2)^{3/2}}, \quad (172)$$

$$\mathcal{Z}_{+-}^{xy} = \frac{\partial n_y}{\partial k_x} = \frac{\lambda (\lambda^2 k_y^2 + B^2)}{(\lambda^2 k^2 + B^2)^{3/2}}, \quad (173)$$

$$\mathcal{Z}_{+-}^{yx} = \frac{\partial n_x}{\partial k_y} = -\frac{\lambda (\lambda^2 k_x^2 + B^2)}{(\lambda^2 k^2 + B^2)^{3/2}}, \quad (174)$$

$$\mathcal{Z}_{+-}^{xz} = \frac{\partial n_z}{\partial k_x} = -\frac{\lambda^2 B k_x}{(\lambda^2 k^2 + B^2)^{3/2}}, \quad (175)$$

$$\mathcal{Z}_{+-}^{yz} = \frac{\partial n_z}{\partial k_y} = -\frac{\lambda^2 B k_y}{(\lambda^2 k^2 + B^2)^{3/2}}. \quad (176)$$

Only the Zeeman Berry curvature  $\mathcal{Z}_{+-}^{xy}$  contributes to a nonzero response because we have

$$\int \mathcal{Z}_{+-}^{xx} d\phi = \int \mathcal{Z}_{+-}^{xz} d\phi = \int \mathcal{Z}_{+-}^{yz} d\phi = 0. \quad (177)$$

We note that  $\mathcal{Z}_{+-}^{xx}$  and  $\mathcal{Z}_{+-}^{xy}$  are singular at  $k = 0$ , while  $\mathcal{Z}_{+-}^{xz}$  and  $\mathcal{Z}_{+-}^{yz}$  are zero for  $B = 0$ .

The static intrinsic gyrotropic magnetic current at zero temperature is calculated as

$$\begin{aligned} \frac{J^{x;y}}{B_y} &= g\mu_B \int d\mathbf{k} \sum_{n>m} f_{nm} \mathcal{Z}_{nm}^{xy} \\ &= g\mu_B \int_{k_-^x}^{k_+^x} k dk d\phi \frac{\lambda (\lambda^2 k_y^2 + B^2)}{(\lambda^2 k^2 + B^2)^{3/2}} \\ &= g\mu_B \sum_{\eta=\pm 1} \pi \lambda \frac{(k_\eta^x)^2}{\sqrt{\lambda^2 (k_\eta^x)^2 + B^2}}. \end{aligned} \quad (178)$$

The electric-field induced spin polarization at zero temperature is calculated as

$$\begin{aligned} \frac{S^{\mu;\nu}}{E^\nu} &= - \int d\mathbf{k} f_{+-} \mathcal{Z}_{+-}^{\nu\mu} \frac{\omega}{\varepsilon_{+-}^2} \sin(\omega t) \\ &= \sum_{\eta=\pm 1} \eta \pi \frac{\lambda (k_\eta^x)^2 + 4B^2}{(\lambda^2 (k_\eta^x)^2 + B^2)^{3/2}} \omega \sin(\omega t). \end{aligned} \quad (179)$$

The Zeeman quantum metrics are calculated as

$$\mathcal{Q}_{+-}^{xx} = \mathcal{Q}_{+-}^{yy} - \frac{B\lambda}{2(\lambda^2 k^2 + B^2)}, \quad (180)$$

$$\mathcal{Q}_{+-}^{xy} = \mathcal{Q}_{+-}^{yx} = 0, \quad (181)$$

$$\mathcal{Q}_{+-}^{xz} = -\frac{\lambda^2 k_y}{2(\lambda^2 k^2 + B^2)}. \quad (182)$$

Only the Zeeman quantum metric  $\mathcal{Q}_{+-}^{xx}$  contributes to a nonzero response because

$$\int \mathcal{Q}_{+-}^{xz} d\phi = 0. \quad (183)$$

The static spin polarization is induced by electric field as

$$\begin{aligned} \frac{S^{x;x}}{E^x} &= - \int d\mathbf{k} f_{+-} \frac{2Q_{+-}^{xx}}{\varepsilon_{+-}} \\ &= - \sum_{\eta=\pm 1} \frac{\eta\pi B}{\lambda \sqrt{\lambda^2 (k_\eta^x)^2 + B^2}}. \end{aligned} \quad (184)$$

The dynamic intrinsic gyrotropic magnetic current is obtained as

$$\begin{aligned} \frac{J^{x;x}}{B^x} &= g\mu_B \int d\mathbf{k} \sum_{n>m} f_{nm} 2Q_{nm}^{xx} \frac{\omega}{\varepsilon_{mn}} \sin \omega t \\ &= g\mu_B \sum_{\eta=\pm 1} \frac{\eta 2\pi B}{\lambda \sqrt{\lambda^2 (k_\eta^x)^2 + B^2}} \omega \sin \omega t. \end{aligned} \quad (185)$$

The spin Berry curvatures are calculated as

$$\mathcal{A}_{+-}^{xy} = -2n_z = -\frac{2B}{\sqrt{\lambda^2 k^2 + B^2}}, \quad (186)$$

$$\mathcal{A}_{+-}^{yz} = -2n_x = \frac{2\lambda k_y}{\sqrt{\lambda^2 k^2 + B^2}}, \quad (187)$$

$$\mathcal{A}_{+-}^{zx} = -2n_y = -\frac{2\lambda k_x}{\sqrt{\lambda^2 k^2 + B^2}}, \quad (188)$$

among which there is only nonzero contribution from  $\mathcal{A}_{+-}^{xy}$  because

$$\int d\phi \mathcal{A}_{+-}^{yz} = \int d\phi \mathcal{A}_{+-}^{zx} = 0. \quad (189)$$

Spin polarization is also induced by magnetic field as

$$\begin{aligned} \frac{S^{x;y}}{B^y} &= g\mu_B \int d\mathbf{k} f_{+-} 2\mathcal{A}_{+-}^{xy} \frac{\omega}{\varepsilon_{+-}^2} \sin \omega t \\ &= g\mu_B \sum_{\eta=\pm 1} \frac{\eta 4\pi B}{\lambda^2 \sqrt{\lambda^2 (k_\eta^x)^2 + B^2}}. \end{aligned} \quad (190)$$

The diagonal spin quantum metrics are calculated as

$$S_{+-}^{xx} = \frac{\lambda^2 k_x^2 + B^2}{\lambda^2 k^2 + B^2}, \quad (191)$$

$$S_{+-}^{yy} = \frac{\lambda^2 k_y^2 + B^2}{\lambda^2 k^2 + B^2}, \quad (192)$$

$$S_{+-}^{zz} = \frac{\lambda^2 k^2}{\lambda^2 k^2 + B^2}, \quad (193)$$

all of which contribute to nonzero responses.

The off-diagonal spin quantum metrics are calculated as

$$S_{+-}^{xy} = \frac{2\lambda^2 k_x k_y}{\lambda^2 k^2 + B^2}, \quad (194)$$

$$S_{+-}^{yz} = -\frac{2B\lambda k_x}{\lambda^2 k^2 + B^2}, \quad (195)$$

$$S_{+-}^{zx} = \frac{2B\lambda k_y}{\lambda^2 k^2 + B^2}, \quad (196)$$

all of which do not contribute to the off-diagonal responses because

$$\int \mathcal{S}_{+-}^{xy} d\phi = \int \mathcal{S}_{+-}^{yz} d\phi = \int \mathcal{S}_{+-}^{zx} d\phi = 0. \quad (197)$$

#### D. Non-Abelian Zeeman quantum geometry

We generalize the Zeeman quantum geometry to the multi-band systems. The Zeeman quantum geometric tensor  $g_{nm}^{\mu\nu}$  is defined by the quantum distance  $ds_{\text{HS}}$  for the infinitesimal translation  $d\mathbf{k}$  of the momentum as

$$(ds_{\text{HS}})^2 \equiv \sqrt{1 - |\langle \psi(\mathbf{k}) | U_{d\theta} U_{d\mathbf{k}} | \psi(\mathbf{k}) \rangle|^2}, \quad (198)$$

where  $|\psi(\mathbf{k})\rangle$  is given by Eq.(57),  $U_{d\theta}$  and  $U_{d\mathbf{k}}$  are given by Eq.(139). The Zeeman quantum geometric tensor is given by

$$\begin{aligned} (ds_{\text{HS}})^2 &= \sum_{\mu\nu} \sum_{n \neq m} g_{nm}^{\mu\nu} dk_\mu dk_\nu + \frac{s_{nm}^{\mu\nu}}{4} d\theta_\mu d\theta_\nu \\ &+ \frac{z_{nm}^{\mu\nu} + z_{mn}^{\mu\nu}}{2} dk_\mu d\theta_\nu, \end{aligned} \quad (199)$$

where

$$g_{nm}^{\mu\nu} \equiv \langle \partial_{k_\mu} \psi_n(\mathbf{k}) | (1 - P(\mathbf{k})) | \partial_{k_\mu} \psi_m(\mathbf{k}) \rangle \quad (200)$$

is the quantum metric,

$$s_{nm}^{\mu\nu} \equiv \langle \psi_n(\mathbf{k}) | \sigma_\mu (1 - P(\mathbf{k})) \sigma_\nu | \psi_m(\mathbf{k}) \rangle \quad (201)$$

is the spin geometric tensor, and

$$z_{nm}^{\mu\nu} \equiv \langle \partial_{k_\mu} \psi_n(\mathbf{k}) | (1 - P(\mathbf{k})) \sigma_\nu | \psi_m(\mathbf{k}) \rangle \quad (202)$$

is the Zeeman geometric tensor. The derivations are shown in Appendix G.

#### V. QUANTUM GEOMETRY FOR NON-HERMITIAN SYSTEMS

##### A. Open quantum system and non-Hermitian Hamiltonian

Non-Hermitian systems attract much attention. It is required that the Hamiltonian is Hermitian in quantum mechanics. However, it becomes non-Hermitian if we consider an open quantum system. An open quantum system is described by the Lindblad equation for the density matrix  $\rho$ ,

$$\frac{d\rho}{dt} = -\frac{i}{\hbar} [H, \rho] + \sum_k \gamma_k \left( L_k \rho L_k^\dagger - \frac{1}{2} \{ L_k^\dagger L_k, \rho \} \right), \quad (203)$$

where  $L_k$  is the Lindblad operator and  $\gamma$  is the strength of the dissipation. The Lindblad equation is rewritten in the form of

$$\frac{d\rho}{dt} = -\frac{i}{\hbar} \left( H_{\text{eff}} \rho - \rho H_{\text{eff}}^\dagger \right) + \sum_k \gamma_k L_k \rho L_k^\dagger, \quad (204)$$

where we have introduced a non-Hermitian Hamiltonian by

$$H_{\text{eff}} \equiv H - \frac{i\hbar}{2} \sum_{k\gamma} \gamma_k L_k^\dagger L_k. \quad (205)$$

## B. Non-Hermitian quantum geometry

Quantum geometry is generalized to non-Hermitian systems[75, 115–118], where  $H^\dagger \neq H$ . There are right and left eigenfunctions and eigenvalues,

$$H = \varepsilon_n^R |\psi_n^R(\mathbf{k})\rangle, \quad \langle \psi_n^L(\mathbf{k}) | H = \langle \psi_n^L(\mathbf{k}) | \varepsilon_n^L, \quad (206)$$

where

$$(|\psi_n^R(\mathbf{k})\rangle)^* \neq \langle \psi_n^L(\mathbf{k}) |$$

in general. However, it is straightforward to generalize quantum geometry to non-Hermitian case. The eigen functions are orthonormalized,

$$\langle \psi_n^L(\mathbf{k}) | \psi_n^R(\mathbf{k}') \rangle = \delta(\mathbf{k}, \mathbf{k}'). \quad (207)$$

If the target bands are  $N$ -fold degenerate, the right and left eigenfunctions are given by

$$|\psi^R(\mathbf{k})\rangle = \sum_{n=1}^N c_n^R |\psi_n^R(\mathbf{k})\rangle, \quad (208)$$

$$\langle \psi^L(\mathbf{k}) | = \sum_{n=1}^N c_n^L \langle \psi_n^L(\mathbf{k}) |. \quad (209)$$

The fidelity is defined by

$$F(\mathbf{k}, \mathbf{k}') \equiv \sqrt{\langle \psi^L(\mathbf{k}) | \psi^R(\mathbf{k}') \rangle \langle \psi^L(\mathbf{k}') | \psi^R(\mathbf{k}) \rangle}. \quad (210)$$

The Hilbert-Schmidt distance is defined by

$$d_{\text{HS}}(\mathbf{k}, \mathbf{k}') \equiv \sqrt{1 - F(\mathbf{k}, \mathbf{k}')^2}. \quad (211)$$

The quantum distance with the infinitesimal momentum translation  $d\mathbf{k}$  is given by

$$d_{\text{SHS}}(\mathbf{k}) \equiv \sqrt{1 - F(\mathbf{k}, \mathbf{k} + d\mathbf{k})^2} \quad (212)$$

with

$$F(\mathbf{k}) = \sqrt{\langle \psi^L(\mathbf{k}) | U_{d\mathbf{k}} |\psi^R(\mathbf{k})\rangle \langle \psi^L(\mathbf{k}) | U_{d\mathbf{k}}^{-1} |\psi^R(\mathbf{k})\rangle}, \quad (213)$$

where  $U_{d\mathbf{k}}$  is given by Eq.(5). The quantum distance for the infinitesimal momentum is expanded in terms of the quantum geometric tensor  $\mathcal{F}_n^{\mu\nu}$  as

$$(d_{\text{SHS}})^2 = \sum_{\mu\nu} \sum_{nm} \mathcal{F}_{nm}^{\mu\nu} dk_\mu dk_\nu, \quad (214)$$

The quantum geometric tensor is

$$\mathcal{F}_{nm}^{\mu\nu}(\mathbf{k}) = \langle \partial_{k_\mu} \psi_n^L(\mathbf{k}) | (1 - P(\mathbf{k})) | \partial_{k_\nu} \psi_m^R(\mathbf{k}) \rangle \quad (215)$$

with the projection operator

$$P(\mathbf{k}) \equiv \sum_{n=1}^N |\psi_n^R(\mathbf{k})\rangle \langle \psi_n^L(\mathbf{k})|. \quad (216)$$

The quantum metric is the real part of the quantum geometric tensor,

$$g_{nm}^{\mu\nu} \equiv \text{Re} \mathcal{F}_{nm}^{\mu\nu} = \frac{\mathcal{F}_{mn}^{\mu\nu}(\mathbf{k}) + (\mathcal{F}_{mn}^{\mu\nu}(\mathbf{k}))^*}{2}, \quad (217)$$

while the Berry curvature is the imaginary part of the quantum geometric tensor,

$$\Omega_{nm}^{\mu\nu} \equiv 2\text{Im} \mathcal{F}_{nm}^{\mu\nu} = i(\mathcal{F}_{mn}^{\mu\nu}(\mathbf{k}) - (\mathcal{F}_{mn}^{\mu\nu}(\mathbf{k}))^*). \quad (218)$$

The Wilczek-Zee connection is given by

$$a_{nm}^\mu(\mathbf{k}) \equiv -i \langle \psi_n^L | \partial_{k_\mu} | \psi_{nm}^R \rangle, \quad (219)$$

while the Berry curvature is given by[120, 122–124, 126]

$$\Omega_n^{\mu\nu}(\mathbf{k}) = \nabla \times \mathbf{a}_n(\mathbf{k}) - i \sum_{n'} [a_{nn'}^\mu, a_{n'm}^\nu]. \quad (220)$$

We note that there are some other generalizations to non-Hermitian systems[75, 115–119].

## C. Two-band systems

We consider a two-band system with the index  $n = \pm$ . The Hamiltonian is generally given by

$$H(\mathbf{k}) = h_0(\mathbf{k}) + \sigma \cdot \mathbf{h}(\mathbf{k}), \quad (221)$$

where

$$h_0(\mathbf{k}) = h_{0\text{Re}}(\mathbf{k}) + ih_{0\text{Im}}(\mathbf{k}), \quad (222)$$

$$\mathbf{h}(\mathbf{k}) = \mathbf{h}_{\text{Re}}(\mathbf{k}) + i\mathbf{h}_{\text{Im}}(\mathbf{k}), \quad (223)$$

where  $h_0(\mathbf{k})$  and  $\mathbf{h}(\mathbf{k})$  are complex functions with  $h_{0\text{Re}}$ ,  $h_{0\text{Im}}$ ,  $\mathbf{h}_{\text{Re}}(\mathbf{k})$  and  $\mathbf{h}_{\text{Im}}(\mathbf{k})$  being real functions. The energy is given by

$$\varepsilon_\pm = h_0(\mathbf{k}) \pm \sqrt{\mathbf{h}(\mathbf{k})^2}, \quad (224)$$

where

$$\mathbf{h}(\mathbf{k})^2 \equiv h_x^2(\mathbf{k}) + h_y^2(\mathbf{k}) + h_z^2(\mathbf{k}). \quad (225)$$

Its right and left eigenvalues are given by[121]

$$|\psi_\pm^R\rangle = \frac{1}{\sqrt{2\varepsilon_\pm(\varepsilon_\pm - h_z)}} (h_x - ih_y, \varepsilon_\pm - h_z)^T, \quad (226)$$

$$\langle \psi_\pm^L | = \frac{1}{\sqrt{2\varepsilon_\pm(\varepsilon_\pm - h_z)}} (h_x + ih_y, \varepsilon_\pm - h_z), \quad (227)$$

which satisfy the biorthogonal condition,  $\langle \psi_\pm^L | \psi_\pm^R \rangle = 1$ . The non-Hermitian Berry connection is calculated as[121]

$$a_\pm^\mu = \frac{h_x \partial_{k_\mu} h_y - h_y \partial_{k_\mu} h_x}{\varepsilon_\pm(\varepsilon_\pm - h_z)}. \quad (228)$$

The non-Hermitian Berry curvature reads[127]

$$\Omega_\pm(\mathbf{k}) = \nabla \times \mathbf{a}_\pm(\mathbf{k}) = \frac{1}{2\varepsilon_\pm^{3/2}} \varepsilon_{\mu\nu\rho} h_\mu \partial_{k_x} h_\nu \partial_{k_y} h_\rho. \quad (229)$$



It is further simplified as

$$\Omega_{\pm}(\mathbf{k}) = \mp \frac{1}{2} \mathbf{n} \cdot (\partial_{k_x} \mathbf{n} \times \partial_{k_y} \mathbf{n}) \quad (230)$$

with

$$\mathbf{n} \equiv \frac{\mathbf{h}(\mathbf{k})}{\sqrt{\mathbf{h}(\mathbf{k})^2}}. \quad (231)$$

It is identical to Eq.(48) for the Hermitian system. Note that

$$\sqrt{\mathbf{h}(\mathbf{k})^2} \neq |\mathbf{h}(\mathbf{k})| \quad (232)$$

for non-Hermitian systems. The non-Hermitian Chern number is defined by[122, 125]

$$C_{\pm} = \frac{1}{2\pi} \int \Omega_{\pm}(\mathbf{k}) d^2k, \quad (233)$$

where the integration is over the Brillouin zone.

We can check

$$g_{\pm}^{\mu\nu}(\mathbf{k}) = \pm \frac{1}{2} (\partial_{k_{\mu}} \mathbf{n}) \cdot (\partial_{k_{\nu}} \mathbf{n}) \quad (234)$$

even for the non-Hermitian systems. It is identical to Eq.(47).

#### D. Dirac system with a complex mass

We consider a Dirac Hamiltonian with a complex mass  $m = B + i\gamma$ , whose Hamiltonian is given by

$$H(\mathbf{k}) = \lambda(\mathbf{k} \times \sigma)_z + (B + i\gamma)\sigma_z, \quad (235)$$

where  $\gamma$  is real. The Berry curvature (229) is calculated as

$$\Omega_{\pm}(\mathbf{k}) = \pm \frac{(m + i\gamma)\lambda^2}{2(\lambda^2 k^2 + (m + i\gamma)^2)^{3/2}}, \quad (236)$$

which leads to the Chern number[128]

$$C_{\pm} = \pm \frac{m + i\gamma}{2|m + i\gamma|}, \quad (237)$$

where  $|C_{\pm}| = 1/2$ .

The quantum metrics are calculated as

$$g_{\pm}^{xx}(\mathbf{k}) = \mp \frac{\lambda^2 \left( (\lambda k_y)^2 + (m + i\gamma)^2 \right)}{\left( (\lambda k)^2 + (m + i\gamma)^2 \right)^2}, \quad (238)$$

$$g_{\pm}^{yy}(\mathbf{k}) = \mp \frac{\lambda^2 \left( (\lambda k_x)^2 + (m + i\gamma)^2 \right)}{\left( (\lambda k)^2 + (m + i\gamma)^2 \right)^2}, \quad (239)$$

$$g_{\pm}^{xy}(\mathbf{k}) = \pm \frac{(\lambda)^2 (\lambda k_x) (\lambda k_y)}{\left( (\lambda k)^2 + (m + i\gamma)^2 \right)^2}, \quad (240)$$

The quantum volume is calculated as

$$\int d\mathbf{k} \sqrt{\det g_{\pm}^{\mu\nu}(\mathbf{k})} = \frac{1}{8} \left( \frac{\lambda}{m + i\gamma} \right)^2. \quad (241)$$

It is negative for pure imaginary mass  $m = 0$  and  $\gamma \neq 0$ .

## VI. QUANTUM INFORMATION GEOMETRY

### A. Uhlmann quantum geometry for density matrix

So far, quantum geometry is constructed for the wave function. It means that it is constructed for pure states. On the other hand, mixed states are important for quantum information, finite temperature system and open quantum systems. They are described by the density matrix

$$\rho(\mathbf{k}) = \sum_{n=1}^N p_n |\psi_n(\mathbf{k})\rangle \langle \psi_n(\mathbf{k})|, \quad (242)$$

where  $p_n = \exp(-\varepsilon_n/k_B T)$ . Quantum geometry for it is constructed by Uhlmann[129–133, 141, 143, 144]. Starting from the fidelity of for the density matrix, we naturally obtain quantum Fisher information, which gives the lower boundary of the quantum fluctuation. Hence, quantum geometry for density matrices is called quantum information geometry.

We start with the Uhlmann fidelity[137, 138] for the density matrix defined by

$$F(\mathbf{k}, \mathbf{k}') = \text{Tr} \sqrt{\sqrt{\rho(\mathbf{k})} \rho(\mathbf{k}') \sqrt{\rho(\mathbf{k})}}. \quad (243)$$

It is symmetric

$$F(\mathbf{k}, \mathbf{k}') = F(\mathbf{k}', \mathbf{k}), \quad (244)$$

because  $\sqrt{\rho(\mathbf{k})} \rho(\mathbf{k}') \sqrt{\rho(\mathbf{k})}$  and  $\sqrt{\rho(\mathbf{k}')} \rho(\mathbf{k}) \sqrt{\rho(\mathbf{k}')}$  have the same eigenvalues. It is bounded as

$$0 \leq F(\mathbf{k}, \mathbf{k}') \leq 1, \quad (245)$$

where

$$F(\mathbf{k}, \mathbf{k}) = 1, \quad (246)$$

because

$$\text{Tr} \rho(\mathbf{k}) = 1. \quad (247)$$

It reduces to the fidelity (1) for the pure states,

$$\begin{aligned} F(\mathbf{k}, \mathbf{k}') &= \text{Tr} \sqrt{\rho(\mathbf{k}) \rho(\mathbf{k}')} \\ &= \text{Tr} \sqrt{|\psi(\mathbf{k})\rangle \langle \psi(\mathbf{k})| |\psi(\mathbf{k}')\rangle \langle \psi(\mathbf{k}')|} \\ &= \sqrt{\langle \psi(\mathbf{k}) | \psi(\mathbf{k}') \rangle \langle \psi(\mathbf{k}') | \psi(\mathbf{k}) \rangle} \\ &= |\langle \psi(\mathbf{k}) | \psi(\mathbf{k}') \rangle|. \end{aligned} \quad (248)$$

With the use of the Uhlmann fidelity (243), the Bures distance[139] is defined by

$$s_B = \sqrt{1 - F(\mathbf{k}, \mathbf{k}')^2}. \quad (249)$$

We make a purification of the density matrix with the use of the amplitude  $W$  satisfying

$$\rho = WW^\dagger, \quad (250)$$

where the amplitude  $W$  is given by

$$W = (\sqrt{p_1} |\psi_1(\mathbf{k})\rangle, \sqrt{p_2} |\psi_2(\mathbf{k})\rangle, \dots, \sqrt{p_N} |\psi_N(\mathbf{k})\rangle), \quad (251)$$

$$W^\dagger = \begin{pmatrix} \sqrt{p_1} \langle \psi_1(\mathbf{k}) | \\ \sqrt{p_2} \langle \psi_2(\mathbf{k}) | \\ \vdots \\ \sqrt{p_N} \langle \psi_N(\mathbf{k}) | \end{pmatrix}. \quad (252)$$

Hence, purification is always possible using the spectral decomposition. It is identical to represent

$$\rho = \text{Tr}_E |\Psi\rangle \langle \Psi| \quad (253)$$

for the extended Hamiltonian

$$H_{\text{ext}} \equiv H \otimes H_E, \quad (254)$$

by attaching an environment Hamiltonian  $H_E$ , where the trace is taken over the environment. It means that the mixed states are represented by a pure state  $|\Psi\rangle$  if we prepare a large system described by  $H_{\text{ext}}$ . Comparing Eq.(250) and Eq.(253),  $W$  and  $W^\dagger$  correspond to  $|\Psi\rangle$  and  $\langle \Psi|$ , respectively.

There is a gauge degrees of freedom  $U'$  in  $W$  as

$$W = \sqrt{\rho} U', \quad (255)$$

where  $U$  is a unitary matrix. By using the purification, the Uhlmann fidelity is rewritten as

$$\begin{aligned} F(\mathbf{k}, \mathbf{k}') &= \text{Tr} \sqrt{W^\dagger(\mathbf{k}) W(\mathbf{k}') W^\dagger(\mathbf{k}') W(\mathbf{k})} \\ &= \text{Tr} |W^\dagger(\mathbf{k}) W(\mathbf{k}')|. \end{aligned} \quad (256)$$

The Bures distance (249) is rewritten as

$$\begin{aligned} s_B^2 &= 2(1 - \text{Tr} |W^\dagger(\mathbf{k}) W(\mathbf{k}')|) \\ &= 2\text{Tr} (W(\mathbf{k}') - W(\mathbf{k})) (W(\mathbf{k}') - W(\mathbf{k}))^\dagger, \end{aligned} \quad (257)$$

where we have used the normalization condition for the density matrix,

$$\text{Tr} \rho(\mathbf{k}) = \text{Tr} W(\mathbf{k}) W^\dagger(\mathbf{k}) = 1, \quad (258)$$

and the Uhlmann parallel transport condition[129]

$$W^\dagger(\mathbf{k}) W(\mathbf{k}') = W^\dagger(\mathbf{k}') W(\mathbf{k}) > 0. \quad (259)$$

The Bures distance for the infinitesimal distance  $d\mathbf{k}$  is given by setting  $\mathbf{k}' = \mathbf{k} + d\mathbf{k}$  as

$$(ds_B)^2 = 2\text{Tr} dW dW^\dagger = 2\text{Tr} |dW|^2. \quad (260)$$

The differential form of the Uhlmann parallel transport condition (259) is given by

$$W^\dagger dW = (dW^\dagger) W. \quad (261)$$

It is fulfilled by the ansatz

$$dW = \frac{1}{2} \mathcal{L} W, \quad \mathcal{L}^\dagger = \mathcal{L}. \quad (262)$$

Indeed, the left and right hand sides of Eq.(261) are given by

$$W^\dagger dW = \frac{1}{2} W^\dagger \mathcal{L} W, \quad (263)$$

$$(dW^\dagger) W = \frac{1}{2} (\mathcal{L} W)^\dagger W = \frac{1}{2} W^\dagger \mathcal{L}^\dagger W = \frac{1}{2} W^\dagger \mathcal{L} W, \quad (264)$$

and identical with the use of Eq.(262).  $\mathcal{L}$  is called the symmetric logarithmic derivative (SLD)[140, 145, 146].

Then, the Bures distance (260) reads

$$\begin{aligned} (ds_B)^2 &= 2\text{Tr} |dW|^2 = 2\text{Tr} \left| \frac{1}{2} \mathcal{L} W \right|^2 \\ &= \frac{1}{2} \text{Tr} \mathcal{L} W W^\dagger \mathcal{L} = \frac{1}{2} \text{Tr} \mathcal{L} \rho \mathcal{L} \\ &= \frac{1}{2} \text{Tr} \rho \mathcal{L}^2 = \frac{1}{2} \langle \mathcal{L}^2 \rangle. \end{aligned} \quad (265)$$

By using one form of the SLD,

$$\mathcal{L} = \mathcal{L}^\mu dk_\mu, \quad (266)$$

we obtain the Uhlmann quantum geometric tensor  $\mathcal{F}_U^{\mu\nu}$  as

$$(ds_B)^2 = \text{Tr} \left[ \rho \sum_{\mu\nu} \mathcal{L}^\mu \mathcal{L}^\nu dk_\mu dk_\nu \right] \equiv \sum_{\mu\nu} \mathcal{F}_U^{\mu\nu} dk_\mu dk_\nu, \quad (267)$$

with

$$\mathcal{F}_U^{\mu\nu} \equiv \text{Tr} [\rho \mathcal{L}^\mu \mathcal{L}^\nu] = \langle \mathcal{L}^\mu \mathcal{L}^\nu \rangle. \quad (268)$$

The Uhlmann quantum geometric tensor  $\mathcal{F}_U^{\mu\nu}$  is decomposed as

$$\mathcal{F}_U^{\mu\nu} = \mathcal{F}_{\text{QFisher}}^{\mu\nu} + i\bar{\mathcal{U}}^{\mu\nu} \quad (269)$$

with the SLD quantum Fisher information[140, 142, 143]

$$\mathcal{F}_{\text{QFisher}}^{\mu\nu} \equiv \frac{1}{2} \text{Tr} [\rho \{\mathcal{L}^\mu, \mathcal{L}^\nu\}] = \frac{1}{2} \langle \{\mathcal{L}^\mu, \mathcal{L}^\nu\} \rangle, \quad (270)$$

and the mean Uhlmann curvature[133, 143]

$$\bar{\mathcal{U}}^{\mu\nu} \equiv -\frac{i}{2} \text{Tr} [\rho [\mathcal{L}^\mu, \mathcal{L}^\nu]] = -\frac{i}{2} \langle [\mathcal{L}^\mu, \mathcal{L}^\nu] \rangle. \quad (271)$$

We note that

$$\mathcal{U}^{\mu\nu} \equiv -\frac{i}{2} [\mathcal{L}^\mu, \mathcal{L}^\nu] \quad (272)$$

is the Uhlmann curvature, which satisfies

$$\bar{\mathcal{U}}^{\mu\nu} = \text{Tr} [\rho \mathcal{U}^{\mu\nu}] = \langle \mathcal{U}^{\mu\nu} \rangle. \quad (273)$$

It follows from Eq.(250) that

$$\begin{aligned} d\rho &= d(WW^\dagger) = (dW)W^\dagger + WdW^\dagger \\ &= \frac{1}{2}\mathcal{L}WW^\dagger + W\frac{1}{2}(\mathcal{L}W)^\dagger \\ &= \frac{1}{2}(\mathcal{L}\rho + \rho\mathcal{L}) = \frac{1}{2}\{\mathcal{L}, \rho\}. \end{aligned} \quad (274)$$

By using Eq.(242) and Eq.(274), the SLD  $\mathcal{L}^\mu$  is explicitly given by[134–136, 140, 143]

$$\mathcal{L}^\mu = \sum_n \frac{\partial \ln p_n}{\partial k_\mu} |\psi_n\rangle \langle \psi_n| + 2i \sum_{n \neq m} \frac{p_m - p_n}{p_m + p_n} a_{nm}^\mu |\psi_n\rangle \langle \psi_m|. \quad (275)$$

The derivation is shown in Appendix.I.

### B. Classical Fisher information

The symmetric logarithmic derivative is decomposed into the classical part  $\mathcal{L}_C^\mu$  and the quantum part  $\mathcal{L}_Q^\mu$  as[143]

$$\mathcal{L}^\mu = \mathcal{L}_C^\mu + \mathcal{L}_Q^\mu, \quad (276)$$

$$\mathcal{L}_C^\mu \equiv \sum_n \frac{\partial \ln p_n}{\partial k_\mu} |\psi_n\rangle \langle \psi_n|, \quad (277)$$

$$\mathcal{L}_Q^\mu \equiv 2i \sum_{n \neq m} \frac{p_m - p_n}{p_m + p_n} a_{nm}^\mu |\psi_n\rangle \langle \psi_m|. \quad (278)$$

When the SLD  $\mathcal{L}^\mu$  commutes with the density matrix  $\rho$ ,

$$[\mathcal{L}^\mu, \rho] = 0, \quad (279)$$

we have  $\mathcal{L}_Q^\mu = 0$  and  $\mathcal{L}^\mu = \mathcal{L}_C^\mu$ . Then, we obtain the classical Fisher information based on the classical part of the SLD as

$$\begin{aligned} &\frac{1}{2} \text{Tr} [\rho \{\mathcal{L}_C^\mu, \mathcal{L}_C^\nu\}] \\ &= \frac{1}{2} \sum_{n=1}^N p_n |\psi_n(\mathbf{k})\rangle \langle \psi_n(\mathbf{k})| \\ &\quad \times \left( \sum_{n'} \frac{\partial \ln p_{n'}}{\partial k_\mu} |\psi_{n'}\rangle \langle \psi_{n'}| \sum_{n''} \frac{\partial \ln p_{n''}}{\partial k_\nu} |\psi_{n''}\rangle \langle \psi_{n''}| \right. \\ &\quad \left. + \sum_{n''} \frac{\partial \ln p_{n''}}{\partial k_\nu} |\psi_{n''}\rangle \langle \psi_{n''}| \sum_{n'} \frac{\partial \ln p_{n'}}{\partial k_\mu} |\psi_{n'}\rangle \langle \psi_{n'}| \right) \\ &= \sum_{n, n', n''=1}^N p_n \frac{\partial \ln p_{n'}}{\partial k_\mu} \frac{\partial \ln p_{n''}}{\partial k_\nu} \delta_{nn'} \delta_{n'n''} \\ &= \sum_{n=1}^N p_n \frac{\partial \ln p_n}{\partial k_\mu} \frac{\partial \ln p_n}{\partial k_\nu} \equiv \mathcal{F}_{\text{CFisher}}^{\mu\nu}. \end{aligned} \quad (280)$$

On the other hand, the classical part of the mean Uhlmann curvature is zero,

$$\bar{\mathcal{U}}^{\mu\nu} \equiv -\frac{i}{2} \text{Tr} [\rho [\mathcal{L}_C^\mu, \mathcal{L}_C^\nu]] = 0. \quad (281)$$

### C. Quantum Cramér-Rao inequality

There is an inequality known as the Quantum Cramér-Rao inequality[142, 145, 146],

$$\mathcal{F}_{\text{CFisher}} \leq \mathcal{F}_{\text{QFisher}}, \quad (282)$$

where we have defined

$$\mathcal{F}_{\text{CFisher}} = \sum_{\mu\nu} a_\mu \mathcal{F}_{\text{CFisher}}^{\mu\nu} a_\nu, \quad (283)$$

$$\mathcal{F}_{\text{QFisher}} = \sum_{\mu\nu} a_\mu \mathcal{F}_{\text{QFisher}}^{\mu\nu} a_\nu \quad (284)$$

for an arbitrary set of parameters  $a_\mu$ . The proof is shown in Appendix.I2.

On the other hand, the classical Cramér-Rao inequality states that the covariance is bounded by the inverse of the classical Fisher information matrix,

$$\begin{aligned} &\sum_{\mu\nu} a_\mu p_n (k_\mu - \langle k_\mu \rangle) (k_\nu - \langle k_\nu \rangle) a_\nu \\ &\geq \frac{1}{N} \sum_{\mu\nu} a_\mu (\mathcal{F}_{\text{CFisher}}^{-1})^{\mu\nu} a_\nu. \end{aligned} \quad (285)$$

Combining the quantum and classical Cramér-Rao inequalities, the lower bound of the covariance is determined by the inverse of the quantum Fisher information.

### D. Quantum Fisher information for a pure state and quantum metric

By inserting Eq.(266) to Eq.(274), we obtain

$$d\rho = \frac{1}{2} \{\mathcal{L}, \rho\} = \frac{1}{2} \{\mathcal{L}^\mu dk_\mu, \rho\}, \quad (286)$$

which leads to

$$\frac{\partial \rho}{\partial k_\mu} = \frac{1}{2} \{\mathcal{L}^\mu, \rho\}. \quad (287)$$

We show that the quantum Fisher information reproduces the quantum metric when the density matrix  $\rho$  describes a pure state  $|\psi_n\rangle$ . By using the relation  $\rho^2 = \rho$ , we have

$$\frac{\partial \rho}{\partial k_\mu} = \frac{\partial \rho^2}{\partial k_\mu} = \rho \frac{\partial \rho}{\partial k_\mu} + \frac{\partial \rho}{\partial k_\mu} \rho = \left\{ \frac{\partial \rho}{\partial k_\mu}, \rho \right\}. \quad (288)$$

Comparing it with Eq.(287), we have

$$\mathcal{L}^\mu = 2 \frac{\partial \rho}{\partial k_\mu}. \quad (289)$$

Then, the quantum Fisher information is rewritten as

$$\mathcal{F}_{\text{QFisher}}^{\mu\nu} = 2\text{Tr} \left[ \rho \left\{ \frac{\partial \rho}{\partial k_\mu}, \frac{\partial \rho}{\partial k_\nu} \right\} \right] = 2 \left\langle \left\{ \frac{\partial \rho}{\partial k_\mu}, \frac{\partial \rho}{\partial k_\nu} \right\} \right\rangle. \quad (290)$$

By inserting

$$\rho = |\psi_n\rangle\langle\psi_n|, \quad (291)$$

the quantum Fisher information is reduced to the quantum metric

$$\begin{aligned} \mathcal{F}_{\text{QFisher}}^{\mu\nu} &= 2\text{Tr} \left[ \frac{\partial\langle\psi_n|}{\partial k_\mu} \frac{\partial|\psi_n\rangle}{\partial k_\nu} - \frac{\partial\langle\psi_n|}{\partial k_\mu} |\psi_n\rangle\langle\psi_n| \frac{\partial|\psi_n\rangle}{\partial k_\nu} \right. \\ &\quad \left. + \frac{\partial\langle\psi_n|}{\partial k_\nu} \frac{\partial|\psi_n\rangle}{\partial k_\mu} - \frac{\partial\langle\psi_n|}{\partial k_\nu} |\psi_n\rangle\langle\psi_n| \frac{\partial|\psi_n\rangle}{\partial k_\mu} \right] \\ &= 2(\mathcal{F}_n^{\mu\nu} + \mathcal{F}_n^{\nu\mu}) = 4g_n^{\mu\nu}. \end{aligned} \quad (292)$$

while the mean Uhlmann curvature is reduced to the Berry curvature

$$\begin{aligned} \bar{\mathcal{U}}^{\mu\nu} &= -2i\text{Tr} \left[ \frac{\partial\langle\psi_n|}{\partial k_\mu} \frac{\partial|\psi_n\rangle}{\partial k_\nu} - \frac{\partial\langle\psi_n|}{\partial k_\mu} |\psi_n\rangle\langle\psi_n| \frac{\partial|\psi_n\rangle}{\partial k_\nu} \right. \\ &\quad \left. - \frac{\partial\langle\psi_n|}{\partial k_\nu} \frac{\partial|\psi_n\rangle}{\partial k_\mu} + \frac{\partial\langle\psi_n|}{\partial k_\nu} |\psi_n\rangle\langle\psi_n| \frac{\partial|\psi_n\rangle}{\partial k_\mu} \right] \\ &= -2i(\mathcal{F}_n^{\mu\nu} + \mathcal{F}_n^{\nu\mu}) = i4\Omega_n^{\mu\nu}. \end{aligned} \quad (293)$$

Then, the quantum Fisher information is reduced to the quantum metric, while the mean Uhlmann curvature is reduced to the Berry curvature. Thus, the Uhlmann quantum geometry is a generalization of quantum geometry. The derivation of Eq.(292) is shown in Appendix.I3.

### E. Fluctuation-dissipation theorem

There is a fluctuation-dissipation theorem[143],

$$-\frac{1}{2\hbar}g_{\text{Bures}}^{\mu\nu} = \frac{\tanh^2 \frac{\hbar\omega}{2k_B T}}{1 - e^{-\hbar\omega/k_B T}} \frac{\chi^{\mu\nu}}{(\hbar\omega)^2}, \quad (294)$$

where  $\chi^{\mu\nu}$  is the susceptibility. It is reduced to Eq.(111) for the pure state.

### F. Quantum geometry at thermal equilibrium

At a thermal equilibrium, the probability is given by

$$p_n = \exp[-\beta\varepsilon_n], \quad (295)$$

where  $\beta \equiv 1/k_B T$  is the inverse temperature. We consider a two-band system with  $n = \pm$ . The SLD operator (275) is given by

$$\begin{aligned} \mathcal{L}^\mu &= -\beta \sum_{n=\pm} \frac{\partial\varepsilon_n}{\partial k_\mu} |\psi_n\rangle\langle\psi_n| \\ &\quad - 2i \tanh \frac{\Delta\varepsilon}{2} (a_{-+}^\mu |\psi_- \rangle\langle\psi_+| - a_{+-}^\mu |\psi_+ \rangle\langle\psi_-|) \end{aligned} \quad (296)$$

with

$$\Delta\varepsilon = \varepsilon_+ - \varepsilon_-, \quad (297)$$

where we have used

$$\frac{e^{-\beta\varepsilon_+} - e^{-\beta\varepsilon_-}}{e^{-\beta\varepsilon_+} + e^{-\beta\varepsilon_-}} = \tanh \frac{\Delta\varepsilon}{2}. \quad (298)$$

It is rewritten as

$$\mathcal{L}^\mu = \Psi^\dagger \begin{pmatrix} -\beta \frac{\partial\varepsilon_+}{\partial k_\mu} & 2i \tanh \frac{\beta\Delta\varepsilon}{2} a_{+-}^\mu \\ -2i \tanh \frac{\beta\Delta\varepsilon}{2} a_{-+}^\mu & -\beta \frac{\partial\varepsilon_-}{\partial k_\mu} \end{pmatrix} \Psi \quad (299)$$

with

$$\Psi \equiv \begin{pmatrix} \langle\psi_+| \\ \langle\psi_-| \end{pmatrix}. \quad (300)$$

The Uhlmann curvature is calculated as

$$\mathcal{U}^{\mu\nu} = -\frac{i}{2} [\mathcal{L}^\mu, \mathcal{L}^\nu] = 2 \tanh \frac{\beta\Delta\varepsilon}{2} \begin{pmatrix} \mathcal{U}^{++} & \mathcal{U}^{+-} \\ \mathcal{U}^{+-} & -\mathcal{U}^{++} \end{pmatrix} \quad (301)$$

with

$$\mathcal{U}^{++} = \Omega^{\mu\nu} \tanh \frac{\beta\Delta\varepsilon}{2}, \quad (302)$$

$$\mathcal{U}^{+-} = \frac{\partial\varepsilon_+}{\partial k_\mu} a_{+-}^\nu - \frac{\partial\varepsilon_+}{\partial k_\nu} a_{+-}^\mu. \quad (303)$$

$\mathcal{U}^{++}$  recovers the Berry curvature at the low temperature limit,  $\beta \rightarrow 0$ ,

$$\mathcal{U}^{++} = -\lim_{\beta \rightarrow 0} 2\Omega^{\mu\nu} \tanh^2 \frac{\beta\Delta\varepsilon}{2} = -2\Omega^{\mu\nu}. \quad (304)$$

We define the quantum Fisher information density by

$$F_{\text{QFisher}}^{\mu\nu} \equiv \frac{1}{2} \{\mathcal{L}^\mu, \mathcal{L}^\nu\}, \quad (305)$$

which satisfies

$$\mathcal{F}_{\text{QFisher}}^{\mu\nu} \equiv \text{Tr} [\rho F_{\text{QFisher}}^{\mu\nu}] = \langle F_{\text{QFisher}}^{\mu\nu} \rangle. \quad (306)$$

It is explicitly given by

$$F_{\text{QFisher}}^{\mu\nu} = \left( \frac{\partial\varepsilon_+}{\partial k_\mu} \frac{\partial\varepsilon_+}{\partial k_\nu} + 4g^{\mu\nu} \tanh^2 \frac{\beta\Delta\varepsilon}{2} \right) I_2, \quad (307)$$

where  $I_2$  is the 2 by 2 identity matrix.

## VII. X-WAVE MAGNETS

### A. Fermi surface symmetry

The Fermi surface of electrons coupled with a ferromagnet is known to have the  $s$ -wave symmetry as shown in Fig.2(a). Recently proposed altermagnets generalize it to Fermi surfaces possessing higher-wave symmetries[42, 43]. The Fermi surface has 0, 1, 2, 3, 4 and 6 nodes for the  $s$ -wave,  $p$ -wave,  $d$ -wave,  $f$ -wave,  $g$ -wave and  $i$ -wave symmetry, respectively. The  $d$ -wave altermagnet has the Fermi surface with the  $d$ -wave symmetry as shown in Fig.2(c1). In the similar way, the

Fermi surface of the  $g$ -wave altermagnet is shown in Fig.2(e1) and that of the  $i$ -wave altermagnet is shown in Fig.2(f1). Altermagnets break time-reversal symmetry. On the other hand, the  $p$ -wave magnet preserves time-reversal symmetry. Its Fermi surface has the  $p$ -wave symmetry as shown in Fig.2(b1). In a similar way, the  $f$ -wave magnet has the Fermi surface with the  $f$ -wave symmetry as shown in Fig.2(d1). We call them the  $X$ -wave magnets with  $X = p, d, f, g, i$ . We note that there are no  $h$ -wave magnets because of the incompatibility between the five-fold rotational symmetry and the lattice symmetry.

The simplest expressions on magnetic terms with higher symmetries in two dimensions are summarized as follows. The  $X$ -wave magnet is characterized by a function  $f_X^{2D}(\mathbf{k})$ , which reads[42, 43, 46, 47, 147],

$$f_s^{2D}(\mathbf{k}) = 1, \quad (308)$$

$$f_p^{2D}(\mathbf{k}) = ak_x = ak \cos \phi, \quad (309)$$

$$f_d^{2D}(\mathbf{k}) = 2a^2 k_x k_y = a^2 k^2 \sin 2\phi, \quad (310)$$

$$f_f^{2D}(\mathbf{k}) = a^3 k_x (k_x^2 - 3k_y^2) = a^3 k^3 \cos 3\phi, \quad (311)$$

$$f_g^{2D}(\mathbf{k}) = 4a^4 k_x k_y (k_x^2 - k_y^2) = a^4 k^4 \sin 4\phi, \quad (312)$$

$$f_i^{2D}(\mathbf{k}) = 2a^6 k_x k_y (3k_x^2 - k_y^2) (k_x^2 - 3k_y^2) = a^6 k^6 \sin 6\phi, \quad (313)$$

where  $k_x = k \cos \phi$ ,  $k_y = k \sin \phi$ . We note that the  $d$ -wave altermagnet described by the function  $f_d^{2D}(\mathbf{k})$  is commonly called the  $d_{xy}$ -wave altermagnet. The  $X$ -wave magnet has  $N_X$  nodes in the band structure, where  $N_X = 1, 2, 3, 4, 6$  for  $X = p, d, f, g, i$ , respectively.

There is another type of the  $X'$ -wave magnet in two dimensions characterized by a function  $f_{X'}^{2D}(\mathbf{k})$  such that

$$f_{p'}^{2D}(\mathbf{k}) = ak_y = ak \sin \phi, \quad (314)$$

$$f_{d'}^{2D}(\mathbf{k}) = a^2 (k_x^2 - k_y^2) = a^2 k^2 \cos 2\phi, \quad (315)$$

$$f_{f'}^{2D}(\mathbf{k}) = a^3 k_y (3k_x^2 - k_y^2) = a^3 k^3 \sin 3\phi, \quad (316)$$

$$\begin{aligned} f_{g'}^{2D}(\mathbf{k}) &= a^4 (k_x^2 - k_y^2 - 2k_x k_y) (k_x^2 - k_y^2 + 2k_x k_y) \\ &= a^4 k^4 \cos 4\phi, \end{aligned} \quad (317)$$

$$\begin{aligned} f_{i'}^{2D}(\mathbf{k}) &= 2a^6 (k_x^2 - k_y^2) (k_x^4 + k_y^4 - 14k_x^2 k_y^2) \\ &= a^6 k^6 \cos 6\phi, \end{aligned} \quad (318)$$

where  $X' = p', d', f', g', i'$ . We note that the  $d'$ -wave altermagnet described by the function  $f_{d'}^{2D}(\mathbf{k})$  is commonly called the  $d_{x^2-y^2}$ -wave altermagnet, which is obtained by rotating the  $d_{xy}$  altermagnet by 45 degrees.

The  $X$ -wave magnet and the  $X'$ -wave magnet are summarized by the function in the form of

$$f_{X,X'}^{2D}(\mathbf{k}) = (ak)^{N_X} \sin N_X \phi, \quad (319)$$

or

$$f_{X,X'}^{2D}(\mathbf{k}) = (ak)^{N_X} \cos N_X \phi. \quad (320)$$

The magnetic terms of the  $X$ -wave magnet in three dimen-

sions are given by

$$f_d^{3D}(\mathbf{k}) = a^2 k_z (k_x + k_y), \quad (321)$$

$$f_f^{3D}(\mathbf{k}) = 2a^3 k_x k_y k_z = a^2 k^2 \cos \theta \sin 2\phi, \quad (322)$$

$$f_g^{3D}(\mathbf{k}) = a^4 k_z k_x (k_x^2 - 3k_y^2) = a^3 k^3 \cos \theta \cos 3\phi, \quad (323)$$

$$f_i^{3D}(\mathbf{k}) = a^6 (k_x^2 - k_y^2) (k_y^2 - k_z^2) (k_z^2 - k_x^2). \quad (324)$$

There are relations between the  $X$ -wave magnet between two and three dimensions,

$$f_f^{3D}(\mathbf{k}) = ak_z f_d^{2D}(\mathbf{k}), \quad (325)$$

$$f_g^{3D}(\mathbf{k}) = ak_z f_f^{2D}(\mathbf{k}). \quad (326)$$

There are also  $X'$ -wave magnets in three dimensions[148],

$$f_{d'}^{3D}(\mathbf{k}) = a^2 k_y (k_x + k_z), \quad (327)$$

$$f_{f'}^{3D}(\mathbf{k}) = a^3 k_z (k_x^2 - k_y^2) = a^2 k^2 \cos \theta \cos 2\phi, \quad (328)$$

$$f_{g'}^{3D}(\mathbf{k}) = a^4 k_z k_y (3k_x^2 - k_y^2) = a^3 k^3 \cos \theta \sin 3\phi. \quad (329)$$

We set  $a = 1$  in the following.

## B. Model Hamiltonian

We consider the two-band Hamiltonian described[46] by

$$H(\mathbf{k}) = \frac{\hbar^2 k^2}{2m} + J f_X(\mathbf{k}) \mathbf{n} \cdot \boldsymbol{\sigma} + \lambda (k_x \sigma_y - k_y \sigma_x) + \mathbf{B} \cdot \boldsymbol{\sigma}. \quad (330)$$

The first term represents the kinetic energy, making the system metallic. The second term represents the  $X$ -wave term with the  $X$ -wave function  $f_X(\mathbf{k})$ , where  $\mathbf{n}$  is the direction of the spin-splitting of the band structure, and  $J$  is the coupling constant induced by the  $X$ -wave magnet. The third term represents the Rashba interaction introduced by making an interface between the  $X$ -wave magnet and the substrate, where  $\lambda$  is the magnitude of the Rashba interaction. The fourth term is the magnetic field term. The Rashba interaction is introduced by placing an altermagnet on the substrate[31, 42, 43, 149–153].

## C. Symmetry

We summarize symmetry properties of the  $X$ -wave magnets[58].

### 1. Spin diagonal case

We consider the Hamiltonian (330) by setting  $\lambda = 0$ ,  $\mathbf{n} = (0, 0, 1)$  and  $\mathbf{B} = 0$ , where the spin is a good quantum number,  $\sigma_z = s = \pm 1$ . The Hamiltonian is diagonal with respect to the spin  $\sigma$ , where  $s = \pm 1$ . Let us use  $s = \uparrow \downarrow$  within indices and  $s = \pm 1$  in equations.

The energy is given by

$$\varepsilon_s = \frac{\hbar^2 k^2}{2m} + s f_X. \quad (331)$$

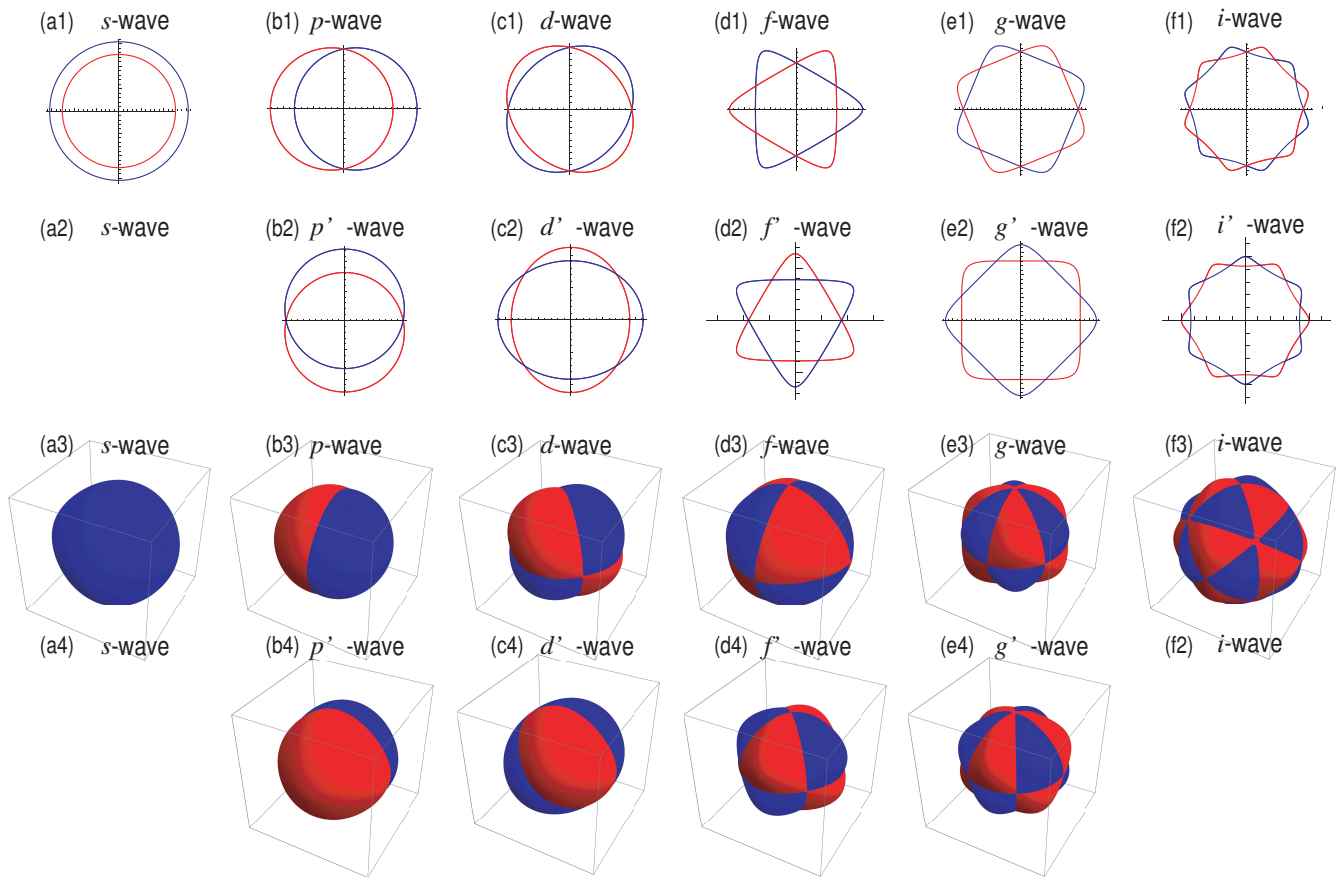


FIG. 2: Fermi surfaces in two and three dimensions. (a1), (a3)  $s$ -wave magnet; (b1), (b3)  $p$ -wave magnet; (c1), (c3)  $d$ -wave altermagnet; (c2)  $d'$ -wave altermagnet; (d1), (d3)  $f$ -wave magnet; (d2)  $f'$ -wave magnet; (e1), (e3)  $g$ -wave altermagnet; (e2)  $g'$ -wave altermagnet; ((f1) and (f3)  $i$ -wave altermagnet. Red (blue) curves indicate up (down)-spin Fermi surfaces.

Time-reversal symmetry is defined by

$$T\varepsilon_s(\mathbf{k})T^{-1} = \varepsilon_{-s}(-\mathbf{k}). \quad (332)$$

Inversion symmetry is defined by

$$P\varepsilon_s(\mathbf{k})P^{-1} = \varepsilon_s(-\mathbf{k}). \quad (333)$$

When there are both symmetries, we have

$$PT\varepsilon_s(\mathbf{k})(PT)^{-1} = \varepsilon_{-s}(\mathbf{k}). \quad (334)$$

Hence, the band with up and down spins are degenerate perfectly. In this sense, the breaking of time-reversal symmetry or inversion symmetry is necessary for spin-splitting band structure. In the  $d$ -wave, the  $g$ -wave and the  $i$ -wave altermagnets, time-reversal symmetry is broken but inversion symmetry is preserved. On the other hand, in the  $p$ -wave and the  $f$ -wave magnets, inversion symmetry is broken but time-reversal symmetry is preserved. Hence, the spin splitting occurs in all  $X$ -wave magnets. These properties are summarized in the following table,

	$p$	$d$	$f$	$g$	$i$
Time-reversal	Yes	No	Yes	No	No
Inversion symmetry	No	Yes	No	Yes	Yes
Spin splitting	Yes	Yes	Yes	Yes	Yes
Altermagnet	No	Yes	No	Yes	Yes

(335)

## 2. Spin nondiagonal case

In the presence of the Rashba interaction, the system is not diagonal with respect to spin  $\sigma_z$ . In this case, time-reversal symmetry is defined by

$$TH(\mathbf{k})T^{-1} = H(-\mathbf{k}) \quad (336)$$

with the time-reversal symmetry operator  $T = i\sigma_y K$ , where  $K$  is the complex conjugation operator. Thus,  $T$  is an anti-unitary operator. Time-reversal symmetry is broken

$$TH(\mathbf{k})T^{-1} = -H(-\mathbf{k}) \quad (337)$$

for the  $d$ -wave, the  $g$ -wave and the  $i$ -wave altermagnets. On the other hand, time-reversal symmetry is preserved for the  $p$ -wave and the  $f$ -wave magnets.

Inversion symmetry is defined by

$$PH(\mathbf{k})P^{-1} = H(-\mathbf{k}) \quad (338)$$

with the inversion symmetry operator  $P = \sigma_z$ , which is a unitary operator. Inversion symmetry is preserved for  $s$ -wave,  $d$ -wave and  $g$ -wave magnets. On the other hand, it is broken

$$PH(\mathbf{k})P^{-1} = -H(-\mathbf{k}) \quad (339)$$

for  $p$ -wave,  $f$ -wave and  $i$ -wave magnets.

PT symmetry is a combination operator of inversion symmetry and time-reversal symmetry. If there is PT symmetry

$$PTH(\mathbf{k})(PT)^{-1} = H(\mathbf{k}), \quad (340)$$

the bands are two-fold degenerate. All  $X$ -wave magnets break PT symmetry, and hence, the band structure is spin split.

The  $X$ -wave symmetric magnets with  $N_X$  are characterized by the spin group, which a combination group of spatial group and spin. The  $\frac{2\pi}{N_X}$ -rotation along the  $z$  axis of the momentum is given by

$$R_z\left(\frac{\pi}{N_X}\right) : \begin{pmatrix} k_x \\ k_y \end{pmatrix} \mapsto \begin{pmatrix} \cos\frac{\pi}{N_X} & \sin\frac{\pi}{N_X} \\ -\sin\frac{\pi}{N_X} & \cos\frac{\pi}{N_X} \end{pmatrix} \begin{pmatrix} k_x \\ k_y \end{pmatrix}, \quad (341)$$

where  $N_X = 1, 2, 3, 4, 6$  for  $X = p, d, f, g, i$ , respectively. The  $X$ -wave symmetric magnets with  $N_X$  in two dimensions have a combinational symmetry of  $\frac{2\pi}{N_X}$ -rotation and time-reversal symmetry

$$\left[ R_z\left(\frac{\pi}{N_X}\right) T \right] H(\mathbf{k}) \left[ R_z\left(\frac{\pi}{N_X}\right) T \right]^{-1} = H(\mathbf{k}). \quad (342)$$

The  $X$ -wave symmetric magnets in three dimensions also have a combinational symmetry of spatial group and time-reversal symmetry.

#### D. Quantum geometry of $X$ -wave magnets

We take  $\mathbf{n} = (0, 0, 1)$  and  $\mathbf{B} = (0, 0, B)$  in the Hamiltonian (330). The Berry curvature is given by

$$\Omega_{\pm}^{xy} = \mp \frac{\lambda^2 (B + Jf_X - Jk\partial_k f_X)}{2(\lambda^2 k^2 + (B + Jf_X))^{3/2}}, \quad (343)$$

while the quantum metrics are given by

$$g_{\pm}^{xx} = \mp \frac{\lambda^2 (\lambda^2 k_y^2 + (B + Jf_X)^2)}{2(\lambda^2 k^2 + (B + Jf_X))^2}, \quad (344)$$

$$g_{\pm}^{xy} = g_{\pm}^{yx} = \mp \frac{-\lambda^4 k_x k_y}{2(\lambda^2 k^2 + (B + Jf_X))^2}, \quad (345)$$

$$g_{\pm}^{yy} = \mp \frac{\lambda^2 (\lambda^2 k_x^2 + (B + Jf_X)^2)}{2(\lambda^2 k^2 + (B + Jf_X))^2}. \quad (346)$$

#### E. Zeeman quantum geometry of $X$ -wave magnets

By inserting Eq.(330) to Eq.(161), the Zeeman Berry curvatures are calculated as

$$\mathcal{Z}_{+-}^{xx} = \frac{\partial n_x}{\partial k_x} = \lambda k_y \frac{\lambda^2 k_x + (B + Jf_X) J\partial_{k_x} f_X}{(\lambda^2 k^2 + (B + Jf_X)^2)^{3/2}}, \quad (347)$$

$$\mathcal{Z}_{+-}^{yy} = \frac{\partial n_y}{\partial k_y} = -\lambda k_x \frac{\lambda^2 k_y + (B + Jf_X) J\partial_{k_y} f_X}{(\lambda^2 k^2 + (B + Jf_X)^2)^{3/2}}, \quad (348)$$

$$\mathcal{Z}_{+-}^{xy} = \frac{\partial n_y}{\partial k_x} = \frac{\lambda}{\sqrt{\lambda^2 k^2 + (B + Jf_X)^2}} - \lambda k_x \frac{2\lambda^2 k_x + 2(B + f_X) J\partial_{k_x} f_X}{2(\lambda^2 k^2 + (B + Jf_X)^2)^{3/2}}, \quad (349)$$

$$\mathcal{Z}_{+-}^{yx} = \frac{\partial n_x}{\partial k_y} = -\frac{\lambda}{\sqrt{\lambda^2 k^2 + (B + Jf_X)^2}} + \lambda k_y \frac{2\lambda^2 k_y + 2(B + f_X) J\partial_{k_y} f_X}{2(\lambda^2 k^2 + (B + Jf_X)^2)^{3/2}}, \quad (350)$$

$$\mathcal{Z}_{+-}^{xz} = \frac{\partial n_z}{\partial k_x} = \lambda^2 \frac{-k_x (B + Jf_X) + Jk^2 J\partial_{k_x} f_X}{2(\lambda^2 k^2 + (B + Jf_X)^2)^{3/2}}, \quad (351)$$

$$\mathcal{Z}_{+-}^{yz} = \frac{\partial n_z}{\partial k_y} = \lambda^2 \frac{-k_y (B + Jf_X) + Jk^2 J\partial_{k_y} f_X}{2(\lambda^2 k^2 + (B + Jf_X)^2)^{3/2}}. \quad (352)$$

By inserting Eq.(330) to Eq.(162), the Zeeman quantum

metrics are calculated as

$$Q_{+-}^{xx} = \frac{n_y \frac{\partial n_z}{\partial k_x} - n_z \frac{\partial n_y}{\partial k_x}}{2} = -\frac{\lambda(B + Jf_X - Jk_x \partial_{k_x} f_X)}{2(\lambda^2 k^2 + (B + Jf_X)^2)}, \quad (353)$$

$$Q_{+-}^{yy} = \frac{n_z \frac{\partial n_x}{\partial k_y} - n_x \frac{\partial n_z}{\partial k_y}}{2} = -\frac{\lambda(B + Jf_X - Jk_y \partial_{k_y} f_X)}{2(\lambda^2 k^2 + (B + Jf_X)^2)}, \quad (354)$$

$$Q_{+-}^{xy} = \frac{n_z \frac{\partial n_x}{\partial k_x} - n_x \frac{\partial n_z}{\partial k_x}}{2} = \frac{\lambda k_y J \partial_{k_x} f_X}{2(\lambda^2 k^2 + (B + Jf_X)^2)}, \quad (355)$$

$$Q_{+-}^{yx} = \frac{n_y \frac{\partial n_z}{\partial k_y} - n_z \frac{\partial n_y}{\partial k_y}}{2} = \frac{\lambda k_x J \partial_{k_y} f_X}{2(\lambda^2 k^2 + (B + Jf_X)^2)}, \quad (356)$$

$$Q_{+-}^{xz} = \frac{n_x \frac{\partial n_y}{\partial k_x} - n_y \frac{\partial n_x}{\partial k_x}}{2} = -\frac{\lambda^2 k_y}{2(\lambda^2 k^2 + (B + Jf_X)^2)}, \quad (357)$$

$$Q_{+-}^{yz} = \frac{n_x \frac{\partial n_y}{\partial k_y} - n_y \frac{\partial n_x}{\partial k_y}}{2} = \frac{\lambda^2 k_x}{2(\lambda^2 k^2 + (B + Jf_X)^2)}. \quad (358)$$

The diagonal spin quantum metrics are calculated as

$$S_{+-}^{xx} = \frac{\lambda^2 k_x^2 + (B + Jf_X)^2}{\lambda^2 k^2 + (B + Jf_X)^2}, \quad (359)$$

$$S_{+-}^{yy} = \frac{\lambda^2 k_y^2 + (B + Jf_X)^2}{\lambda^2 k^2 + (B + Jf_X)^2}, \quad (360)$$

$$S_{+-}^{zz} = \frac{\lambda^2 k^2}{\lambda^2 k^2 + (B + Jf_X)^2}. \quad (361)$$

The off-diagonal spin quantum metrics are calculated as

$$S_{+-}^{xy} = \frac{\lambda^2 k_x k_y}{\sqrt{\lambda^2 k^2 + (B + Jf_X)^2}}, \quad (362)$$

$$S_{+-}^{yz} = -\frac{(B + Jf_X) k_x}{\sqrt{\lambda^2 k^2 + (B + Jf_X)^2}}, \quad (363)$$

$$S_{+-}^{zx} = \frac{(B + f_X) k_y}{\sqrt{\lambda^2 k^2 + (B + Jf_X)^2}}. \quad (364)$$

The spin Berry curvatures are calculated as

$$\mathcal{A}_{+-}^{xy} = -2 \frac{B + Jf_X}{\sqrt{\lambda^2 k^2 + (B + Jf_X)^2}}, \quad (365)$$

$$\mathcal{A}_{+-}^{yz} = \frac{2\lambda k_y}{\sqrt{\lambda^2 k^2 + (B + Jf_X)^2}}, \quad (366)$$

$$\mathcal{A}_{+-}^{zx} = -\frac{2\lambda k_x}{\sqrt{\lambda^2 k^2 + (B + Jf_X)^2}}. \quad (367)$$

## F. Zeeman quantum geometry induced cross response

We study the X-wave magnet coupled with the Rashba interaction without applying magnetic field[112], where we set  $J \neq 0$  and  $B = 0$ . It is possible to determine whether there is a response by integrating the quantum geometric tensors  $\mathcal{Z}_{+-}^{\mu\nu}$  and  $\mathcal{Q}_{+-}^{\mu\nu}$  over the angle  $\phi$ . Most of them vanishes by integration over the angle  $\phi$ .

First, we study the spin polarization  $S^{\mu;\nu}$  induced by electric field  $E^\nu$ . It is determined by  $\mathcal{Q}_{+-}^{\mu\nu}$  as in Eq.(159).

### 1) $S^{x;x}/E^x$

In the absence of the X-wave magnet, there is no response in the absence of magnetic field, while there is nonzero response in the presence of magnetic field. Only in the  $d_{x^2-y^2}$  altermagnet, there emerges the diagonal spin polarization  $S^{\mu;\mu}$  by applying electric field  $E^\mu$  with  $\mu = x, y$  in the absence of magnetic field. Once magnetic field is turned on, there is nonzero response for all X-wave magnets.

### 2) $S^{x;y}/E^y$

In addition, only in the  $d_{xy}$  altermagnet, there emerges the off-diagonal spin polarization  $S^x$  ( $S^y$ ) by applying electric field  $E^y$  ( $E^x$ ) due to the contribution from the Zeeman quantum metric  $\mathcal{Z}_{+-}^{xy}$  ( $\mathcal{Z}_{+-}^{yx}$ ). Diagonal spin polarization  $S^\mu$  is induced by electric field  $E^\mu$  for all X-wave and X'-wave magnets, which originate from the contribution of the Rashba interaction.

Next, we study current  $J^{\mu;\nu}$  induced by magnetic field  $B^\nu$ . It is determined by  $\mathcal{Z}_{+-}^{\mu\nu}$  as in Eq.(158).

### 3) $J^{x;x}/B^x$

The diagonal current  $J^{\mu;\mu}$  is not induced by magnetic field  $B^\mu$ .

### 4) $J^{x;y}/B^y$

On the other hand, the off-diagonal current  $J^{x;y}$  ( $J^{y;x}$ ) is induced by magnetic field  $B^y$  ( $B^x$ ) when there is nonzero Rashba interaction irrespective of the presence of the X-wave magnet.

They are summarized in the following table. Detailed derivations are shown in Appendix.H,



5. *i*-wave altermagnet

	$S^{x;x}/E^x$	$S^{x;y}/E^y$	$J^{x;x}/B^x$	$J^{x;y}/B^y$
Quantum geometry	$Q_{+-}^{xx}$	$Q_{+-}^{xy}$	$Z_{+-}^{xx}$	$Z_{+-}^{xy}$
Rashba ( $B = 0$ )	Zero	Zero	Zero	Nonzero
Rashba ( $B \neq 0$ )	Nonzero	Zero	Zero	Nonzero
X-wave ( $B = 0$ )	$d_{x^2-y^2}$	$d_{xy}$	Zero	Nonzero
X-wave ( $B \neq 0$ )	Nonzero	$d_{xy}$	Zero	Nonzero

(368)

## G. Materials

We summarize materials realizing *X*-wave magnets[52, 58]. Altermagnets have a collinear spin texture[42, 43], while *p*-wave magnets have a spiral spin texture[44, 154].

1. *p*-wave magnet

It was theoretically proposed that CeNiAsO is a *p*-wave magnet[45] and experimentally realized[155]. They were recently realized experimentally in[156] Gd<sub>3</sub>Ru<sub>4</sub>Al<sub>12</sub> and in[157] NiI<sub>2</sub>. It was also theoretically proposed that a *p*-wave magnet is realized in graphene by introducing spin nematic order[158].

2. *d*-wave altermagnet

The *d*-wave magnet in two dimensions was theoretically proposed in organic materials[37], perovskite materials[39], and twisted magnetic Van der Waals bilayers[159]. The *d*-wave altermagnet in three dimensions is experimentally realized in RuO<sub>2</sub>[160–164], Mn<sub>5</sub>Si<sub>3</sub>[165], FeSb<sub>2</sub>[166], KV<sub>2</sub>Se<sub>2</sub>[167].

3. *f*-wave magnet

It was theoretically proposed that an *f*-wave magnet is theoretically proposed in Ba<sub>3</sub>MnNb<sub>2</sub>O<sub>9</sub>[168], FePO<sub>4</sub>[44] and in graphene by introducing spin nematic order[158].

4. *g*-wave altermagnet

A *g*-wave altermagnet in two-dimensions was theoretically proposed in twisted magnetic Van der Waals bilayers[159]. The Fermi surface splitting of the *g*-wave altermagnet in three dimensions is experimentally observed in MnTe[169–174], CrSb[175–179], V<sub>1/3</sub>NbS<sub>2</sub>[180] and FeS[181].

An *i*-wave altermagnet in two dimensions was theoretically proposed in twisted magnetic Van der Waals bilayers[159] and in MnP(S,Se)<sub>3</sub>[182].

VIII. TRANSPORT PROPERTIES OF *X*-WAVE MAGNETS

## A. Without Rashba interaction

## 1. Spin current generation

One of the key feature of the *d*-wave altermagnet is that spin current is generated without using the Rashba interaction[37]. We analytically show it.

The current is given by

$$\mathbf{j} = -e \int dk f \mathbf{v}, \quad (369)$$

where  $f$  is the Fermi distribution function in the presence of  $\mathbf{E}$ ;  $\mathbf{v}$  is the velocity,

$$\mathbf{v} = \frac{1}{\hbar} \frac{\partial \varepsilon}{\partial \mathbf{k}}, \quad (370)$$

where  $\varepsilon$  is the energy of the Hamiltonian, and we have dropped the anomalous velocity term proportional to  $-e\mathbf{E} \times \boldsymbol{\Omega}/\hbar$  because the Berry curvature  $\boldsymbol{\Omega}$  is zero due to the single band condition.

We expand the current in terms of electric field  $E$  as

$$j_b = \sum_{\ell_1, \ell_2=0} \sigma^{x^{\ell_1} y^{\ell_2}; b} (E_x)^{\ell_1} (E_y)^{\ell_2}. \quad (371)$$

Then, the  $(\ell_1 + \ell_2)$ -th order conductivity is defined by

$$\sigma^{x^{\ell_1} y^{\ell_2}; b} = \frac{1}{\ell_1! \ell_2!} \frac{\partial^{\ell_1 + \ell_2} j_b}{\partial E_x^{\ell_1} \partial E_y^{\ell_2}}. \quad (372)$$

The semi-classical Boltzmann equation in the presence of electric field  $\mathbf{E}$  is given by

$$\partial_t f - \frac{e\mathbf{E}}{\hbar} \cdot \nabla_{\mathbf{k}} f = -\frac{f - f^{(0)}}{\tau}, \quad (373)$$

where  $\tau$  is the relaxation time, and  $f^{(0)}$  is the Fermi distribution function at the equilibrium with the chemical potential  $\mu$ ,

$$f^{(0)} = 1 / (\exp(\varepsilon - \mu) + 1). \quad (374)$$

Corresponding to Eq.(371), we expand the Fermi distribution in powers of  $\mathbf{E}$ ,

$$f = f^{(0)} + f^{(1)} + \dots. \quad (375)$$

The recursive solution gives[29]

$$f^{(\ell_1+\ell_2)} = \left( \frac{e/\hbar}{i\omega + 1/\tau} \right)^{\ell_1+\ell_2} \frac{\partial^{\ell_1+\ell_2} f^{(0)}}{\partial k_x^{\ell_1} \partial k_y^{\ell_2}} (E_x)^{\ell_1} (E_x)^{\ell_2}, \quad (376)$$

where  $\omega$  is the frequency of the applied electric field  $\mathbf{E}$ . The current (369) is expanded as in Eq.(375) with

$$\begin{aligned} j_b^{(\ell_1+\ell_2)} &= -e \int d\mathbf{k} f^{(\ell_1+\ell_2)} v_b \\ &= -\frac{e}{\hbar} \left( \frac{e/\hbar}{i\omega + 1/\tau} \right)^{\ell_1+\ell_2} \\ &\quad \times \int d\mathbf{k} \frac{\partial \varepsilon}{\partial k_b} \frac{\partial^{\ell_1+\ell_2} f^{(0)}}{\partial k_x^{\ell_1} \partial k_y^{\ell_2}} (E_x)^{\ell_1} (E_x)^{\ell_2}. \end{aligned} \quad (377)$$

The  $(\ell_1 + \ell_2)$ -th nonlinear Drude conductivity is defined by

$$\sigma^{x^{\ell_1} y^{\ell_2}; b} = \frac{(-e/\hbar)^{\ell_1+\ell_2+1}}{(i\omega + 1/\tau)^{\ell_1+\ell_2}} \int d\mathbf{k} f^{(0)} \frac{\partial^{\ell_1+\ell_2+1} \varepsilon}{\partial k_x^{\ell_1} \partial k_y^{\ell_2} \partial k_b}. \quad (378)$$

The static limit is obtained simply by setting  $\omega = 0$  in this equation.

We define the  $\ell$ -th order spin-dependent Drude conductivity for each spin  $s$  by the formula

$$\sigma_s^{x^{\ell_1} y^{\ell_2}; b} = \frac{(-e/\hbar)^{\ell_1+\ell_2+1}}{(i\omega + 1/\tau)^{\ell_1+\ell_2}} \int d\mathbf{k} f_s^{(0)} \frac{\partial^{\ell_1+\ell_2+1} \varepsilon_s}{\partial k_x^{\ell_1} \partial k_y^{\ell_2} \partial k_b}. \quad (379)$$

This formula is nontrivial only when

$$\frac{\partial^{\ell_1+\ell_2+1} \varepsilon_s}{\partial k_x^{\ell_1} \partial k_y^{\ell_2} \partial k_b} \neq 0, \quad (380)$$

which leads to a conclusion that there is no  $\ell$ -th order nonlinear spin-Drude conductivity for  $\ell \geq \ell_1 + \ell_2$ . It is necessary to calculate explicitly the  $\ell$ -th order nonlinear spin-Drude conductivity for  $\ell = 0, 1, \dots, \ell_1 + \ell_2 - 1$ . In particular, the choice of  $\ell = 0$  and 1 yield the persistent spin current without electric field and the linear spin conductivity, respectively.

We define the  $(\ell_1 + \ell_2)$ -th order nonlinear spin-Drude conductivity by

$$\sigma_{\text{spin}}^{x^{\ell_1} y^{\ell_2}; b} = \frac{\sigma_{\uparrow}^{x^{\ell_1} y^{\ell_2}; b} - \sigma_{\downarrow}^{x^{\ell_1} y^{\ell_2}; b}}{2}. \quad (381)$$

On the other hand, the charge conductivity is given by

$$\sigma_{\text{charge}}^{x^{\ell_1} y^{\ell_2}; b} = \sigma_{\uparrow}^{x^{\ell_1} y^{\ell_2}; b} + \sigma_{\downarrow}^{x^{\ell_1} y^{\ell_2}; b}. \quad (382)$$

Spin current is generated in linear response only for the  $d$ -wave altermagnet. The second-order nonlinear spin current is generated in the  $f$ -wave magnet, the third-order nonlinear spin current is generated in the  $g$ -wave altermagnet and the fifth-order nonlinear spin current is generated in the  $i$ -wave altermagnet[147]. The results are summarized in the following table.

	$s$	$p$	$d$	$f$	$g$	$i$
nodes	0	1	2	3	4	6
$\ell$			linear	2nd NL	3rd NL	5th NL
2D	None	None	$\sigma_{\text{spin}}^{y;x}$	$\sigma_{\text{spin}}^{xx;y}$	$\sigma_{\text{spin}}^{yyy;x}$	$\sigma_{\text{spin}}^{yyyy;x}$
3D	None	None	$\sigma_{\text{spin}}^{y;x}$	$\sigma_{\text{spin}}^{z;y;x}$	$\sigma_{\text{spin}}^{xxx;z}$	$\sigma_{\text{spin}}^{yyyy;x}$

(383)

## 2. Spin Nernst effects

The spin Nernst effect is an effect that spin current is generated perpendicularly to the thermal gradient. It is discussed in the  $d$ -wave altermagnet[37]. So far, there is no analytic result on it, which we derive.

Its momentum derivative reads

$$\frac{\partial f}{\partial \mathbf{k}} = \frac{\partial \varepsilon(\mathbf{k})}{\partial \mathbf{k}} \frac{\partial f}{\partial \varepsilon}, \quad (384)$$

while its spatial derivative reads

$$\frac{\partial f}{\partial \mathbf{r}} = \frac{\partial T(\mathbf{r})}{\partial \mathbf{r}} \frac{\partial f}{\partial T}. \quad (385)$$

We rewrite the Boltzmann equation as

$$\begin{aligned} \frac{df}{dt} &= \frac{\partial f}{\partial t} + \frac{\partial \mathbf{k}}{\partial t} \cdot \frac{\partial f}{\partial \mathbf{k}} + \frac{\partial \mathbf{r}}{\partial t} \cdot \frac{\partial f}{\partial \mathbf{r}} \\ &= \frac{\partial \mathbf{k}}{\partial t} \cdot \left( \frac{\partial \varepsilon(\mathbf{k})}{\partial \mathbf{k}} \frac{\partial f}{\partial \varepsilon} \right) + \frac{\partial \mathbf{r}}{\partial t} \cdot \left( \frac{\partial T(\mathbf{r})}{\partial \mathbf{r}} \frac{\partial f}{\partial T} \right) \\ &= -\frac{f - f^{(0)}}{\tau}. \end{aligned} \quad (386)$$

We use the kinetic equation

$$\frac{\partial \mathbf{r}}{\partial t} = \frac{1}{\hbar} \frac{\partial \varepsilon(\mathbf{k})}{\partial \mathbf{k}}, \quad (387)$$

$$\frac{\partial \mathbf{k}}{\partial t} = 0, \quad (388)$$

and obtain

$$\frac{1}{\hbar} \left( \frac{\partial \varepsilon(\mathbf{k})}{\partial \mathbf{k}} \cdot \frac{\partial T(\mathbf{r})}{\partial \mathbf{r}} \right) \frac{\partial f}{\partial T} = -\frac{f - f^{(0)}}{\tau}. \quad (389)$$

The first order expansion reads

$$\frac{1}{\hbar} \left( \frac{\partial \varepsilon(\mathbf{k})}{\partial \mathbf{k}} \cdot \frac{\partial T(\mathbf{r})}{\partial \mathbf{r}} \right) \frac{\partial f^{(0)}}{\partial T} = -\frac{f^{(1)}}{\tau}, \quad (390)$$

whose solution is given by

$$f^{(1)} = -\frac{\tau}{\hbar} \left( \frac{\partial \varepsilon(\mathbf{k})}{\partial \mathbf{k}} \cdot \frac{\partial T(\mathbf{r})}{\partial \mathbf{r}} \right) \frac{\partial f^{(0)}}{\partial T}. \quad (391)$$

The current driven by temperature gradient is given by

$$\begin{aligned} j_b &= -e \int d\mathbf{k} f^{(1)} v_b \\ &= \frac{e\tau}{\hbar^2} \int d\mathbf{k} \left( \frac{\partial \varepsilon(\mathbf{k})}{\partial \mathbf{k}} \cdot \frac{\partial T(\mathbf{r})}{\partial \mathbf{r}} \right) \frac{\partial \varepsilon}{\partial k_b} \frac{\partial f^{(0)}}{\partial T}. \end{aligned} \quad (392)$$

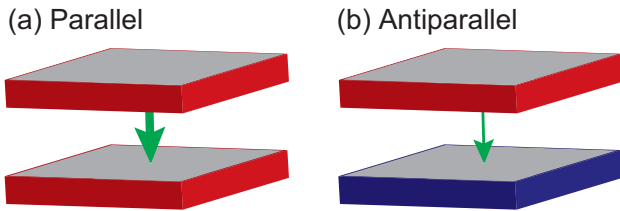


FIG. 3: Illustration of a bilayer magnetic tunneling junction made of magnets. (a) Parallel configuration, where the spin directions are identical at each lattice site between the two layers. (b) Antiparallel configuration, where the spin directions are opposite at each lattice site between the two layers. The green arrow indicates the tunneling current, which is larger in the parallel configuration.

Especially, current  $j_x$  and  $j_y$  flow when the temperature gradient is along the  $x$  axis,

$$j_x = e\tau \int d\mathbf{k} \left( \frac{1}{\hbar} \frac{\partial \varepsilon}{\partial k_x} \right)^2 \frac{\partial T(\mathbf{r})}{\partial x} \frac{\partial f^{(0)}}{\partial T}, \quad (393)$$

which is known as the Seebeck effect, and

$$\begin{aligned} j_y &= -e \int d\mathbf{k} f^{(1)} v_y \\ &= \frac{e\tau}{\hbar^2} \int d\mathbf{k} \frac{\partial \varepsilon}{\partial k_x} \cdot \frac{\partial T(\mathbf{r})}{\partial x} \frac{\partial \varepsilon}{\partial k_y} \frac{\partial f^{(0)}}{\partial T}, \end{aligned} \quad (394)$$

which is known as the Nernst effect. We assume that the temperature gradient is linear,

$$T(\mathbf{r}) = ax. \quad (395)$$

When  $\varepsilon(\mathbf{k}) - \mu \gg k_B T(\mathbf{r})$ , we approximate the Fermi distribution by the Boltzmann distribution,

$$f = \frac{1}{\exp\left(\frac{\varepsilon(\mathbf{k}) - \mu}{k_B T(\mathbf{r})}\right) + 1} \simeq \exp\left(-\frac{\varepsilon(\mathbf{k}) - \mu}{k_B T(\mathbf{r})}\right). \quad (396)$$

Then, the spin Hall conductivity is obtained as

$$j_s = \frac{e\tau}{\hbar^2} \frac{8e^{\mu/k_B T} J m \pi (2T - \mu)}{\sqrt{1 - 4J^2 m^2}} \quad (397)$$

for the  $d$ -wave altermagnet. It is proportional to the coupling constant  $J$  of the  $X$ -wave magnet in the Hamiltonian (330). Hence, it is possible to detect the sign of  $J$  by the spin Nernst effect. On the other hand, there is no spin current generation for the other  $X$ -wave magnets.

### 3. Tunneling magnetoresistance

Magnetic tunneling junction is a most successful spintronic device[183, 184]. It consists of the bilayer ferromagnets spaced by an insulator as shown in Fig.3, where the resistance is low (large) if the directions of spins are identical (opposite). It is called the tunneling magnetoresistance (TMR).

The spin direction of the memory can be readout by using the TMR. Tunneling magnetoresistance is discussed in the  $d$ -wave altermagnet[43, 185–191] and the  $p$ -wave magnet[192].

The differential conductance  $G = dI/dV$  is calculated based on the Green function[192],

$$\frac{G}{4e\pi^3} = \sum_{s=\pm 1} \sum_{\mathbf{k}_1, \mathbf{k}_2} |T_{\mathbf{k}_1, \mathbf{k}_2}|^2 \text{Tr} [\text{Im} \mathcal{G}_s^T(0; \mathbf{k}_1) \text{Im} \mathcal{G}_s^B(0; \mathbf{k}_2)], \quad (398)$$

where  $\mathcal{G}_s^T$  ( $\mathcal{G}_s^B$ ) is the retarded Green function of the top (bottom) layer defined by

$$\mathcal{G}_s^T(\omega; \mathbf{k}) \equiv \mathcal{G}_s^B(\omega; \mathbf{k}) \equiv \mathcal{G}_s(\omega; \mathbf{k}) \quad (399)$$

for the parallel configuration, and

$$\mathcal{G}_s^T(\omega; \mathbf{k}) \equiv \mathcal{G}_s(\omega; \mathbf{k}), \quad \mathcal{G}_s^B(\omega; \mathbf{k}) \equiv \mathcal{G}_{-s}(\omega; \mathbf{k}) \quad (400)$$

for the antiparallel configuration, where we have defined

$$\mathcal{G}_s(\omega; \mathbf{k}) \equiv \frac{1}{\hbar\omega - \varepsilon_s + i\Gamma} \quad (401)$$

with the self-energy  $\Gamma$  and the energy  $\varepsilon_s$ .  $\text{Im} \mathcal{G}_s(0; \mathbf{k}_1)$  represents the density of states depending on the spin  $s$ , which is shown in Fig.4(a) and (b).

The differential conductivity is determined by the overlap of the density of states  $\text{Im} \mathcal{G}_s(0; \mathbf{k}_1)$ , which is shown in Fig.4(c) and (d).

The differential conductivity for the parallel configuration is analytically given by[47]

$$\lim_{\Gamma \rightarrow 0} \frac{G_P}{4e\pi^3} = \frac{2m\pi^2}{\hbar^2\Gamma}, \quad (402)$$

while that for the antiparallel configuration is analytically given by

$$\lim_{\Gamma \rightarrow 0} \frac{G_{AP}}{4e\pi^3} = \sqrt{\frac{m}{2\mu}} \frac{N_X \pi^2}{\hbar a |J|}, \quad (403)$$

where  $J$  is the strength of the  $X$ -wave magnet,  $\Gamma$  is the self-energy,  $\mu$  is the chemical potential,  $a$  is the lattice constant and  $m$  is the mass of electrons. Hence, the TMR ratio is given by

$$\lim_{\Gamma \rightarrow 0} \text{TMR}_{\text{ratio}} \equiv \lim_{\Gamma \rightarrow 0} \frac{G_P - G_{AP}}{G_{AP}} = \frac{2a|J|\sqrt{2m\mu}}{N_X \hbar \Gamma}. \quad (404)$$

It is to be contrasted with the TMR ratio based on ferromagnets, where it is given by

$$\lim_{\Gamma \rightarrow 0} \text{TMR}_{\text{ratio}} = \frac{2J^2}{\Gamma^2}. \quad (405)$$

Therefore, the TMR ratio is larger in ferromagnets for  $|J| > \Gamma$ . However, the  $X$ -wave magnets are expected to achieve high-speed and ultra-dense memory owing to the zero net magnetization.

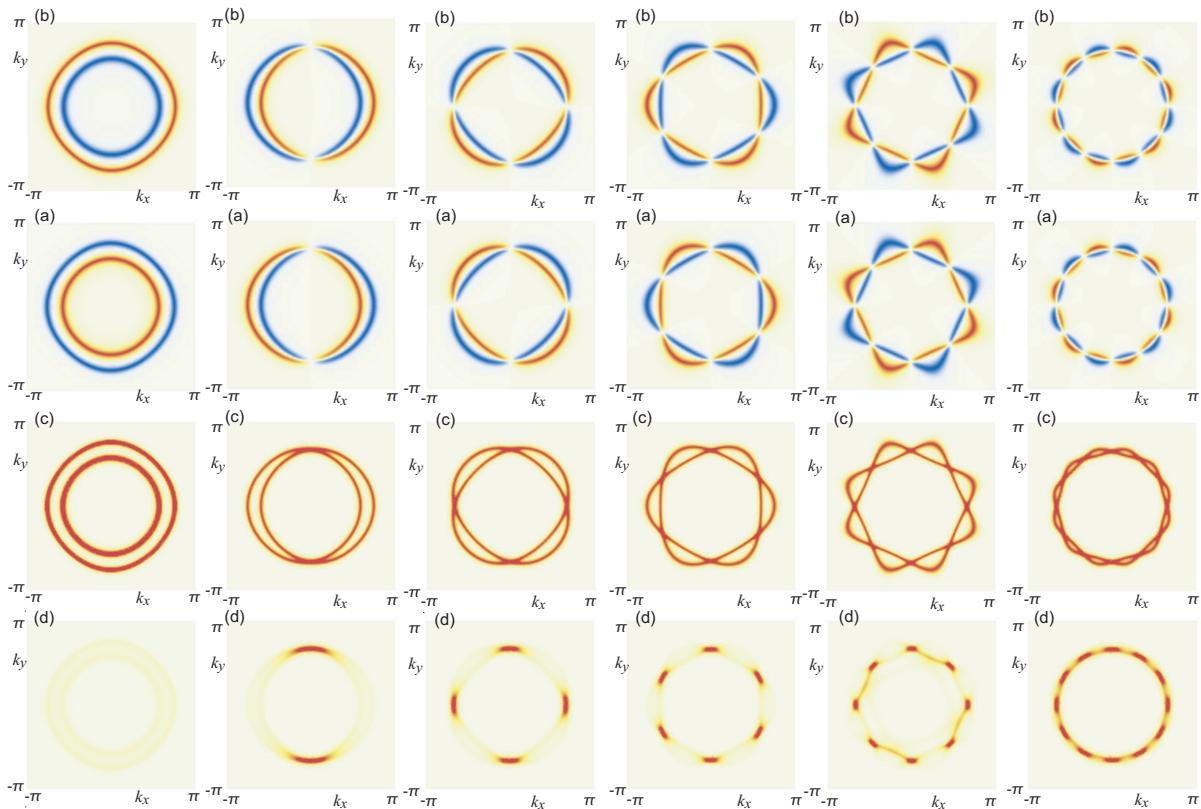


FIG. 4: (a) Spin density  $\langle S_z \rangle$  when  $J > 0$ , and (b) that when  $J < 0$  in one layer. Red (blue) color indicates up (down) spin. (c) Overlap  $\mathcal{O}_P$  for the parallel configuration, and (d) overlap  $\mathcal{O}_{AP}$  for the antiparallel configuration. Red color indicates a large overlap.

## B. With Rashba interaction

### 1. Anomalous Hall effects

One of the motivation of studying altermagnets is that the Néel vector can be readout by measuring anomalous Hall conductivity because time-reversal symmetry is broken[162, 165, 193, 194]. Actually, it is verified by the density-functional theory and experiments.

The Berry curvature is obtained as

$$\Omega_X = -\frac{\lambda^2 (B + Jf_X - Jk\partial_k f_X)}{2 \left( (B + Jf_X)^2 + \lambda^2 k^2 \right)^{3/2}}. \quad (406)$$

The Hall conductivity is calculated as

$$\frac{1}{2\pi} \int \Omega_X d\mathbf{k} = -\frac{1}{2} \text{sgn} B. \quad (407)$$

It does not depend on  $J$ . Hence, it is impossible to detect the sign of  $J$  by measuring the anomalous Hall conductivity based on the two-band model. It is necessary to introduce the orbital degrees of freedom to the two-band model.

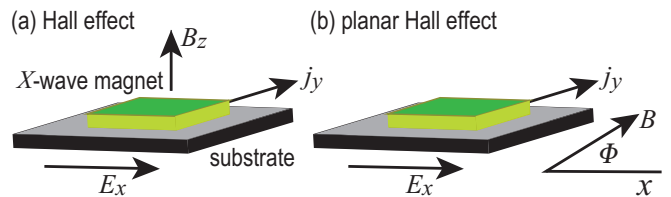


FIG. 5: Illustration for (a) Hall effect and (b) planar Hall effect. In the planar Hall effect, when the electric field is applied along the  $x$  axis and the magnetic field  $(B \cos \Phi, B \sin \Phi, 0)$  is applied parallel to the system, the Hall current flows along the  $y$  axis. The Hall conductivity is predicted to be given by the formula (411).

### 2. Planar Hall effects

The Hall effect is a prominent phenomenon in two-dimensional materials. A current flows into a direction perpendicular to the applied electric field, when the magnetic field is applied perpendicular to the plane, as illustrated in Fig.5(a). Similarly, a current flows into a direction perpendicular to the applied electric field, when the magnetic field is applied parallel to the plane, as illustrated in Fig.5(b). It is the planar Hall effect[195–201]. The planar Hall effect is discussed in  $d$ -wave altermagnets[202, 203].

The planar Hall effect is discussed in the  $X$ -wave magnet[46]. The Dirac point shifts in the presence of the

in-plane magnetic field. The shifted Dirac point is given by  $(k'_x, k'_y) = 0$ , where

$$k'_x = k_x + \frac{B_y}{\lambda}, \quad k'_y = k_y - \frac{B_x}{\lambda}, \quad (408)$$

by solving the equation

$$\lambda(k_x \sigma_y - k_y \sigma_x) + B_x \sigma_x + B_y \sigma_y = 0. \quad (409)$$

The Dirac gap is explicitly determined as

$$\Delta = (-1)^{s_X} \frac{B^{N_X}}{\lambda^{N_X}} \sin N_X \Phi, \quad (410)$$

which leads to the Hall conductance

$$\sigma_{xy} = \frac{e^2}{h} \frac{(-1)^{s_X}}{2} \text{sgn} \left( J \frac{B^{N_X}}{\lambda^{N_X}} \sin N_X \Phi \right), \quad (411)$$

where  $s_X = 1, 1, -1, -1, 1$  for  $X = p, d, f, g, i$ , respectively.

## IX. QUANTUM HALL EFFECTS

### A. Landau levels

If we apply magnetic field perpendicular to the sample, Landau levels are formed. Landau levels are obtained for the  $d$ -wave altermagnet[204, 205]. We apply a homogeneous magnetic field  $\mathbf{B} = \nabla \times \mathbf{A} = (0, 0, -B)$  with  $B > 0$  along the  $z$  axis to the sample. The Hamiltonian under magnetic field is obtained by replacing the momentum  $k_i$  to the co-variant momentum  $P_i \equiv k_i + eA_i$ . We introduce a pair of Landau-level ladder operators,

$$\hat{a} = \frac{\ell_B(P_x + iP_y)}{\sqrt{2\hbar}}, \quad \hat{a}^\dagger = \frac{\ell_B(P_x - iP_y)}{\sqrt{2\hbar}}, \quad (412)$$

satisfying the bosonic commutation relation  $[\hat{a}, \hat{a}^\dagger] = 1$ , where  $\ell_B = \sqrt{\hbar/eB}$  is the magnetic length. The inverse relations read

$$P_x = \frac{\hbar}{\sqrt{2}\ell_B} (\hat{a} + \hat{a}^\dagger), \quad P_y = \frac{\hbar}{i\sqrt{2}\ell_B} (\hat{a} - \hat{a}^\dagger). \quad (413)$$

The Hamiltonian for free electrons reads

$$H_0 = \hbar\omega_0 \hat{a}^\dagger \hat{a}. \quad (414)$$

#### 1. $p$ -wave magnets and coherent states

By inserting Eq.(413) to Eq.(309), the  $p$ -wave term under magnetic field reads

$$f_p^{2D}(\mathbf{k}) = \frac{a\hbar}{\sqrt{2}\ell_B} (\hat{a} + \hat{a}^\dagger). \quad (415)$$

The Hamiltonian is identical to that of the coherent state

$$\hat{H} = \hbar\omega_0 \hat{a}^\dagger \hat{a} + c^* \hat{a} + c \hat{a}^\dagger \quad (416)$$

provided

$$c = c^* = \frac{a\hbar}{\sqrt{2}\ell_B}. \quad (417)$$

It is diagonalized as

$$\hat{H} = \hbar\omega \hat{b}^\dagger \hat{b} - c^2/\hbar\omega, \quad (418)$$

where we have introduced displaced operators

$$\hat{b} \equiv \hat{a} + c/\hbar\omega, \quad \hat{b}^\dagger \equiv \hat{a}^\dagger + c/\hbar\omega. \quad (419)$$

The energy of the landau level is obtained as

$$\hat{H} = \hbar\omega N - \frac{a^2\hbar}{2\ell_B^2\omega}, \quad (420)$$

while the eigenstate is determined as

$$|N\rangle_b \equiv \frac{1}{\sqrt{N!}} (\hat{b}^\dagger)^N |0\rangle. \quad (421)$$

#### 2. $d$ -wave altermagnets and squeezed states

By inserting Eq.(413) to Eq.(310), the  $d$ -wave term under magnetic field reads

$$f_{d'}^{2D}(\mathbf{k}) = \frac{\hbar^2 a^2}{2\ell_B^2} \left( (\hat{a} + \hat{a}^\dagger)^2 + (\hat{a} - \hat{a}^\dagger)^2 \right) \quad (422)$$

$$= \frac{\hbar^2 a^2}{\ell_B^2} \left( (\hat{a}^\dagger)^2 + \hat{a}^2 \right). \quad (423)$$

The Hamiltonian is identical to that of the squeezed state,

$$\hat{\mathcal{H}} \equiv \hbar\omega_0 + \frac{c}{2} (\hat{a}^\dagger)^2 + \frac{c^*}{2} \hat{a}^2 \quad (424)$$

provided

$$c = c^* = \frac{2\hbar^2 a^2}{\ell_B^2}. \quad (425)$$

It is diagonalized as

$$H = \hbar\omega \hat{b}^\dagger \hat{b} - \hbar \frac{\omega_0 - \omega}{2} \quad (426)$$

with

$$\omega = \sqrt{\omega_0^2 - c^2}, \quad (427)$$

where we have made the Bogoliubov transformation of bosons

$$\begin{pmatrix} \hat{b} \\ \hat{b}^\dagger \end{pmatrix} = \begin{pmatrix} \cosh r & -\sinh r \\ -\sinh r & \cosh r \end{pmatrix} \begin{pmatrix} \hat{a} \\ \hat{a}^\dagger \end{pmatrix} \quad (428)$$

with

$$\tanh 2r = c/\hbar\omega. \quad (429)$$

The energy of the landau level is obtained as

$$E_n = \hbar\omega N - \hbar \frac{\omega_0 - \omega}{2}, \quad (430)$$

while the eigenstate is determined as

$$|N\rangle_b \equiv \frac{1}{\sqrt{N!}} (\hat{b}^\dagger)^N |0\rangle. \quad (431)$$

### 3. $X$ -wave magnets

In general, it is hard to exactly diagonalize the Hamiltonian except for the  $p$ -wave magnet and the  $d$ -wave altermagnet because the Hamiltonian contains more than quadratic order of the creation and annihilation operators. However, it is possible to numerically obtain the energy of the Landau levels by using the states

$$|N\rangle = \frac{1}{\sqrt{N!}} (a^\dagger)^N |0\rangle. \quad (432)$$

### B. Magneto-optical conductivity

Optical absorption between Landau levels are known as magneto-optical conductivity, which is calculated by the Kubo formula[206–209],

$$\begin{aligned} \sigma_{\mu\nu}(\omega) &= -i\hbar e^2 \int d\mathbf{k} \\ &\times \sum_{n \neq m} \frac{f(\varepsilon_n(\mathbf{k})) - f(\varepsilon_m(\mathbf{k}))}{(\varepsilon_n(\mathbf{k}) - \varepsilon_m(\mathbf{k}))(\varepsilon_n(\mathbf{k}) - \varepsilon_m(\mathbf{k}) + \hbar\omega + i\Gamma)} \\ &\times [\langle \psi_n(\mathbf{k}) | v_\mu | \psi_m(\mathbf{k}) \rangle \langle \psi_m(\mathbf{k}) | v_\nu | \psi_n(\mathbf{k}) \rangle] \end{aligned} \quad (433)$$

with the velocity operators

$$v_x \equiv \frac{\partial H}{\partial P_x}, \quad v_y \equiv \frac{\partial H}{\partial P_y}. \quad (434)$$

Especially, the magneto-optical conductivity for the  $d$ -wave altermagnet is studied[204].

#### 1. $p$ -wave magnets

We first study magneto-optical conductivity for the  $p$ -wave magnet. The velocity operators are explicitly obtained as

$$\begin{aligned} v_x &= \frac{\partial H}{\partial P_x} = \frac{\partial \hat{b}^\dagger}{\partial P_x} \frac{\partial H}{\partial \hat{b}^\dagger} + \frac{\partial \hat{b}}{\partial P_x} \frac{\partial H}{\partial \hat{b}} \\ &= \frac{\ell_B \omega}{\sqrt{2}} (\hat{b} + \hat{b}^\dagger), \end{aligned} \quad (435)$$

and

$$\begin{aligned} v_y &= \frac{\partial H}{\partial P_y} = \frac{\partial \hat{b}^\dagger}{\partial P_y} \frac{\partial H}{\partial \hat{b}^\dagger} + \frac{\partial \hat{b}}{\partial P_y} \frac{\partial H}{\partial \hat{b}} \\ &= i \frac{\ell_B \omega}{\sqrt{2}} (-\hat{b} + \hat{b}^\dagger), \end{aligned} \quad (436)$$

where we have used

$$\hat{b} = \frac{\ell_B}{\sqrt{2}\hbar} (P_x + iP_y) + \frac{c}{\hbar\omega}, \quad (437)$$

$$\hat{b}^\dagger = \frac{\ell_B}{\sqrt{2}\hbar} (P_x - iP_y) + \frac{c^*}{\hbar\omega}, \quad (438)$$

derived from Eq.(419). The interband matrix elements  $\langle \psi_n(\mathbf{k}) | v_\mu | \psi_m(\mathbf{k}) \rangle$  and  $\langle \psi_m(\mathbf{k}) | v_\nu | \psi_n(\mathbf{k}) \rangle$  are nonzero for  $m = n \pm 1$ . Then, the optical absorption occurs between the adjacent Landau levels. There are nonzero  $\text{Re}\sigma_{xx}$ ,  $\text{Re}\sigma_{yy}$  and  $\text{Im}\sigma_{xy}$  because  $v_x$  is real and  $v_y$  is imaginary.

#### 2. $d$ -wave altermagnets

We next study magneto-optical conductivity for the  $d$ -wave altermagnet. The velocity operators are explicitly obtained as

$$\begin{aligned} v_x &= \frac{\partial H}{\partial P_x} = \frac{\partial \hat{b}^\dagger}{\partial P_x} \frac{\partial H}{\partial \hat{b}^\dagger} + \frac{\partial \hat{b}}{\partial P_x} \frac{\partial H}{\partial \hat{b}} \\ &= \frac{\ell_B \omega}{\sqrt{2} (\cosh r + \sinh r)} (\hat{b} + \hat{b}^\dagger), \end{aligned} \quad (439)$$

and

$$\begin{aligned} v_y &= \frac{\partial H}{\partial P_y} = \frac{\partial \hat{b}^\dagger}{\partial P_y} \frac{\partial H}{\partial \hat{b}^\dagger} + \frac{\partial \hat{b}}{\partial P_y} \frac{\partial H}{\partial \hat{b}} \\ &= \frac{-i\ell_B \omega}{\sqrt{2} (\cosh r - \sinh r)} (\hat{b} - \hat{b}^\dagger) \end{aligned} \quad (440)$$

where we have used

$$\hat{b} = \frac{\ell_B}{\sqrt{2}} \left( \frac{P_x}{\cosh r + \sinh r} + \frac{iP_y}{\cosh r - \sinh r} \right), \quad (441)$$

$$\hat{b}^\dagger = \frac{\ell_B}{\sqrt{2}} \left( \frac{P_x}{\cosh r + \sinh r} - \frac{iP_y}{\cosh r - \sinh r} \right), \quad (442)$$

derived from Eq.(428). The interband matrix elements  $\langle \psi_n(\mathbf{k}) | v_\mu | \psi_m(\mathbf{k}) \rangle$  and  $\langle \psi_m(\mathbf{k}) | v_\nu | \psi_n(\mathbf{k}) \rangle$  are nonzero for  $m = n \pm 1$ . Then, the optical absorption occurs between the adjacent Landau levels. There are nonzero  $\text{Re}\sigma_{xx}$ ,  $\text{Re}\sigma_{yy}$  and  $\text{Im}\sigma_{xy}$  because  $v_x$  is real and  $v_y$  is imaginary.

### C. Magnetic circular dichroism

Circular dichroism is a phenomenon that the optical absorption is different between the right-hand and left-hand polarized light,

$$\sigma_\pm = \sigma_{xx} \pm i\sigma_{xy}. \quad (443)$$

Its real part is given by

$$\text{Re}\sigma_\pm = \text{Re}\sigma_{xx} \mp \text{Im}\sigma_{xy}. \quad (444)$$

By using it, the degree of the circular dichroism is evaluated by the quantity

$$I_{\text{CD}} \equiv \frac{\text{Re}\sigma_+ - \text{Re}\sigma_-}{\text{Re}\sigma_+ + \text{Re}\sigma_-} = -\frac{\text{Im}\sigma_{xy}}{\text{Re}\sigma_{xx}}. \quad (445)$$

Hence, circular dichroism occurs when  $\text{Im}\sigma_{xy} \neq 0$ . Indeed, it occurs in the case of the  $p$ -wave magnet and the  $d$ -wave altermagnet, where  $\text{Im}\sigma_{xy} \neq 0$  as we have seen.

## X. FRIEDEL OSCILLATION

We study the effect of an impurity. Friedel oscillation is that the local the density of states (LDOS) oscillates in the presence of the impurity. We show that this LDOS has the  $X$ -wave symmetry for the  $X$ -wave magnet. The energy-dependent LDOS is determined by

$$\rho(\omega, \mathbf{r}) = -\frac{1}{\pi} \text{Im} G^{\text{R}}(\omega, \mathbf{r}, \mathbf{r}), \quad (446)$$

where  $G(\omega, \mathbf{r}, \mathbf{r})$  is the real space representation of the retarded Green function in the presence of the impurity defined by

$$G^{\text{R}}(\omega, \mathbf{r}, \mathbf{r}') \equiv \langle \mathbf{r} | \frac{1}{\hbar\omega - H + i\eta} | \mathbf{r}' \rangle. \quad (447)$$

The Green function is obtained by using the Dyson equation

$$\begin{aligned} G^{\text{R}}(\omega, \mathbf{r}, \mathbf{r}') \\ = G_0^{\text{R}}(\omega, \mathbf{r}, \mathbf{r}') \\ + \int d\mathbf{r}_1 d\mathbf{r}_2 G_0^{\text{R}}(\omega, \mathbf{r}, \mathbf{r}_1) T(\omega, \mathbf{r}_1, \mathbf{r}_2) G_0^{\text{R}}(\omega, \mathbf{r}_2, \mathbf{r}') \end{aligned} \quad (448)$$

with the T matrix

$$T(\omega, \mathbf{r}, \mathbf{r}_1) \equiv V(1 - G_0^{\text{R}}(\omega, \mathbf{r}, \mathbf{r}_1)V)^{-1}. \quad (449)$$

We assume that the impurity is described by the delta function potential

$$(V_0\sigma_0 + V_s\sigma_z)\delta(r), \quad (450)$$

where  $V_0$  describes a non-magnetic impurity and  $V_s$  describes a magnetic impurity. It is enough to study spin-dependent potential

$$(V_0 + V_s s)\delta(r) \quad (451)$$

with  $s = \pm 1$  because the spin operator is diagonal. In this case, the T matrix has a form

$$T(\omega, \mathbf{r}, \mathbf{r}_1) = T(\omega)\delta(\mathbf{r})\delta(\mathbf{r}'), \quad (452)$$

which leads to the Dyson equation

$$\begin{aligned} G^{\text{R}}(\omega, \mathbf{r}, \mathbf{r}') \\ = G_0^{\text{R}}(\omega, \mathbf{r}, \mathbf{r}') + G_0^{\text{R}}(\omega, \mathbf{r}, \mathbf{0}) T(\omega) G_0^{\text{R}}(\omega, \mathbf{0}, \mathbf{r}'). \end{aligned} \quad (453)$$

For small  $V$ , the difference of the local density of states is simply given by

$$\begin{aligned} \delta\rho &\equiv -\frac{1}{\pi} \text{Im} [G^{\text{R}}(\omega, \mathbf{r}, \mathbf{r}) - G^{\text{R}}(\omega, \mathbf{r}, \mathbf{r}')] \\ &= -\frac{1}{\pi} \text{Im} [VG_0^{\text{R}}(\omega, \mathbf{r}, \mathbf{0})G_0^{\text{R}}(\omega, \mathbf{0}, \mathbf{r}')]^2. \end{aligned} \quad (454)$$

The real space Green function is obtained by the Fourier transformation of the momentum space Green function as

$$\begin{aligned} G_0^{\text{R}}(\omega, \mathbf{r}, \mathbf{r}') &= G_0^{\text{R}}(\omega, \mathbf{r} - \mathbf{r}', \mathbf{0}) \\ &\equiv \frac{1}{(2\pi)^2} \int e^{-\mathbf{k}\cdot(\mathbf{r}-\mathbf{r}')} G_0^{\text{R}}(\omega, \mathbf{k}) d\mathbf{k}, \end{aligned} \quad (455)$$

with

$$G_0^{\text{R}}(\omega, \mathbf{k}) \equiv \frac{1}{i\omega - H + i\eta} \quad (456)$$

where we have used the translational symmetry of the Green function in the absence of the impurity.

### A. Free electrons

First, we review the Friedel oscillation of free electrons. We derive the real space representation of the Green function in the presence of the impurity and determine the symmetry of the LDOS. The Green function for free electrons is given by

$$G_0^{\text{R}}(\omega, \mathbf{k}) = \frac{1}{\frac{\hbar^2}{2m}(k_0^2 - k^2) + i\eta}, \quad (457)$$

where we have set

$$\omega = \frac{\hbar^2 k_0^2}{2m}. \quad (458)$$

We make a Fourier transformation

$$\begin{aligned} G_0^{\text{R}}(r) &= \frac{1}{(2\pi)^2} \int_0^\infty k \frac{e^{ikr \cos(\theta-\phi)}}{\frac{\hbar^2}{2m}(k_0^2 - k^2) + i\eta} dk d\theta \\ &= \frac{1}{2\pi} \int_0^\infty \frac{k J_0(kr)}{\frac{\hbar^2}{2m}(k_0^2 - k^2) + i\eta} dk, \end{aligned} \quad (459)$$

where  $J_0$  is the Bessel function and we have used the formula

$$\int_0^{2\pi} e^{ikr \cos \theta} d\theta = 2\pi J_0(kr). \quad (460)$$

The Bessel function is decomposed as the Hankel function

$$J_0(kr) = \frac{H_0^{(1)}(kr) + H_0^{(2)}(kr)}{2}, \quad (461)$$

where  $H_0^{(1)}(kr)$  ( $H_0^{(2)}(kr)$ ) is the Hankel function the first (second) kind. The asymptotic forms of the Hankel functions are given by

$$H_0^{(1)}(kr) \sim \sqrt{\frac{2}{\pi kr}} e^{i(kr - \frac{\pi}{4})}, \quad (462)$$

$$H_0^{(2)}(kr) \sim \sqrt{\frac{2}{\pi kr}} e^{-i(kr - \frac{\pi}{4})}. \quad (463)$$

We make a complex integral

$$G_0(r) = \frac{1}{16\pi} \int_{-\infty}^{\infty} k \frac{(H_0^{(1)}(kr) + H_0^{(2)}(kr))}{\frac{\hbar^2}{2m}(k_0^2 - k^2) + i\eta} dk, \quad (464)$$

where poles exist at

$$k = \pm k_0 + i\eta. \quad (465)$$

We take the upper half circle for  $H_0^{(1)}(kr)$  and the lower half circle for  $H_0^{(2)}(kr)$  so that the complex integral converges. Only the contribution from  $H_0^{(1)}(kr)$  is nonzero and the Green function is calculated as

$$\begin{aligned} G_0(r) &= \frac{1}{16\pi} \int_{-\infty}^{\infty} \frac{k H_0^{(1)}(kr)}{\frac{\hbar^2}{2m}(k_0^2 - k^2) + i\eta} dk \\ &= \frac{i}{8} \left( H_0^{(1)}(k_0 r) + H_0^{(1)}(-k_0 r) \right) \\ &= \frac{i}{4} H_0^{(1)}(k_0 r). \end{aligned} \quad (466)$$

Then, the LDOS has the  $s$ -wave symmetry.

### B. $p$ -wave magnets

Second, we study the Friedel oscillation of the  $p$ -wave magnet[211]. We calculate the real space representation of the Green function

$$\begin{aligned} G(r) &= \frac{1}{(2\pi)^2} \int_0^{\infty} k \frac{e^{ikr \cos(\theta-\phi)}}{\frac{\hbar^2}{2m}(k_0^2 - k^2) - sJk \cos \phi + i\eta} dk d\theta \\ &= \frac{1}{2\pi} \int_0^{\infty} \frac{k J_0(kr)}{\frac{\hbar^2}{2m}(k_0^2 - k^2) - sJk \cos \phi + i\eta} dk. \end{aligned} \quad (467)$$

Poles exist at

$$k_p = -\frac{sJm \cos \phi}{\hbar^2} \pm \sqrt{k_0^2 + \frac{J^2 m^2}{\hbar^4} \cos^2 \phi + i\eta}, \quad (468)$$

and we obtain

$$G(r) = \frac{i}{4} H_0^{(1)}(k_p r). \quad (469)$$

Then, the LDOS has the  $p$ -wave symmetry and spin dependence.

### C. $d$ -wave altermagnets

Third, we study the Friedel oscillation of the  $d$ -wave altermagnet[210, 211]. We calculate the real space representation of the Green function

$$\begin{aligned} G(r) &= \frac{1}{(2\pi)^2} \int_0^{\infty} k \frac{e^{ikr \cos(\theta-\phi)}}{k_0^2 - k^2 - sJk^2 \cos \phi + i\eta} dk d\theta \\ &= \frac{1}{2\pi} \int_0^{\infty} \frac{k J_0(kr)}{\frac{\hbar^2}{2m}(k_0^2 - k^2) - sJk^2 \cos \phi + i\eta} dk \end{aligned} \quad (470)$$

Poles exist at

$$k_d = \pm \frac{k_0}{\sqrt{1 + \frac{2msJ}{\hbar^2} \cos \phi}} + i\eta, \quad (471)$$

and we obtain

$$G(r) = \frac{i}{4} H_0^{(1)}(k_d r). \quad (472)$$

Then, the LDOS has the  $d$ -wave symmetry.

### D. $X$ -wave magnets

Finally, we study the Friedel oscillation of the  $X$ -wave magnet. We calculate the real space representation of the Green function

$$\begin{aligned} G(r) &= \frac{1}{(2\pi)^2} \int_0^{\infty} k \frac{e^{ikr \cos(\theta-\phi)}}{k_0^2 - k^2 - f_{X,X'}^{2D}(\mathbf{k}) + i\eta} dk d\theta \\ &= \frac{1}{2\pi} \int_0^{\infty} \frac{k J_0(kr)}{\frac{\hbar^2}{2m}(k_0^2 - k^2) - f_{X,X'}^{2D}(\mathbf{k}) + i\eta} dk \end{aligned} \quad (473)$$

The pole is determined by the solution of

$$\frac{\hbar^2}{2m}(k_0^2 - k_{X,X'}^2) - f_{X,X'}^{2D}(\mathbf{k}_{X,X'}) + i\eta = 0, \quad (474)$$

which has the  $X$ -wave symmetry although it is hard to obtain analytic formula except for the  $p$ -wave magnet and the  $d$ -wave altermagnet. By using it, we obtain

$$G(r) = \frac{i}{4} H_0^{(1)}(k_{X,X'} r). \quad (475)$$

Then, the LDOS has the  $X$ -wave symmetry and spin dependence.

## XI. SUMMARIES, DISCUSSIONS AND OUTLOOKS

We reviewed recent progress on quantum geometry and  $X$ -wave magnets. We systematically formulated quantum geometry based on the quantum distance. Quantum geometry is generalized to the Zeemann quantum geometry, non-Hermitian quantum geometry and quantum information geometry. Then, we reviewed the  $X$ -wave magnets including altermagnets and  $p$ -wave magnets in a universal manner. Universal transport properties were discussed for the  $X$ -wave magnets.

In this paper, we have derived various analytic formulas based on the two-band Hamiltonian. However, actual materials are more complicated. For example, four-band models including the orbital degrees of freedom have been studied[45, 148]. Nevertheless, if there are only two bands at the Fermi energy, the effective Hamiltonian is reduced to be a two-band Hamiltonian[32]. In addition, optical absorption is well described by the two-band Hamiltonian consisting of the valence and conduction bands. The two-band Hamiltonian reveals the basic structure of the relevant phenomena in these cases. It is an interesting problem to study based on more realistic models.

In passing, we give some outlooks. The general relativistic quantities such as the Christoffel symbols are defined based



on the quantum metric as shown in Sec.IIF. However, it is not clear whether there are physical observable quantities such as nonlinear conductivities or nonlinear optical conductivities directly relating to them. Quantum geometry is mainly studied in the context of condensed matter physics. Applications of the notion of quantum geometry to quantum information and quantum computing are still rare, where quantum information geometry for density matrices will be useful. There will be developments in this direction. Zeeman quantum geometry will be useful for spintronics.

Magnonic properties of the  $X$ -wave magnets will also be interesting, which are mainly studied so far for  $d$ -wave altermagnets[212, 213] and  $g$ -wave altermagnets[214]. The magnon spectrum is given by[215]

$$E_{\pm}(\mathbf{k}) = vk + \kappa k^3 \pm Jk^{N_x} \sin N_X \phi \quad (476)$$

for the  $X$ -wave magnet in general. With respect to material realization of the  $X$ -wave magnets, there are no experiments on the  $f$ -wave,  $g$ -wave and  $i$ -wave magnets in two dimensions and the  $f$ -wave and  $i$ -wave magnets in three dimensions. In this paper, we have mainly focused on electronic and optical properties coupled with the  $X$ -wave magnet. On the other hand, the control of the magnetism of the  $X$ -wave magnet is also important. It is a nontrivial problem to switch the direction of the spins of the  $X$ -wave magnet. In order to switch the direction of spins, multiferroic altermagnets[216, 217] are promising because the spin direction is reversed by applying electric field. It is a fascinating problem both theoretically and experimentally to search universal physics in the viewpoint of the  $X$ -wave magnets.

### Acknowledgements

The author is grateful to N. Nagaosa, M. Hirschberger, S. Okumura, Y. Motome, T. Morimoto, H. Seo, J. Wang, B. J. Yang and W. Chen for helpful discussions on the subject. This work is supported by CREST, JST (Grants No. JPMJCR20T2) and Grants-in-Aid for Scientific Research from MEXT KAKENHI (Grant No. 23H00171).

### Appendices

#### Appendix A: Quantum distance and Abelian quantum geometric tensor

The Hilbert-Schmidt distance is defined by

$$(d_{\text{SHS}})^2 \equiv 1 - |\langle \psi_n(\mathbf{k}) | \psi_n(\mathbf{k}) + d\mathbf{k} \rangle|^2. \quad (A1)$$

The wave function is expanded as

$$\begin{aligned} & |\psi_n(\mathbf{k} + d\mathbf{k})\rangle \\ &= |\psi_n(\mathbf{k})\rangle + |\partial_{k_\mu} \psi_n(\mathbf{k})\rangle dk_\mu \\ &+ \frac{1}{2} |\partial_{k_\mu} \partial_{k_\nu} \psi_n(\mathbf{k})\rangle dk_\mu dk_\nu + \dots \end{aligned} \quad (A2)$$

The inner product reads

$$\begin{aligned} & |\langle \psi_n(\mathbf{k}) | \psi_n(\mathbf{k}') \rangle|^2 \\ &= \langle \psi_n(\mathbf{k}') | \psi_n(\mathbf{k}) \rangle \langle \psi_n(\mathbf{k}) | \psi_n(\mathbf{k}') \rangle \\ &= \langle \psi_n(\mathbf{k}) | \psi_n(\mathbf{k}) \rangle \\ &+ (\langle \partial_{k_\mu} \psi_n(\mathbf{k}) | \psi_n(\mathbf{k}) \rangle + \langle \psi_n(\mathbf{k}) | \partial_{k_\mu} \psi_n(\mathbf{k}) \rangle) dk_\mu \\ &+ \left( \frac{1}{2} \langle \partial_{k_\mu} \partial_{k_\nu} \psi_n(\mathbf{k}) | \psi_n(\mathbf{k}) \rangle + \frac{1}{2} \langle \psi_n(\mathbf{k}) | \partial_{k_\mu} \partial_{k_\nu} \psi_n(\mathbf{k}) \rangle \right) \\ &+ \langle \partial_{k_\mu} \psi_n(\mathbf{k}) | \psi_n(\mathbf{k}) \rangle \langle \psi_n(\mathbf{k}) | \partial_{k_\mu} \psi_n(\mathbf{k}) \rangle dk_\mu dk_\nu. \end{aligned} \quad (A3)$$

The term proportional to  $dk_\mu$  is zero because

$$\begin{aligned} & (\langle \partial_{k_\mu} \psi_n(\mathbf{k}) | \psi_n(\mathbf{k}) \rangle + \langle \psi_n(\mathbf{k}) | \partial_{k_\mu} \psi_n(\mathbf{k}) \rangle) \\ &= \partial_{k_\mu} (\langle \psi_n(\mathbf{k}) | \psi_n(\mathbf{k}) \rangle) = 0, \end{aligned} \quad (A4)$$

where we have used the normalization condition  $\langle \psi_n(\mathbf{k}) | \psi_n(\mathbf{k}) \rangle = 1$ . By using the relation

$$\begin{aligned} & \partial_{k_\mu} \partial_{k_\nu} (\langle \psi_n(\mathbf{k}) | \psi_n(\mathbf{k}) \rangle) \\ &= \langle \partial_{k_\mu} \partial_{k_\nu} \psi_n(\mathbf{k}) | \psi_n(\mathbf{k}) \rangle + \langle \psi_n(\mathbf{k}) | \partial_{k_\mu} \partial_{k_\nu} \psi_n(\mathbf{k}) \rangle \\ &+ \langle \partial_{k_\mu} \psi_n(\mathbf{k}) | \partial_{k_\nu} \psi_n(\mathbf{k}) \rangle + \langle \partial_{k_\nu} \psi_n(\mathbf{k}) | \partial_{k_\mu} \psi_n(\mathbf{k}) \rangle, \end{aligned} \quad (A5)$$

we have

$$\begin{aligned} & \frac{1}{2} \langle \partial_{k_\mu} \partial_{k_\nu} \psi_n(\mathbf{k}) | \psi_n(\mathbf{k}) \rangle + \frac{1}{2} \langle \psi_n(\mathbf{k}) | \partial_{k_\mu} \partial_{k_\nu} \psi_n(\mathbf{k}) \rangle \\ &= -\frac{1}{2} (\langle \partial_{k_\mu} \psi_n(\mathbf{k}) | \partial_{k_\nu} \psi_n(\mathbf{k}) \rangle \\ &+ \langle \partial_{k_\nu} \psi_n(\mathbf{k}) | \partial_{k_\mu} \psi_n(\mathbf{k}) \rangle) dk_\mu dk_\nu \\ &= -\langle \partial_{k_\mu} \psi_n(\mathbf{k}) | \partial_{k_\nu} \psi_n(\mathbf{k}) \rangle dk_\mu dk_\nu. \end{aligned} \quad (A6)$$

Then, the inner product is written as

$$\begin{aligned} & |\langle \psi_n(\mathbf{k}) | \psi_n(\mathbf{k}') \rangle|^2 \\ &= 1 + (\langle \partial_{k_\mu} \psi_n(\mathbf{k}) | \psi_n(\mathbf{k}) \rangle \langle \psi_n(\mathbf{k}) | \partial_{k_\mu} \psi_n(\mathbf{k}) \rangle \\ &- \langle \partial_{k_\mu} \psi_n(\mathbf{k}) | \partial_{k_\nu} \psi_n(\mathbf{k}) \rangle) dk_\mu dk_\nu \\ &= 1 + \langle \partial_{k_\mu} \psi_n(\mathbf{k}) | (\langle \psi_n(\mathbf{k}) \rangle \langle \psi_n(\mathbf{k}) | - 1) | \partial_{k_\mu} \psi_n(\mathbf{k}) \rangle dk_\mu dk_\nu, \end{aligned} \quad (A7)$$

and the quantum distance reads

$$\begin{aligned} & (d_{\text{SHS}})^2 \\ &\equiv \langle \partial_{k_\mu} \psi_n(\mathbf{k}) | \left( 1 - |\psi_n(\mathbf{k})\rangle \langle \psi_n(\mathbf{k})| \right) | \partial_{k_\mu} \psi_n(\mathbf{k}) \rangle dk_\mu dk_\nu \\ &= \mathcal{F}_n^{\mu\nu} dk_\mu dk_\nu. \end{aligned} \quad (A8)$$

This is Eq.(7) in the main text.

#### Appendix B: Quantum distance and non-Abelian quantum geometric tensor

We summarize non-Abelian quantum geometry for the  $N$ -fold degenerate wave functions[3].

The Hilbert-Schmidt distance is defined by

$$(ds_{\text{HS}})^2 \equiv 1 - |\langle u(\mathbf{k}) | u(\mathbf{k} + d\mathbf{k}) \rangle|^2. \quad (\text{B1})$$

where  $|u(\mathbf{k})\rangle$  is the wave function of  $N$ -fold degenerate bands

$$|u(\mathbf{k})\rangle = \sum_{n=1}^N c_n |\psi_n(\mathbf{k})\rangle, \quad (\text{B2})$$

where

$$\sum_{n=1}^N |c_n|^2 = 1. \quad (\text{B3})$$

The inner product is calculated as

$$\begin{aligned} & |\langle u(\mathbf{k}) | u(\mathbf{k} + d\mathbf{k}) \rangle|^2 \\ &= \langle u(\mathbf{k}) | u(\mathbf{k}) \rangle \\ &+ (\langle \partial_{k_\mu} u(\mathbf{k}) | u(\mathbf{k}) \rangle + \langle u(\mathbf{k}) | \partial_{k_\mu} u(\mathbf{k}) \rangle) dk_\mu \\ &+ \left( \frac{1}{2} \langle \partial_{k_\mu} \partial_{k_\nu} u(\mathbf{k}) | u(\mathbf{k}) \rangle + \frac{1}{2} \langle u(\mathbf{k}) | \partial_{k_\mu} \partial_{k_\nu} u(\mathbf{k}) \rangle \right) \\ &+ \langle \partial_{k_\mu} u(\mathbf{k}) | u(\mathbf{k}) \rangle \langle u(\mathbf{k}) | \partial_{k_\mu} u(\mathbf{k}) \rangle dk_\mu dk_\nu \\ &= 1 + \left( -\frac{1}{2} \langle \partial_{k_\mu} u(\mathbf{k}) | \partial_{k_\nu} u(\mathbf{k}) \rangle - \frac{1}{2} \langle \partial_{k_\nu} u(\mathbf{k}) | \partial_{k_\mu} u(\mathbf{k}) \rangle \right) \\ &+ \langle \partial_{k_\mu} u(\mathbf{k}) | u(\mathbf{k}) \rangle \langle u(\mathbf{k}) | \partial_{k_\mu} u(\mathbf{k}) \rangle dk_\mu dk_\nu \\ &= 1 + \langle \partial_{k_\mu} u(\mathbf{k}) | (|u(\mathbf{k})\rangle \langle u(\mathbf{k})| - 1) | \partial_{k_\mu} u(\mathbf{k}) \rangle dk_\mu dk_\nu. \end{aligned} \quad (\text{B4})$$

Then, we have

$$(ds_{\text{HS}})^2 = \langle \partial_{k_\mu} u(\mathbf{k}) | (1 - P(\mathbf{k})) | \partial_{k_\mu} u(\mathbf{k}) \rangle dk_\mu dk_\nu, \quad (\text{B5})$$

where  $P(\mathbf{k}) \equiv |u(\mathbf{k})\rangle \langle u(\mathbf{k})|$  is the projection operator to the  $N$ -fold degenerate bands satisfying  $P(\mathbf{k})^2 = P(\mathbf{k})$ . By diagonalizing it, we obtain

$$P(\mathbf{k}) \equiv \sum_{n=1}^N |\psi_n(\mathbf{k})\rangle \langle \psi_n(\mathbf{k})|. \quad (\text{B6})$$

This is Eq.(61) in the main text.

### Appendix C: Hellmann-Feynman theorem

By differentiating the eigenvalue equation

$$H |\psi_n(\mathbf{k})\rangle = \varepsilon_n(\mathbf{k}) |\psi_n(\mathbf{k})\rangle \quad (\text{C1})$$

with respect to  $k_\mu$ , we obtain

$$\begin{aligned} & \partial_{k_\mu} H |\psi_n(\mathbf{k})\rangle + H(\mathbf{k}) \partial_{k_\mu} |\psi_n(\mathbf{k})\rangle \\ &= \partial_{k_\mu} \varepsilon_n(\mathbf{k}) |\psi_n(\mathbf{k})\rangle + \varepsilon_n(\mathbf{k}) \partial_{k_\mu} |\psi_n(\mathbf{k})\rangle. \end{aligned} \quad (\text{C2})$$

Applying  $\langle \psi_m(\mathbf{k}) |$  to the above equation, we obtain

$$\begin{aligned} & \langle \psi_m(\mathbf{k}) | \partial_{k_\mu} H(\mathbf{k}) | \psi_n(\mathbf{k}) \rangle \\ &+ \langle \psi_m(\mathbf{k}) | H(\mathbf{k}) \partial_{k_\mu} | \psi_n(\mathbf{k}) \rangle \\ &= \langle \psi_m(\mathbf{k}) | \partial_{k_\mu} \varepsilon_n(\mathbf{k}) | \psi_n(\mathbf{k}) \rangle \\ &+ \langle \psi_m(\mathbf{k}) | \varepsilon_n(\mathbf{k}) \partial_{k_\mu} | \psi_n(\mathbf{k}) \rangle. \end{aligned} \quad (\text{C3})$$

Using (C1) and defining the velocity

$$v_\mu = \frac{\partial H(\mathbf{k})}{\hbar \partial k_\mu}, \quad (\text{C4})$$

we obtain

$$\begin{aligned} & \hbar \langle \psi_m(\mathbf{k}) | v_\mu | \psi_n(\mathbf{k}) \rangle \\ &+ \langle \psi_m(\mathbf{k}) | \varepsilon_m(\mathbf{k}) \partial_{k_\mu} | \psi_n(\mathbf{k}) \rangle \\ &= \langle \psi_m(\mathbf{k}) | \partial_{k_\mu} \varepsilon_n(\mathbf{k}) | \psi_n(\mathbf{k}) \rangle \\ &+ \varepsilon_n(\mathbf{k}) \langle \psi_m(\mathbf{k}) | \partial_{k_\mu} | \psi_n(\mathbf{k}) \rangle, \end{aligned} \quad (\text{C5})$$

where we have used the eigenequation

$$\langle \psi_m(\mathbf{k}) | H(\mathbf{k}) = \langle \psi_m(\mathbf{k}) | \varepsilon_m(\mathbf{k}). \quad (\text{C6})$$

This equation is rewritten as

$$\begin{aligned} & \langle \psi_m(\mathbf{k}) | v_\mu | \psi_n(\mathbf{k}) \rangle \\ &= \frac{1}{\hbar} \partial_{k_\mu} \varepsilon_n(\mathbf{k}) \langle \psi_m(\mathbf{k}) | \psi_n(\mathbf{k}) \rangle \\ &+ \frac{1}{\hbar} (\varepsilon_n(\mathbf{k}) - \varepsilon_m(\mathbf{k})) \langle \psi_m(\mathbf{k}) | \partial_{k_\mu} | \psi_n(\mathbf{k}) \rangle. \end{aligned} \quad (\text{C7})$$

It is Eq.(68) in the main text. Assuming that the states satisfy the orthonormalization condition  $\langle \psi_m(\mathbf{k}) | \psi_n(\mathbf{k}) \rangle = \delta_{mn}$  we find

$$\begin{aligned} & \langle \psi_m(\mathbf{k}) | v_\mu | \psi_n(\mathbf{k}) \rangle \\ &= \frac{1}{\hbar} (\varepsilon_n(\mathbf{k}) - \varepsilon_m(\mathbf{k})) \langle \psi_m(\mathbf{k}) | \partial_{k_\mu} | \psi_n(\mathbf{k}) \rangle, \quad \text{for } m \neq n. \end{aligned} \quad (\text{C8})$$

Indeed, when  $n$  is the band index, it is obvious that  $\langle \psi_m(\mathbf{k}) | \psi_n(\mathbf{k}) \rangle = 0$  for  $m \neq n$ . Furthermore, it is always possible to normalize as  $\langle \psi_n(\mathbf{k}) | \psi_n(\mathbf{k}) \rangle = 1$  at each  $\mathbf{k}$ .

By applying  $\langle \psi_m(\mathbf{k}) |$  to Eq.(C7) and taking a sum of  $m$ , we have

$$\begin{aligned} & \sum_m |\psi_m(\mathbf{k})\rangle \langle \psi_m(\mathbf{k}) | v_\mu | \psi_n(\mathbf{k}) \rangle \\ &= \frac{1}{\hbar} \partial_{k_\mu} \varepsilon_n(\mathbf{k}) \sum_m |\psi_m(\mathbf{k})\rangle \langle \psi_m(\mathbf{k}) | \psi_n(\mathbf{k}) \rangle \\ &+ \frac{1}{\hbar} (\varepsilon_n(\mathbf{k}) - \varepsilon_m(\mathbf{k})) \\ &\times \sum_m |\psi_m(\mathbf{k})\rangle \langle \psi_m(\mathbf{k}) | \partial_{k_\mu} | \psi_n(\mathbf{k}) \rangle \\ &= \frac{1}{\hbar} \partial_{k_\mu} \varepsilon_n(\mathbf{k}) \sum_m |\psi_m(\mathbf{k})\rangle \delta_{mn} \\ &+ \frac{1}{\hbar} (\varepsilon_n(\mathbf{k}) - \varepsilon_m(\mathbf{k})) \sum_m |\psi_m(\mathbf{k})\rangle \langle \psi_m(\mathbf{k})|. \end{aligned} \quad (\text{C9})$$

We have

$$\begin{aligned} & \sum_m |\psi_m(\mathbf{k})\rangle \langle \psi_m(\mathbf{k}) | \partial_{k_\mu} | \psi_n(\mathbf{k}) \rangle \\ &= \sum_{m \neq n} |\psi_m(\mathbf{k})\rangle \frac{\langle \psi_m(\mathbf{k}) | \hbar v_\mu | \psi_n(\mathbf{k}) \rangle}{\varepsilon_n(\mathbf{k}) - \varepsilon_m(\mathbf{k})}. \end{aligned} \quad (\text{C10})$$

for  $m \neq n$ . By using the complete condition  $\sum_m |\psi_m(\mathbf{k})\rangle \langle \psi_m(\mathbf{k})| = 1$ , we have

$$\partial_{k_\mu} |\psi_n(\mathbf{k})\rangle = \sum_{m \neq n} |\psi_m(\mathbf{k})\rangle \frac{\langle \psi_m(\mathbf{k}) | \hbar v_\mu | \psi_n(\mathbf{k}) \rangle}{\varepsilon_n(\mathbf{k}) - \varepsilon_m(\mathbf{k})}. \quad (\text{C11})$$

We use Eq.(C11) to analyze the diagonal component of the quantum metric

$$\begin{aligned} \mathcal{F}_{nn}^{\mu\nu}(\mathbf{k}) &= \langle \partial_{k_\mu} \psi_n(\mathbf{k}) | \mathcal{Q}(\mathbf{k}) | \partial_{k_\nu} \psi_n(\mathbf{k}) \rangle \\ &= \sum_{m' \neq n} \frac{\langle \psi_n(\mathbf{k}) | \hbar v_\mu | \psi_{m'}(\mathbf{k}) \rangle \langle \psi_{m'}(\mathbf{k}) |}{\varepsilon_n(\mathbf{k}) - \varepsilon_{m'}(\mathbf{k})} \\ &\quad \times \left( 1 - \sum_{m''=1}^N |\psi_{m''}(\mathbf{k})\rangle \langle \psi_{m''}(\mathbf{k})| \right) \\ &\quad \times \sum_{n' \neq n} |\psi_{n'}(\mathbf{k})\rangle \frac{\langle \psi_{n'}(\mathbf{k}) | \hbar v_\nu | \psi_n(\mathbf{k}) \rangle}{\varepsilon_n(\mathbf{k}) - \varepsilon_{n'}(\mathbf{k})}. \end{aligned} \quad (\text{C12})$$

We have

$$\begin{aligned} &\langle \psi_{m'}(\mathbf{k}) | \left( 1 - \sum_{m''=1}^N |\psi_{m''}(\mathbf{k})\rangle \langle \psi_{m''}(\mathbf{k})| \right) | \psi_{n'}(\mathbf{k}) \rangle \\ &= \delta_{m'n'} - \sum_{m''=1}^N \delta_{m'm''} \delta_{m''n'} = 0, \end{aligned}$$

when  $m''$  is the occupied band, while

$$\begin{aligned} &\langle \psi_{m'}(\mathbf{k}) | \left( 1 - \sum_{m''=1}^N |\psi_{m''}(\mathbf{k})\rangle \langle \psi_{m''}(\mathbf{k})| \right) | \psi_{n'}(\mathbf{k}) \rangle \\ &= \delta_{m'n'}, \end{aligned} \quad (\text{C13})$$

when  $m''$  is the unoccupied band.

$$\begin{aligned} \mathcal{F}_{nn}^{\mu\nu}(\mathbf{k}) &= \sum_{m \in \text{Unoccupied}} \frac{\langle \psi_n(\mathbf{k}) | \hbar v_x | \psi_m(\mathbf{k}) \rangle \langle \psi_m(\mathbf{k}) | \hbar v_y | \psi_n(\mathbf{k}) \rangle}{[\varepsilon_n(\mathbf{k}) - \varepsilon_m(\mathbf{k})]^2}. \end{aligned} \quad (\text{C14})$$

The quantum metric reads

$$g_n^{\mu\nu} = \text{Re} \sum_{m \in \text{Unoccupied}} \frac{\langle \psi_n(\mathbf{k}) | \hbar v_x | \psi_m(\mathbf{k}) \rangle \langle \psi_m(\mathbf{k}) | \hbar v_y | \psi_n(\mathbf{k}) \rangle}{[\varepsilon_n(\mathbf{k}) - \varepsilon_m(\mathbf{k})]^2}, \quad (\text{C15})$$

while the Berry curvature reads

$$\Omega_n^{\mu\nu} = 2\text{Im} \sum_{m \in \text{Unoccupied}} \frac{\langle \psi_n(\mathbf{k}) | \hbar v_x | \psi_m(\mathbf{k}) \rangle \langle \psi_m(\mathbf{k}) | \hbar v_y | \psi_n(\mathbf{k}) \rangle}{[\varepsilon_n(\mathbf{k}) - \varepsilon_m(\mathbf{k})]^2}. \quad (\text{C16})$$

#### Appendix D: Bulk photovoltaic effects

We apply alternating and monochromatic electric fields,

$$E_x(t) = E_x(\omega) e^{-i\omega t} + E_x(-\omega) e^{i\omega t} \quad (\text{D1})$$

with  $\omega > 0$ . We assume that the electric field is real,

$$E_x(t) = E_x^*(t), \quad (\text{D2})$$

or

$$E_x(\omega) = E_x^*(-\omega). \quad (\text{D3})$$

Excited electrons from the valence band and the conduction band contribute to the bulk photovoltaic current.

#### 1. Injection currents

We derive the injection current. We consider an acceleration due to the static electric field and an optical excitation from the valence band to the conduction band due to the oscillatory electric field, separately[218–221]. The equation of motion of electrons is

$$\hbar \frac{d\mathbf{k}}{dt} = -e \frac{\partial \mathbf{A}_0}{\partial t}, \quad (\text{D4})$$

where  $\mathbf{A}_0 = (A_0, 0, 0)$  is the vector potential. The static electric field is obtained from the vector potential as

$$E_x(0) \equiv -\frac{\partial A_0}{\partial t}, \quad (\text{D5})$$

or  $A_0 = -E_x(0)t + \text{constant}$ . The Bloch velocity under electric field is given by the minimal substitution,

$$v_n(k_x) \rightarrow v_n(k_x - eA_0/\hbar). \quad (\text{D6})$$

A comment is in order. We have only considered the contribution from the static electric field in the vector potential. Even if we take into account the contribution from the oscillatory electric field in the vector potential, the time evolution of the mean momentum does not change. It is understood as follows. The equation of motion under the oscillatory electric field reads

$$\hbar \frac{dk}{dt} = eE_x(0) + eE_x(\omega) \cos \omega t, \quad (\text{D7})$$

whose solution is given by

$$k = \frac{e}{\hbar} \left( tE_x(0) + \frac{E_x(\omega)}{\omega} \sin \omega t \right) + k_0. \quad (\text{D8})$$

Its mean for one period with respect to the time  $t$  is zero. Hence, it is enough only to consider the static electric field the vector potential.

We expand Eq.(D6) in powers of  $E_x(0)$ , and obtain

$$\frac{d^2 v_n^x}{dt^2} = \left( \frac{e}{\hbar} \right)^2 \frac{\partial^3 \omega_n}{\partial k_x^3} [E_x(0)]^2, \quad (\text{D9})$$

where we have used

$$\frac{dv_n^x}{dt} = \frac{dk_x}{dt} \frac{dv_n^x}{dk_x} = -\left( \frac{e}{\hbar} \right) \frac{\partial A_0}{\partial t} \frac{d^2 \omega_n}{dk_x^2} = \frac{e}{\hbar} \frac{d^2 \omega_n}{dk_x^2} E_x(0). \quad (\text{D10})$$

The current is given by

$$J = \frac{e}{V} \sum_{n,\mathbf{k}} f_n v_n^x, \quad (\text{D11})$$

with the velocity along the  $x$  direction

$$v_n^x \equiv \frac{\partial \omega_n}{\partial k_x}. \quad (\text{D12})$$

The injection current originates in  $dJ^{x;x^2}/dt$ . The injection current is obtained as

$$\frac{dJ_{\text{inject}}^{x;x^2}}{dt} = \frac{e}{V} \sum_n \sum_{s=0}^1 \binom{\ell-1}{s} \frac{d^s f_n}{dt^s} \frac{d^{1-s} v_n^x}{dt^{1-s}}. \quad (\text{D13})$$

The term proportional to  $E_x(\omega) E_x(-\omega)$  is given by taking the terms with  $s=1$  from Eq.(D13) as

$$\frac{dJ_{\text{inject}}^{x;x^2}}{dt} = \frac{e}{V} \sum_n \frac{df_n}{dt} v_n^x. \quad (\text{D14})$$

The Fermi golden rule reads

$$\frac{df_{\pm}}{dt} = \pm \frac{2\pi e^2}{\hbar^2} |\mathbf{E}(\omega) \cdot \mathbf{a}_{+-}|^2 \delta(\omega_{+-} - \omega), \quad (\text{D15})$$

where

$$\begin{aligned} \mathbf{E}(\omega) \cdot \mathbf{r}_{+-}^2 &= |E_x(\omega) a_{+-}^x|^2 = E_x(\omega) a_{+-}^x E_x^*(\omega) a_{+-}^{x*} \\ &= -E_x(\omega) E_x(-\omega) a_{+-}^x a_{+-}^x, \end{aligned} \quad (\text{D16})$$

with the use of the Hermitian condition Eq.(17).

Inserting it into Eq.(D14), we have

$$\begin{aligned} J_{\text{inject}}^{x;x^2} &= \frac{2\pi e^2}{\hbar^2} \frac{e}{V} a_{-+}^x a_{+-}^x \delta(\omega_{+-} - \omega) \\ &\times \frac{\partial^3 \omega_{+-}}{\partial k_x^3} E_x(\omega) E_x(-\omega). \end{aligned} \quad (\text{D17})$$

By assuming a monochromatic oscillation  $J^{x;x^2} \propto e^{-i\omega_0 t}$ , we obtain the  $\ell$ -th order current  $J^{x;x^\ell}$ ,

$$\begin{aligned} J_{\text{inject}}^{x;x^\ell} &= \frac{1}{i\omega_0 + 1/\tau} \frac{2\pi e^3}{\hbar^2 V} a_{-+}^x a_{+-}^x \delta(\omega_{+-} - \omega) \\ &\times \frac{\partial \omega_{+-}}{\partial k_x} E_x(\omega) E_x(-\omega) [E_x(0)]^{\ell-2}, \end{aligned} \quad (\text{D18})$$

where we have introduced a cutoff by the relaxation time  $\tau$ . When we concentrate on the direct current component  $\omega_0 = 0$ , it is proportional to  $\tau$ . The longitudinal component is

$$\frac{\sigma_{\text{inject}}^{x;x^2}}{\sigma_{\text{inject}}} = \sum_{\mathbf{k}} f_{-+} \frac{\partial \omega_{+-}}{\partial k_x} a_{-+}^x a_{+-}^x \delta(\omega_{+-} - \omega), \quad (\text{D19})$$

with

$$\sigma_{\text{inject}} \equiv 2\pi V \frac{e^3}{\hbar^2} \tau. \quad (\text{D20})$$

This is Eq.(120) in the main text.

## 2. Shift currents

The shift current is induced by the difference of the position between the valence band and the conduction band when electrons are excited from the valence band to the conduction band. It induces the electric dipole  $E_x(t) a_{+-}^x$ . Hence, the shift current originates in a quantum interference[221] between the oscillation of  $\rho_{mn}$  and the oscillation of the dipole velocity  $E_x a_{nm;x}^x$ ,

$$J_{\text{shift}}^{x;x^2} = -\frac{e^2}{\hbar V} \sum_{\mathbf{k}} E_x a_{+-;x}^x \rho_{+-}^{(1)}, \quad (\text{D21})$$

which is defined by the interband contributions  $a_{+-;x}^x$  and  $\rho_{+-}^{(1)}(t)$ .

The density matrix is obtained by solving the von-Neumann equation[89, 90, 221],

$$\begin{aligned} &\frac{\partial \rho_{mn}}{\partial t} + i\omega_{mn} \rho_{mn} \\ &= \frac{e}{i\hbar} \sum_s E_x (\rho_{ml} a_{sn}^x - a_{ms}^x \rho_{sn}) - \frac{e}{\hbar} E_x \rho_{mn;x}. \end{aligned} \quad (\text{D22})$$

For the two-band system, it is rewritten as

$$i(\omega_{+-} - \omega_0) \rho_{+-} = \frac{e}{i\hbar} E_x a_{+-}^x (\rho_{++} - \rho_{--}) - \frac{e}{\hbar} E_x \rho_{+-;x}, \quad (\text{D23})$$

where we have used  $a_{nn}^x = 0$  and assumed a monochromatic solution  $\rho_{mn} \propto e^{-i\omega_0 t}$ . This definition recovers properly the definition of the shift current for  $\ell=2$ .

The zeroth order solution is given by

$$\rho_{\pm}^{(0)} = f_{\pm}, \quad (\text{D24})$$

because electric field is not applied. The first order solution is given by

$$\begin{aligned} \rho_{+-}^{(1)} &= \frac{ie}{\hbar(\omega_{+-} - \omega_0)} E_x a_{+-}^x (\rho_{++}^{(0)} - \rho_{--}^{(0)}) e^{-i\omega_0 t} \\ &= \frac{ie}{\hbar(\omega_{+-} - \omega_0)} E_x a_{+-}^x f_{-+} e^{-i\omega_0 t}. \end{aligned} \quad (\text{D25})$$

Especially, we have  $\rho_{++}^{(1)} = 0$  because  $f_{++} \equiv f_+ - f_+ = 0$ . Hence, the shift current is obtained as

$$\begin{aligned} J_{\text{shift}}^{x;x^2} &= -\frac{e^2}{\hbar V} \sum_{\mathbf{k}} E_x a_{+-;x}^x \rho_{+-}^{(1)} \\ &= -\frac{e^2}{\hbar V} e^{-i\omega_0 t} \sum_{\mathbf{k}} a_{+-;x}^x f_{-+} a_{+-}^x E_x^l. \end{aligned} \quad (\text{D26})$$

We use the monochromatic condition (D1) and study the direct current component,

$$\begin{aligned} J_{\text{shift}}^{x;x^2} &= \sigma_{\text{shift}}^{x;x^2} (0; \omega, -\omega, 0, 0, \dots, 0) \\ &\times E_x(\omega) E_x(-\omega). \end{aligned} \quad (\text{D27})$$

Then, the shift current is obtained as

$$J_{\text{shift}}^{x;x^2} = -\frac{e^2}{\hbar V} \sum_{\mathbf{k}} a_{+;-}^x a_{+;-}^x \times f_{-+} E_x(\omega) E_x(-\omega) \delta(\omega_{+-} - \omega). \quad (\text{D28})$$

It is independent of  $\tau$ . The shift conductivity is given by

$$\frac{\sigma_{\text{shift}}^{x;x^2}}{\sigma_{\text{shift}}} = \frac{1}{V} \sum_{\mathbf{k}} f_{-+} a_{+;-}^x a_{+;-}^x \delta(\omega_{+-} - \omega), \quad (\text{D29})$$

with

$$\sigma_{\text{shift}} \equiv -\frac{e^3}{\hbar^2}. \quad (\text{D30})$$

This is Eq.(123) in the main text.

### Appendix E: Quantum distance and Zeeman quantum geometric tensor

The Zeeman quantum geometric tensor  $g_{nm}^{\mu\nu}$  is defined by the quantum distance  $ds_{\text{HS}}$  for the infinitesimal translation  $d\mathbf{k}$  of the momentum as[110–113]

$$ds_{\text{HS}}(\mathbf{k}) \equiv \sqrt{1 - |\langle \psi_n(\mathbf{k}) | U_{d\theta} U_{d\mathbf{k}} | \psi_n(\mathbf{k}) \rangle|^2}, \quad (\text{E1})$$

where

$$U_{d\theta} \equiv e^{-\frac{i}{2} d\theta \cdot \sigma}, \quad U_{d\mathbf{k}} \equiv e^{-i d\mathbf{k} \cdot \mathbf{r}} \quad (\text{E2})$$

are the generators of the spin angular momentum  $d\theta$  and the momentum  $d\mathbf{k}$ . By using the relation

$$\begin{aligned} & U_{d\theta} U_{d\mathbf{k}} | \psi_n \rangle \\ &= \left( 1 - \frac{i\sigma_\mu}{2} d\theta_\nu - \frac{\sigma_\mu \sigma_\nu}{8} d\theta_\mu d\theta_\nu \dots \right) \\ & \times \left( 1 + \partial_{k_\mu} dk_\mu + \frac{1}{2} |\partial_{k_\mu} \partial_{k_\nu} \psi_n(\mathbf{k})\rangle dk_\mu dk_\nu \dots \right) | \psi_n \rangle \\ &= 1 + \frac{1}{2} |\partial_{k_\mu} \partial_{k_\nu} \psi_n(\mathbf{k})\rangle dk_\mu dk_\nu \\ & - \frac{i\sigma_\mu}{2} | \psi_n \rangle d\theta^\mu - \frac{1}{8} | \psi_n \rangle d\theta^\mu d\theta^\mu - \frac{i\sigma_\nu}{2} \partial_{k_\mu} | \psi_n \rangle dk_\mu d\theta^\nu + \dots, \end{aligned} \quad (\text{E3})$$

the quantum distance is given by

$$\begin{aligned} (ds_{\text{HS}})^2 &= \sum_{n \neq m} g_{nm}^{\mu\nu} dk_\mu dk_\nu + \sum_{n \neq m} s_{nm}^{\mu\nu} \frac{d\theta_\mu d\theta_\nu}{4} \\ & + \sum_{n \neq m} (z_{nm}^{\mu\nu} + z_{mn}^{\mu\nu}) dk_\mu \frac{d\theta_\nu}{2}, \end{aligned} \quad (\text{E4})$$

where  $g_{nm}^{\mu\nu}$  is the quantum metric,  $s_{nm}^{\mu\nu}$  is the spin quantum geometric tensor and  $z_{nm}^{\mu\nu}$  is the Zeeman quantum geometric tensor.

We determine  $z_{nm}^{\mu\nu}$  by calculating the coefficient of  $dk_\mu \frac{d\theta_\nu}{2}$ . The fidelity is calculated as

$$\begin{aligned} & |\langle \psi_n(\mathbf{k}) | \psi_n(\mathbf{k} + d\mathbf{k}) \rangle|^2 \\ &= \langle \psi_n(\mathbf{k} + d) | \psi_n(\mathbf{k}) \rangle \langle \psi_n(\mathbf{k}) | \psi_n(\mathbf{k} + d) \rangle \\ &= \langle \psi_n(\mathbf{k}) | \psi_n(\mathbf{k}) \rangle + (\langle \partial_{k_\mu} \psi_n(\mathbf{k}) | \psi_n(\mathbf{k}) \rangle \\ & + \langle \psi_n(\mathbf{k}) | \partial_{k_\mu} \psi_n(\mathbf{k}) \rangle) dk_\mu \\ & + (-\frac{i}{2} \langle \partial_{k_\mu} \psi_n(\mathbf{k}) | \psi_n(\mathbf{k}) \rangle \langle \psi_n(\mathbf{k}) | \sigma_\nu | \psi_n(\mathbf{k}) \rangle \\ & + \frac{i}{2} \langle \psi_n(\mathbf{k}) | \sigma_\nu | \psi_n(\mathbf{k}) \rangle \langle \psi_n(\mathbf{k}) | \partial_{k_\mu} \psi_n(\mathbf{k}) \rangle \\ & + \frac{i}{2} \langle \partial_{k_\mu} \psi_n(\mathbf{k}) | \sigma_\nu | \psi_n(\mathbf{k}) \rangle \\ & - \frac{i}{2} \langle \psi_n(\mathbf{k}) | \sigma_\nu | \partial_{k_\mu} \psi_n(\mathbf{k}) \rangle) dk_\mu d\theta_\nu \\ &= 1 + \frac{i}{2} (\langle \partial_{k_\mu} \psi_n(\mathbf{k}) | (1 - P(\mathbf{k})) \sigma_\nu | \psi_n(\mathbf{k}) \rangle \\ & - \frac{i}{2} \langle \psi_n(\mathbf{k}) | (1 - P(\mathbf{k})) \sigma_\nu | \partial_{k_\mu} \psi_n(\mathbf{k}) \rangle) dk_\mu \frac{d\theta_\nu}{2} \\ &= 1 + \frac{i}{2} \left( \sum_{m \neq n} \langle \partial_{k_\mu} \psi_n(\mathbf{k}) | \psi_m(\mathbf{k}) \rangle \langle \psi_m(\mathbf{k}) | \sigma_\nu | \psi_n(\mathbf{k}) \rangle \right. \\ & \left. - \langle \psi_n(\mathbf{k}) | \sigma_\nu | \psi_m(\mathbf{k}) \rangle \langle \psi_m(\mathbf{k}) | \partial_{k_\mu} \psi_n(\mathbf{k}) \rangle \right) dk_\mu \frac{d\theta_\nu}{2} \\ &= 1 - \frac{1}{2} \sum_{m \neq n} \langle \psi_n(\mathbf{k}) | \partial_{k_\mu} \psi_m(\mathbf{k}) \rangle \langle \psi_m(\mathbf{k}) | \sigma_\nu | \psi_n(\mathbf{k}) \rangle \\ & + \langle \psi_n(\mathbf{k}) | \sigma_\nu | \psi_m(\mathbf{k}) \rangle \langle \psi_m(\mathbf{k}) | \partial_{k_\mu} \psi_n(\mathbf{k}) \rangle dk_\mu \frac{d\theta_\nu}{2} \\ &= 1 - \frac{1}{2} \sum_{m \neq n} (a_{nm}^\mu s_{mn}^\nu + s_{nm}^\nu a_{mn}^\mu) dk_\mu \frac{d\theta_\nu}{2}, \end{aligned} \quad (\text{E5})$$

where we have used Eq.(15). By comparing it to Eq.(E4), we obtain

$$z_{nm}^{\mu\nu} = a_{nm}^\mu s_{mn}^\nu, \quad (\text{E6})$$

which is the Zeeman geometric tensor. This is Eq.(143) in the main text.

We calculate  $s_{nm}^{\mu\nu}$  as

$$\begin{aligned} & |\langle \psi_n(\mathbf{k}) | \psi_n(\mathbf{k}') \rangle|^2 \\ &= \langle \psi_n(\mathbf{k}') | \psi_n(\mathbf{k}) \rangle \langle \psi_n(\mathbf{k}) | \psi_n(\mathbf{k}') \rangle \\ &= \left( \langle \psi_n(\mathbf{k}) | + \langle \psi_n(\mathbf{k}) | \frac{i\sigma_\mu}{2} d\theta^\mu + \dots \right) | \psi_n(\mathbf{k}) \rangle \\ & \left\langle \psi_n(\mathbf{k}) \left| \left( | \psi_n(\mathbf{k}) \rangle + \frac{i\sigma_\mu}{2} | \psi_n(\mathbf{k}) \rangle d\theta^{\mu\nu} + \dots \right) \right. \right\rangle \\ &= \langle \psi_n(\mathbf{k}) | \psi_n(\mathbf{k}) \rangle \\ & + \left( \frac{i}{2} \langle \psi_n(\mathbf{k}) | \sigma_\mu | \psi_n(\mathbf{k}) \rangle - \frac{i\sigma_\mu}{2} \langle \psi_n(\mathbf{k}) | \sigma_\mu | \psi_n(\mathbf{k}) \rangle \right) d\theta^\mu \\ & + \left( -\frac{1}{4} \langle \psi_n(\mathbf{k}) | \sigma_\mu | \psi_n(\mathbf{k}) \rangle \langle \psi_n(\mathbf{k}) | \sigma_\nu | \psi_n(\mathbf{k}) \rangle \right) d\theta^\mu d\theta^\nu \\ &= 1 + \frac{1}{4} \langle \psi_n(\mathbf{k}) | \sigma_\mu | \psi_n(\mathbf{k}) \rangle \langle \psi_n(\mathbf{k}) | \sigma_\nu | \psi_n(\mathbf{k}) \rangle d\theta^\mu d\theta^\nu \end{aligned} \quad (\text{E7})$$

Then, we have

$$s_{nm}^{\mu\nu} \equiv s_{nm}^{\mu} s_{mn}^{\nu} \quad (\text{E8})$$

with

$$s_{nm}^{\mu} \equiv \langle \psi_n(\mathbf{k}) | \sigma_{\mu} | \psi_n(\mathbf{k}) \rangle. \quad (\text{E9})$$

is the spin geometric tensor. This is Eq.(142) in the main text.

## Appendix F: Zeeman quantum geometry induced intrinsic cross responses

### 1. Hall current and AC Hall current

Inserting the density matrix (153) to Eq.(154) and assuming  $\omega \ll \varepsilon_{mn}$ , the current is calculated as

$$\begin{aligned} J^{\mu;\nu} &= \frac{1}{2} \sum_{nm} \sum_{\omega_1=\pm\omega} \int d\mathbf{k} v_{nm}^{\mu} f_{nm} a_{mn}^{\nu} \frac{E^{\nu} e^{-i\omega_1 t}}{\hbar\omega_1 - \varepsilon_{mn} + i\eta} \\ &= \frac{1}{2} \sum_{nm} \sum_{\omega_1=\pm\omega} \int d\mathbf{k} f_{nm} i\varepsilon_{nm} a_{nm}^{\mu} a_{mn}^{\nu} \frac{E^{\nu} e^{-i\omega_1 t}}{\hbar\omega_1 - \varepsilon_{mn} + i\eta}. \end{aligned} \quad (\text{F1})$$

We assume the off-resonant condition

$$\hbar\omega_1 - \varepsilon_{mn} \neq 0. \quad (\text{F2})$$

Then, we can expand the denominator in Eq.(F1)

$$\frac{1}{\hbar\omega_1 - \varepsilon_{mn} + i\eta} = - \sum_{j=1}^{\infty} \frac{\omega_1^{j-1}}{\varepsilon_{mn}^j}. \quad (\text{F3})$$

By using it, we obtain

$$\begin{aligned} J^{\mu;\nu} &= -\frac{1}{2} \sum_{nm} \sum_{\omega_1=\pm\omega} \int d\mathbf{k} f_{nm} i\varepsilon_{nm} a_{nm}^{\mu} a_{mn}^{\nu} \\ &\quad \times E^{\nu} e^{-i\omega_1 t} \sum_{j=1}^{\infty} \frac{\omega_1^{j-1}}{\varepsilon_{mn}^j} \\ &= \frac{1}{2} \sum_{nm} \sum_{\omega_1=\pm\omega} \int d\mathbf{k} f_{nm} i a_{nm}^{\mu} a_{mn}^{\nu} E^{\nu} e^{-i\omega_1 t} \sum_{j=0}^{\infty} \frac{\omega_1^j}{\varepsilon_{mn}^j} \\ &= \frac{1}{2} \int d\mathbf{k} \sum_{n>m} \sum_{\omega_1=\pm\omega} \sum_{j=0}^{\infty} f_{nm} \\ &\quad \times i [a_{nm}^{\mu} a_{mn}^{\nu} - a_{mn}^{\mu} a_{nm}^{\nu}] \frac{\omega_1^{2j}}{\varepsilon_{mn}^{2j}} E^{\nu} e^{-i\omega_1 t} \\ &\quad + i [a_{nm}^{\mu} a_{mn}^{\nu} + a_{mn}^{\mu} a_{nm}^{\nu}] \frac{\omega_1^{2j+1}}{\varepsilon_{mn}^{2j+1}} E^{\nu} e^{-i\omega_1 t}, \end{aligned} \quad (\text{F4})$$

where we have used the relations

$$f_{nm} \equiv f_n - f_m = -f_{mn}, \quad (\text{F5})$$

and

$$\varepsilon_{nm} \equiv \varepsilon_n - \varepsilon_m = -\varepsilon_{mn}. \quad (\text{F6})$$

By taking the sum of  $\omega_1 = \pm\omega$ , we obtain

$$\begin{aligned} J^{\mu;\nu} &= \int d\mathbf{k} \sum_{n>m} \sum_{j=0}^{\infty} f_{nm} \left[ \Omega_{nm}^{\mu\nu} \frac{\omega^{2j}}{\varepsilon_{mn}^{2j}} E^{\nu} \cos \omega t \right. \\ &\quad \left. + 2g_{nm}^{\mu\nu} \frac{\omega^{2j+1}}{\varepsilon_{mn}^{2j+1}} E^{\nu} \sin \omega t \right] \\ &= \int d\mathbf{k} \sum_{n>m} f_{nm} \left[ \Omega_{nm}^{\mu\nu} \frac{1}{1 - (\omega/\varepsilon_{mn})^2} E^{\nu} \cos \omega t \right. \\ &\quad \left. + 2g_{nm}^{\mu\nu} \frac{\omega/\varepsilon_{mn}}{1 - (\omega/\varepsilon_{mn})^2} E^{\nu} \sin \omega t \right]. \end{aligned} \quad (\text{F7})$$

Only the order of  $\Omega^0$  and  $\Omega$  are valid in the linear response theory. Then, we obtain the current

$$\frac{J^{\mu;\nu}}{E^{\nu}} = \int d\mathbf{k} \sum_{n>m} f_{nm} \left[ \Omega_{nm}^{\mu\nu} + 2g_{nm}^{\mu\nu} \frac{\omega}{\varepsilon_{mn}} \sin \omega t \right], \quad (\text{F8})$$

which is Eq.(157) in the main text.

In the static limit  $\Omega = 0$ , it recovers the TKNN formula

$$J^{\mu\nu} = \int d\mathbf{k} \sum_{n>m} f_{nm} \Omega_{nm}^{\mu\nu} E^{\nu}. \quad (\text{F9})$$

### 2. Intrinsic gyrotropic magnetic current

The current under external magnetic field is calculated as

$$\begin{aligned} J^{\mu;\nu} &= -\frac{g\mu_B}{2} \sum_{nm} \sum_{\omega_1=\pm\omega} \int d\mathbf{k} v_{nm}^{\mu} \frac{f_{nm} s_{mn}^{\nu} B^{\nu} e^{-i\omega_1 t}}{\hbar\omega_1 - \varepsilon_{mn} + i\eta} \\ &= g\mu_B \int d\mathbf{k} \sum_{n>m} f_{nm} \left[ \mathcal{Z}_{nm}^{\mu\nu} \frac{1}{1 - (\omega/\varepsilon_{mn})^2} \right. \\ &\quad \left. + 2\mathcal{Q}_{nm}^{\mu\nu} \frac{\omega/\varepsilon_{mn}}{1 - (\omega/\varepsilon_{mn})^2} \sin \omega t \right] B^{\nu}. \end{aligned} \quad (\text{F10})$$

It is

$$J^{\mu;\nu} = g\mu_B \int d\mathbf{k} \sum_{n>m} f_{nm} \left[ \mathcal{Z}_{nm}^{\mu\nu} \cos \omega t + 2\mathcal{Q}_{nm}^{\mu\nu} \frac{\omega}{\varepsilon_{mn}} \sin \omega t \right] B^{\nu}. \quad (\text{F11})$$

up to the linear order in  $\omega$ , which is Eq.(158) in the main text.

### 3. Intrinsic electric field induced spin density

The spin polarization under external electric field is calculated as

$$\begin{aligned} S^{\mu} &= \frac{1}{2} \sum_{nm} \sum_{\omega_1=\pm\omega} \int d\mathbf{k} s_{nm}^{\mu} f_{nm} v_{mn}^{\nu} \frac{E^{\nu} e^{-i\omega_1 t}}{\hbar\omega_1 - \varepsilon_{mn} + i\eta} \\ &= - \int d\mathbf{k} \sum_{n>m} f_{nm} \left[ \frac{2\mathcal{Q}_{nm}^{\nu\mu}}{\varepsilon_{mn}} \frac{1}{1 - (\omega/\varepsilon_{mn})^2} \right. \\ &\quad \left. + \mathcal{Z}_{nm}^{\nu\mu} \frac{\omega/\varepsilon_{mn}^2}{1 - (\omega/\varepsilon_{mn})^2} \sin \omega t \right] E^{\nu}. \end{aligned} \quad (\text{F12})$$

It is

$$S^\mu = - \int d\mathbf{k} \sum_{n>m} f_{nm} \left[ \frac{2Q_{nm}^{\nu\mu}}{\varepsilon_{mn}} \cos \omega t + Z_{nm}^{\nu\mu} \frac{\omega}{\varepsilon_{mn}^2} \sin \omega t \right] E^\nu. \quad (\text{F13})$$

up to the linear order in  $\omega$ , which is Eq.(159) in the main text.

#### 4. Intrinsic magnetic field induced spin density

The spin polarization under external magnetic field is calculated as

$$\begin{aligned} S^{\mu;\nu} &= - \frac{g\mu_B}{2} \sum_{\omega_1=\pm\omega} \int d\mathbf{k} s_{nm}^\mu \frac{f_{nm} s_{mn}^\nu B^\nu e^{-i\omega_1 t}}{\hbar\omega_1 - \varepsilon_{mn} + i\eta} \\ &= g\mu_B \int d\mathbf{k} \sum_{n>m} f_{nm} \left[ \frac{S_{nm}^{\mu\nu}}{\varepsilon_{mn}} \frac{1}{1 - (\omega/\varepsilon_{mn})^2} B^\nu \right. \\ &\quad \left. + 2\mathcal{A}_{nm}^{\mu\nu} \frac{\omega/\varepsilon_{mn}^2}{1 - (\omega/\varepsilon_{mn})^2} B^\nu \sin \omega t \right]. \quad (\text{F14}) \end{aligned}$$

It is

$$S^{\mu;\nu} = g\mu_B \int d\mathbf{k} \sum_{n>m} f_{nm} \left[ \frac{S_{nm}^{\mu\nu}}{\varepsilon_{mn}} \cos \omega t + 2\mathcal{A}_{nm}^{\mu\nu} \frac{\omega}{\varepsilon_{mn}^2} \sin \omega t \right] B^\nu \quad (\text{F15})$$

up to the linear order in  $\omega$ , which is Eq.(160) in the main text.

## Appendix G: Zeeman quantum geometry for two-band systems

### 1. Zeeman Berry curvature

By inserting  $n = +$  and  $m = -$  in Eq.(146), we obtain

$$\begin{aligned} Z_{+-}^{xx} &= i (r_{+-}^x s_{+-}^x - r_{-+}^x s_{-+}^x) \\ &= \frac{\partial \theta}{\partial k_x} \cos \theta \cos \phi - \frac{\partial \phi}{\partial k_x} \sin \theta \sin \phi = \frac{\partial n_x}{\partial k_x}, \quad (\text{G1}) \end{aligned}$$

$$\begin{aligned} Z_{+-}^{yy} &= i (r_{+-}^y s_{+-}^y - r_{-+}^y s_{-+}^y) \\ &= \frac{\partial \theta}{\partial k_y} \cos \theta \sin \phi + \frac{\partial \phi}{\partial k_y} \cos \theta \sin \phi = \frac{\partial n_y}{\partial k_y}, \quad (\text{G2}) \end{aligned}$$

$$\begin{aligned} Z_{+-}^{xy} &= i (r_{+-}^x s_{+-}^y - r_{-+}^x s_{-+}^y) \\ &= \frac{\partial \theta}{\partial k_x} \cos \theta \sin \phi + \frac{\partial \phi}{\partial k_x} \sin \theta \cos \phi = \frac{\partial n_y}{\partial k_x}, \quad (\text{G3}) \end{aligned}$$

$$\begin{aligned} Z_{+-}^{yx} &= i (r_{+-}^y s_{+-}^x - r_{-+}^y s_{-+}^x) \\ &= \frac{\partial \theta}{\partial k_y} \cos \theta \cos \phi - \frac{\partial \phi}{\partial k_y} \sin \theta \sin \phi = \frac{\partial n_x}{\partial k_y}, \quad (\text{G4}) \end{aligned}$$

$$\begin{aligned} Z_{+-}^{zz} &= i (r_{+-}^x s_{+-}^z - r_{-+}^x s_{-+}^z) \\ &= - \frac{\partial \theta}{\partial k_x} \sin \theta = \frac{\partial n_z}{\partial k_x}, \quad (\text{G5}) \end{aligned}$$

$$\begin{aligned} Z_{+-}^{yz} &= i (r_{+-}^y s_{+-}^z - r_{-+}^y s_{-+}^z) \\ &= - \frac{\partial \theta}{\partial k_y} \sin \theta = \frac{\partial n_z}{\partial k_y}. \quad (\text{G6}) \end{aligned}$$

They are summarized as

$$Z_{+-}^{\mu\nu} = -Z_{-+}^{\mu\nu} = \frac{\partial n_\nu}{\partial k_\mu}. \quad (\text{G7})$$

This is Eq.(161) in the main text.

### 2. Zeeman quantum metric

The expectation value of the spin

$$s_{nm}^\mu \equiv \langle \psi_n(\mathbf{k}) | \sigma_\mu | \psi_m(\mathbf{k}) \rangle \quad (\text{G8})$$

is calculated as

$$s_{-+}^x = -i \sin \phi + \cos \theta \cos \phi, \quad (\text{G9})$$

$$s_{-+}^y = i \cos \phi + \cos \theta \sin \phi, \quad (\text{G10})$$

$$s_{-+}^z = -\sin \theta. \quad (\text{G11})$$

By inserting  $n = +$  and  $m = -$  in Eq.(145), we obtain

$$\begin{aligned} Q_{+-}^{xx} &= \frac{r_{+-}^x - s_{+-}^x + r_{-+}^x + s_{-+}^x}{2} \\ &= -\frac{\sin \phi}{2} \frac{\partial \theta}{\partial k_x} - \frac{\cos \phi}{2} \sin \theta \cos \theta \frac{\partial \phi}{\partial k_x} \\ &= \frac{1}{2} \left( n_y \frac{\partial n_z}{\partial k_x} - n_z \frac{\partial n_y}{\partial k_x} \right), \end{aligned} \quad (\text{G12})$$

$$\begin{aligned} Q_{+-}^{yy} &= \frac{r_{+-}^y - s_{+-}^y + r_{-+}^y + s_{-+}^y}{2} \\ &= \frac{\cos \phi}{2} \frac{\partial \theta}{\partial k_y} - \frac{\sin \phi}{2} \sin \theta \cos \theta \frac{\partial \phi}{\partial k_y} \\ &= \frac{1}{2} \left( n_z \frac{\partial n_x}{\partial k_y} - n_x \frac{\partial n_z}{\partial k_y} \right), \end{aligned} \quad (\text{G13})$$

$$\begin{aligned} Q_{+-}^{xy} &= \frac{r_{+-}^x - s_{+-}^y + r_{-+}^x + s_{-+}^y}{2} \\ &= \frac{\cos \phi}{2} \frac{\partial \theta}{\partial k_x} - \frac{\sin \phi}{2} \sin \theta \cos \theta \frac{\partial \phi}{\partial k_x} \\ &= \frac{1}{2} \left( n_z \frac{\partial n_x}{\partial k_x} - n_x \frac{\partial n_z}{\partial k_x} \right), \end{aligned} \quad (\text{G14})$$

$$\begin{aligned} Q_{+-}^{yx} &= \frac{r_{+-}^y - s_{+-}^x + r_{-+}^y + s_{-+}^x}{2} \\ &= \frac{\cos \phi}{2} \frac{\partial \theta}{\partial k_y} - \frac{\sin \phi}{2} \sin \theta \cos \theta \frac{\partial \phi}{\partial k_y} \\ &= \frac{1}{2} \left( n_y \frac{\partial n_z}{\partial k_y} - n_z \frac{\partial n_y}{\partial k_y} \right), \end{aligned} \quad (\text{G15})$$

$$Q_{+-}^{xz} = \frac{\sin^2 \theta}{2} \frac{\partial \phi}{\partial k_x} = \frac{1}{2} \left( n_x \frac{\partial n_y}{\partial k_x} - n_y \frac{\partial n_x}{\partial k_x} \right), \quad (\text{G16})$$

$$Q_{+-}^{yz} = \frac{\sin^2 \theta}{2} \frac{\partial \phi}{\partial k_y} = \frac{1}{2} \left( n_x \frac{\partial n_y}{\partial k_y} - n_y \frac{\partial n_x}{\partial k_y} \right), \quad (\text{G17})$$

where we have used the relations

$$\frac{\partial n_x}{\partial k_\mu} = \cos \theta \cos \phi \frac{\partial \theta}{\partial k_\mu} - \sin \theta \sin \phi \frac{\partial \phi}{\partial k_\mu}, \quad (\text{G18})$$

$$\frac{\partial n_y}{\partial k_\mu} = \cos \theta \sin \phi \frac{\partial \theta}{\partial k_\mu} + \sin \theta \cos \phi \frac{\partial \phi}{\partial k_\mu}, \quad (\text{G19})$$

$$\frac{\partial n_z}{\partial k_\mu} = -\sin \theta \frac{\partial \theta}{\partial k_\mu}. \quad (\text{G20})$$

They are summarized as

$$Q_{+-}^{\mu\nu} = \frac{1}{2} \varepsilon_{\nu\rho\sigma} n_\rho \frac{\partial n_\sigma}{\partial k_\mu}. \quad (\text{G21})$$

This is Eq.(162) in the main text.

### 3. Spin quantum geometry

By inserting  $n = +$  and  $m = -$  in Eq.(142), we obtain the diagonal components,

$$\begin{aligned} s_{+-}^{xx} &= s_{+-}^x - s_{-+}^x = \frac{1}{4} (3 + \cos 2\theta - 2 \cos 2\phi \sin^2 \theta) \\ &= n_y^2 + n_z^2 = 1 - n_x^2, \end{aligned} \quad (\text{G22})$$

$$\begin{aligned} s_{+-}^{yy} &= s_{+-}^y - s_{-+}^y = \frac{1}{4} (3 + \cos 2\theta + 2 \cos 2\phi \sin^2 \theta) \\ &= n_x^2 + n_z^2 = 1 - n_y^2, \end{aligned} \quad (\text{G23})$$

$$s_{+-}^{zz} = s_{+-}^z - s_{-+}^z = \sin^2 \theta = 1 - n_z^2. \quad (\text{G24})$$

They are summarized as

$$s_{+-}^{\mu\mu} = 1 - n_\mu^2. \quad (\text{G25})$$

We also obtain the off-diagonal components,

$$\begin{aligned} s_{+-}^{xy} &= i \cos \theta - \sin^2 \theta \sin \phi \cos \phi \\ &= i n_z - n_x n_y, \end{aligned} \quad (\text{G26})$$

$$\begin{aligned} s_{+-}^{yx} &= -i \cos \theta - \sin^2 \theta \sin \phi \cos \phi \\ &= -i n_z - n_x n_y = (s_{+-}^{xy})^*, \end{aligned} \quad (\text{G27})$$

$$\begin{aligned} s_{+-}^{xz} &= -\sin \theta (i \sin \phi \cos \theta + \cos \phi) \\ &= -i n_y - n_z n_x, \end{aligned} \quad (\text{G28})$$

$$\begin{aligned} s_{+-}^{yz} &= \sin \theta (+i \cos \phi - \cos \theta \sin \phi) \\ &= i n_x - n_z n_y. \end{aligned} \quad (\text{G29})$$

They are summarized as

$$s_{+-}^{\mu\nu} = i \varepsilon_{\mu\nu\rho} n_\rho - n_\mu n_\nu \quad (\text{G30})$$

for  $\mu \neq \nu$ . Eqs.(G25) and (G30) are summarized as

$$s_{+-}^{\mu\nu} = \delta_{\mu\nu} + i \varepsilon_{\mu\nu\rho} n_\rho - n_\mu n_\nu. \quad (\text{G31})$$

The spin quantum metric (147) is given by

$$S_{+-}^{\mu\nu} = \delta_{\mu\nu} - n_\mu n_\nu. \quad (\text{G32})$$

This is Eq.(163) in the main text.

The spin Berry curvature (148) is given by

$$A_{+-}^{\mu\nu} = -2 \varepsilon_{\mu\nu\rho} n_\rho. \quad (\text{G33})$$

This is Eq.(164) in the main text.

#### Appendix H: Zeeman geometry induced cross responses in X-wave magnets

We evaluate whether there is a response by integrating the Zeeman quantum geometric quantities  $Z_{+-}^{\mu\nu}$  and  $Q_{+-}^{\mu\nu}$ . It is determined by the integration over  $\phi$ .

$$1) J^{x;x} / E^x$$



$Z_{+-}^{xx}$  is expanded as

$$\begin{aligned} Z_{+-}^{xx} &= \frac{\lambda^3 k_x k_y}{(\lambda^2 k^2 + B^2)^{3/2}} \\ &+ J\lambda k_y \left( -\frac{3B\lambda^2 k_x f_X}{(\lambda^2 k^2 + B^2)^{5/2}} + \frac{B\partial_{k_x} f_X}{(\lambda^2 k^2 + B^2)^{3/2}} \right) \end{aligned} \quad (\text{H1})$$

up to the first order in  $J$ . The integration is

$$\int Z_{+-}^{xx} d\phi = 0 \quad (\text{H2})$$

for  $f_X = k^{N_X} \cos N_X \phi$ , and  $f_X = k^{N_X} \sin N_X \phi$  with all  $N_X$ . Hence there is no response  $J^{x;x}/E^x$ .

2)  $J^{y;y}/E^y$

$Z_{+-}^{yy}$  is expanded as

$$\begin{aligned} Z_{+-}^{yy} &= -\frac{\lambda^3 k_x k_y}{(\lambda^2 k^2 + B^2)^{3/2}} \\ &+ J\lambda k_x \left( \frac{3B\lambda^2 k_y f_X}{(\lambda^2 k^2 + B^2)^{5/2}} - \frac{B\partial_{k_y} f_X}{(\lambda^2 k^2 + B^2)^{3/2}} \right) \end{aligned} \quad (\text{H3})$$

up to the first order in  $J$ . The integration is

$$\int Z_{+-}^{yy} d\phi = 0 \quad (\text{H4})$$

for  $f_X = k^{N_X} \cos N_X \phi$ , and  $f_X = k^{N_X} \sin N_X \phi$  with all  $N_X$ . Hence there is no response  $J^{y;y}/E^y$ .

3)  $J^{x;y}/E^y$

$Z_{+-}^{xy}$  is expanded as

$$\begin{aligned} Z_{+-}^{xy} &= \frac{\lambda(\lambda^2 k_y^2 + B^2)}{(\lambda^2 k^2 + (B + Jf_X)^2)^{3/2}} \\ &+ J\lambda \left( -\frac{3B(\lambda^2 k_y^2 + B^2) f_X}{(\lambda^2 k^2 + B^2)^{5/2}} + B \frac{2f_X - k_x \partial_{k_y} f_X}{(\lambda^2 k^2 + B^2)^{3/2}} \right) \end{aligned} \quad (\text{H5})$$

up to the first order in  $J$ . It is nonzero for all  $N_X$  due to the first term.

4)  $S^{x;x}/E^x$

We show that  $S^{x;x}/E^x$  is nonzero only for the  $d_{x^2-y^2}$ -wave altermagnet. We have  $S^{x;x}/E^x \neq 0$  only for  $d' = d_{x^2-y^2}$  as in shown as follows.  $Q_{+-}^{xx}/\varepsilon_{mn}$  is expanded as

$$\begin{aligned} \frac{Q_{+-}^{xx}}{\varepsilon_{mn}} &= -\frac{\lambda B}{2(\lambda^2 k^2 + B^2)^{3/2}} - \frac{J\lambda^2 k^2 (f_X - k_x \partial_{k_x} f_X)}{2(\lambda^2 k^2 + B^2)^{5/2}} \\ &+ \frac{JB^2 (2f_X + k_x \partial_{k_x} f_X)}{2(\lambda^2 k^2 + B^2)^{5/2}} \end{aligned} \quad (\text{H6})$$

up to the first order in  $J$ .

First, we consider the case with  $J = 0$ , where

$$\frac{Q_{+-}^{xx}}{\varepsilon_{mn}} = -\frac{\lambda B}{2(\lambda^2 k^2 + B^2)^{3/2}}. \quad (\text{H7})$$

We have

$$\int_0^\infty k dk \int \frac{Q_{+-}^{xx}}{\varepsilon_{mn}} d\phi = -\frac{B}{2|B|\lambda}. \quad (\text{H8})$$

Hence, there is nonzero response in the presence of nonzero  $B$ .

Next, we consider the case with  $B = 0$ , where

$$\frac{Q_{+-}^{xx}}{\varepsilon_{mn}} = -\frac{J\lambda^2 k^2 (f_X - k_x \partial_{k_x} f_X)}{2(\lambda^2 k^2 + B^2)^{5/2}}. \quad (\text{H9})$$

By using

$$\partial_{k_x} = \cos \phi \partial_k - \frac{\sin \phi}{k} \partial_\phi, \quad (\text{H10})$$

$$\partial_{k_y} = \sin \phi \partial_k + \frac{\cos \phi}{k} \partial_\phi, \quad (\text{H11})$$

we have

$$\begin{aligned} f_X - k_x \partial_{k_x} f_X &= f_X - k \cos \phi \left( \cos \phi \partial_k f_X - \frac{\sin \phi}{k} \partial_\phi f_X \right). \end{aligned} \quad (\text{H12})$$

For  $f_X = k^{N_X} \cos N_X \phi$ , we have

$$\begin{aligned} f_X - k_x \partial_{k_x} f_X &= -\frac{k^{N_X}}{2} (N_X \cos(N_X - 2)\phi \\ &+ (N_X - 2) \cos N_X \phi). \end{aligned} \quad (\text{H13})$$

It is nonzero only for  $N_X = 2$ . It is nonzero contribution only for the  $d_{x^2-y^2}$ -wave altermagnet. For  $f_X = k^{N_X} \sin N_X \phi$ , we also have

$$\begin{aligned} f_X - k_x \partial_{k_x} f_X &= -\frac{k^{N_X}}{2} (N_X \sin(N_X - 2)\phi \\ &+ (N_X - 2) \sin N_X \phi), \end{aligned} \quad (\text{H14})$$

which is zero for all  $N_X$ . It leads to

$$\begin{aligned} \frac{S^{x;x}}{E^x} &= -\int d^2 k f_{+-} \frac{2Q_{+-}^{xx}}{\varepsilon_{+-}} \\ &= -2\pi J m \sqrt{m(\lambda^2 + 2\mu)} \text{sgn}(\lambda) \\ &- \frac{\pi B}{2\lambda^3} (BJ + \lambda^2) \\ &+ B \ln \frac{B^2 + 2m\lambda^2 \{m\lambda^2 + \mu - M\}}{B^2 + 2m\lambda^2 \{m\lambda^2 + \mu + M\}} \end{aligned} \quad (\text{H15})$$

with

$$M \equiv \sqrt{(m\lambda^2)^2 + 2\mu m\lambda^2 + B^2} \quad (\text{H16})$$

up to the first order in  $J$ . For  $B = 0$ , we obtain

$$\frac{S^x}{E^x} = -\frac{2mJ\pi}{\lambda}.$$

It is nonzero even for  $B = 0$ .

5)  $S^{y;y}/E^y$

We show that  $S^{y;y}/E^y$  is nonzero only for the  $d_{xy}$ -wave alternagnet. We have  $S^{y;y}/E^y \neq 0$  only for  $d' = d_{xy}$  as in shown as follows.  $Q_{+-}^{yy}/\varepsilon_{mn}$  is expanded as

$$\frac{Q_{+-}^{yy}}{\varepsilon_{mn}} = -\frac{\lambda B}{2(\lambda^2 k^2 + B^2)^{3/2}} + \frac{J\lambda^2 k^2 (f_X - k_y \partial_{k_y} f_X)}{2(\lambda^2 k^2 + B^2)^{5/2}} + \frac{JB^2 (2f_X + k_y \partial_{k_y} f_X)}{2(\lambda^2 k^2 + B^2)^{5/2}} \quad (\text{H17})$$

up to the first order in  $J$ . As in the case of  $Q_{+-}^{xx}$ , there is nonzero response for  $B \neq 0$ .

We consider the case with  $B = 0$ , where

$$\frac{Q_{+-}^{yy}}{\varepsilon_{mn}} = \frac{J\lambda^2 k^2 (f_X - k_y \partial_{k_y} f_X)}{2(\lambda^2 k^2 + B^2)^{5/2}}. \quad (\text{H18})$$

For  $f_X = k^{N_X} \cos N_X \phi$ , we have

$$f_X - k_x \partial_{k_x} f_X = \frac{k^{N_X}}{2} (N_X \sin(N_X - 2)\phi + N_X \sin N_X \phi + 2 \cos N_X \phi). \quad (\text{H19})$$

On the other hand, for  $f_X = k^{N_X} \sin N_X \phi$ , we have

$$f_X - k_x \partial_{k_x} f_X = -\frac{k^{N_X}}{2} (N_X \cos(N_X - 2)\phi + N_X \cos N_X \phi - 2 \sin N_X \phi), \quad (\text{H20})$$

which is nonzero only for  $N_X = 2$  because

$$\int (f_X - k_x \partial_{k_x} f_X) d\phi = -2k^2 \pi \delta_{N_X, 2}. \quad (\text{H21})$$

It leads to

$$\begin{aligned} \frac{S^{y;y}}{E^y} &= -\int d^2 k f_{+-} \frac{2Q_{+-}^{yy}}{\varepsilon_{+-}} \\ &= -2\pi J m \sqrt{m(\lambda^2 + 2\mu)} \text{sgn}(\lambda) \\ &\quad - \frac{\pi B}{2\lambda^3} (BJ + \lambda^2) \\ &\quad + B \ln \frac{B^2 + 2m\lambda^2 \{m\lambda^2 + \mu - M\}}{B^2 + 2m\lambda^2 \{m\lambda^2 + \mu + M\}} \end{aligned} \quad (\text{H22})$$

Hence, we have nonzero contribution only for the  $d_{xy}$ -wave alternagnet.

6)  $S^{x;y}/E^y$

We show that  $S^{x;y}/E^y$  is nonzero only for the  $d_{xy}$ -wave alternagnet.  $Q_{+-}^{xy}$  is expanded as

$$Q_{+-}^{xy} = \frac{\lambda k_y J \partial_{k_x} f_X}{2(\lambda^2 k^2 + B^2)^{3/2}} \quad (\text{H23})$$

up to the first order in  $J$ . It is evaluated as follows. The numerator of  $Q_{+-}^{xy}$  reads

$$k_y \partial_{k_x} f_X = N k^{N_X} \cos(N_X - 1)\phi \sin \phi \quad (\text{H24})$$

for  $f_X = k^{N_X} \cos N_X \phi$ , whose integration over  $\phi$  is zero,

$$\int k_y \partial_{k_x} f_X d\phi = 0. \quad (\text{H25})$$

We also have

$$k_y \partial_{k_x} f_X = N k^{N_X} \sin(N_X - 1)\phi \sin \phi, \quad (\text{H26})$$

for  $f_X = k^{N_X} \sin N_X \phi$ , whose integration over  $\phi$  is obtained as

$$\int k_y \partial_{k_x} f_X d\phi = -2k^2 \pi \delta_{N_X, 2}. \quad (\text{H27})$$

Then, we have the static electric-field induced spin polarization

$$\begin{aligned} \frac{S^{x;y}}{E^y} &= -\int d^2 k f_{+-} \frac{2Q_{+-}^{xy}}{\varepsilon_{+-}} \\ &= -\frac{J\pi}{\lambda^3} \sum_{\eta=\pm} \eta \frac{2(B^2 + m\lambda^2)(m\lambda^2 + \mu + \eta M)}{\sqrt{B^2 + 2m\lambda^2}(m\lambda^2 + \mu + \eta M)} \end{aligned} \quad (\text{H28})$$

up to the first order in  $J$ . For  $B = 0$ , it is simplified as

$$\frac{S^x}{E^y} = -\frac{2mJ\pi}{\lambda} \quad (\text{H29})$$

for  $\mu > 0$ . Hence,  $S^{x;y}/E^y$  is nonzero only for the  $d_{xy}$ -wave alternagnet.

7)  $S^{y;x}/E^x$

We show that  $S^{y;x}/E^x$  is nonzero only for the  $d_{xy}$ -wave alternagnet.  $Q_{+-}^{yx}$  is expanded as

$$Q_{+-}^{yx} = \frac{\lambda k_x J \partial_{k_y} f_X}{2(\lambda^2 k^2 + B^2)^{3/2}} \quad (\text{H30})$$

up to the first order in  $J$ . It is evaluated as follows. We study  $Q_{+-}^{yx}$ , whose numerator is  $k_x \partial_{k_y} f_X$ .

$$k_x \partial_{k_y} f_X = N k^{N_X} \sin(N_X - 1)\phi \cos \phi \quad (\text{H31})$$

for  $f_X = k^{N_X} \cos N_X \phi$ , whose integration over  $\phi$  is

$$\int k_x \partial_{k_y} f_X d\phi = 0. \quad (\text{H32})$$

We also have

$$k_x \partial_{k_y} f_X = N k^{N_X} \cos(N_X - 1)\phi \cos \phi \quad (\text{H33})$$

for  $f_X = k^{N_X} \sin N_X \phi$ , whose integration is obtained as

$$\int k_x \partial_{k_y} f_X d\phi = 2k^2 \pi \delta_{N_X, 2}. \quad (\text{H34})$$

Then, we have the static electric-field induced spin polarization

$$\begin{aligned} \frac{S^{y;x}}{E^x} &= -\int d^2 k f_{+-} \frac{2Q_{+-}^{yx}}{\varepsilon_{+-}} \\ &= \frac{J\pi}{\lambda^3} \sum_{\eta=\pm} \eta \frac{2(B^2 + m\lambda^2)(m\lambda^2 + \mu + \eta M)}{\sqrt{B^2 + 2m\lambda^2}(m\lambda^2 + \mu + \eta M)} \end{aligned} \quad (\text{H35})$$

up to the first order in  $J$ . For  $B = 0$ , it is simplified as

$$\frac{S^x}{E^y} = \frac{2mJ\pi}{\lambda} \quad (\text{H36})$$

for  $\mu > 0$ . Hence,  $S^{y;x}/E^x$  is nonzero only for the  $d_{xy}$ -wave altermagnet.

### Appendix I: Uhlmann geometry

We prove Eq.(275) in the main text. We first calculate

$$\begin{aligned} & \langle \psi_n(\mathbf{k}) | d\rho | \psi_m(\mathbf{k}) \rangle \\ &= \sum_{n'} \partial_{k_\mu} p_{n'} \delta_{nn'} \delta_{n'm} \\ & \quad - i p_{n'} a_{nn'}^\mu(\mathbf{k}) \delta_{n'm} - i p_{n'} \delta_{nn'} a_{mn'}^{\mu*}(\mathbf{k}) \\ &= \delta_{nm} \partial_{k_\mu} p_n - i p_n a_{nm}^\mu(\mathbf{k}) + i p_m a_{nm}^\mu(\mathbf{k}), \end{aligned} \quad (\text{I1})$$

where we have used

$$\begin{aligned} d\rho &= \sum_{n'} \partial_{k_\mu} p_{n'} |\psi_{n'}(\mathbf{k})\rangle \langle \psi_{n'}(\mathbf{k})| \\ & \quad + p_{n'} (\partial_{k_\mu} |\psi_{n'}(\mathbf{k})\rangle) \langle \psi_{n'}(\mathbf{k})| \\ & \quad + p_{n'} |\psi_{n'}(\mathbf{k})\rangle (\partial_{k_\mu} \langle \psi_{n'}(\mathbf{k})|). \end{aligned} \quad (\text{I2})$$

On the other hand, we have

$$\begin{aligned} & \langle \psi_n(\mathbf{k}) | \frac{\mathcal{L}\rho + \rho\mathcal{L}}{2} | \psi_m(\mathbf{k}) \rangle \\ &= \langle \psi_n(\mathbf{k}) | \left( \sum_{n'} \frac{1}{2} \frac{\partial_{k_\mu} p_{n'}}{p_{n'}} |\psi_{n'}\rangle \langle \psi_{n'}| \right. \\ & \quad \times \sum_{m'} p_{m'} |\psi_{m'}(\mathbf{k})\rangle \langle \psi_{m'}(\mathbf{k})| \\ & \quad + i \sum_{n' \neq m'} \frac{p_{m'} - p_{n'}}{p_{m'} + p_{n'}} a_{n'm'}^\mu |\psi_{n'}\rangle \langle \psi_{m'}| \\ & \quad \times \sum_{m''} p_{m''} |\psi_{m''}(\mathbf{k})\rangle \langle \psi_{m''}(\mathbf{k})| \\ & \quad + \sum_{m''} p_{m''} |\psi_{m''}(\mathbf{k})\rangle \langle \psi_{m''}(\mathbf{k})| \\ & \quad \times \sum_{n'} \frac{1}{2} \frac{\partial_{k_\mu} p_{n'}}{p_{n'}} |\psi_{n'}\rangle \langle \psi_{n'}| \\ & \quad \left. + \sum_{m'} p_{m'} |\psi_{m'}(\mathbf{k})\rangle \langle \psi_{m'}(\mathbf{k})| \right) | \psi_m(\mathbf{k}) \rangle. \end{aligned} \quad (\text{I3})$$

It is further calculated as

$$\begin{aligned} & \sum_{n'} \delta_{nn'} \frac{1}{2} \frac{\partial_{k_\mu} p_{n'}}{p_{n'}} \delta_{n'm'} p_{m'} \delta_{m'm} \\ & \quad + i \sum_{n' \neq m'} \frac{p_{m'} - p_{n'}}{p_{m'} + p_{n'}} a_{n'm'}^\mu \delta_{nn'} \delta_{m'm'} \delta_{m''m} \\ & \quad + \sum_{m'} p_{m'} \delta_{nm'} \sum_{n'} \frac{1}{2} \frac{\partial_{k_\mu} p_{n'}}{p_{n'}} \delta_{m'n'} \delta_{n'm} \\ & \quad + \sum_{n' \neq m'} \delta_{nm'} p_{m'} \frac{p_{m'} - p_{n'}}{p_{m'} + p_{n'}} a_{n'm'}^\mu \delta_{m'n'} \delta_{m'm} \\ &= \delta_{nm} \frac{1}{2} \frac{\partial_{k_\mu} p_n}{p_n} p_n + i \frac{p_m - p_n}{p_m + p_n} a_{nm}^\mu p_m \\ & \quad + \delta_{nm} p_n \frac{1}{2} \frac{\partial_{k_\mu} p_n}{p_n} + i p_n \frac{p_m - p_n}{p_m + p_n} a_{nm}^\mu \\ &= \delta_{nm} \partial_{k_\mu} p_n + i (p_m - p_n) a_{nm}^\mu, \end{aligned} \quad (\text{I4})$$

which is identical to Eq.(I1).

### 1. Positive Operator-Valued Measure

Positive Operator-Valued Measure (POVM)  $\Pi_n$  satisfies[222]

$$p_n = \text{Tr} \rho \Pi_n, \quad (\text{I5})$$

and

$$\sum_{n=1}^N \Pi_n = 1. \quad (\text{I6})$$

It is a generalization of the projective measurement. These two conditions lead to the conservation of the provability,

$$\sum_{n=1}^N p_n = \sum_{n=1}^N \text{Tr} \rho \Pi_n = \text{Tr} \rho \sum_{n=1}^N \Pi_n = \text{Tr} \rho = 1. \quad (\text{I7})$$

By using it, the classical Fisher information (280) is rewritten as

$$\begin{aligned} \mathcal{F}_{\text{CFisher}}^{\mu\nu} &= \sum_{n=1}^N \text{Tr} \rho \Pi_n \frac{\text{Tr} \frac{\partial \rho}{\partial k_\mu} \Pi_n}{\text{Tr} \rho \Pi_n} \frac{\text{Tr} \frac{\partial \rho}{\partial k_\nu} \Pi_n}{\text{Tr} \rho \Pi_n} \\ &= \sum_{n=1}^N \frac{1}{\text{Tr} \rho \Pi_n} \text{Tr} \left( \frac{\partial \rho}{\partial k_\mu} \Pi_n \right) \text{Tr} \left( \frac{\partial \rho}{\partial k_\nu} \Pi_n \right). \end{aligned} \quad (\text{I8})$$

### 2. Quantum Cramér-Rao inequality

We prove the quantum Cramér-Rao inequality (282). It is enough to show[140]

$$\sum_{\mu\nu} a_\mu \mathcal{F}_{\text{CFisher}}^{\mu\nu} a_\nu < \sum_{\mu\nu} a_\mu \mathcal{F}_{\text{QFisher}}^{\mu\nu} a_\nu \quad (\text{I9})$$

for arbitrary set of  $a_\mu$ . By introducing

$$\tilde{\mathcal{L}} = \sum_{\mu} a_{\mu} \mathcal{L}^{\mu}, \quad (\text{I10})$$

we define  $\mathcal{F}_{\text{CFisher}}$  as

$$\begin{aligned} \mathcal{F}_{\text{CFisher}} &\equiv \sum_{n=1}^N \frac{1}{\text{Tr} \rho \Pi_n} \left( \text{Tr} \left( \frac{1}{2} (\tilde{\mathcal{L}} \rho + \rho \tilde{\mathcal{L}}) \Pi_n \right) \right)^2 \\ &= \sum_{n=1}^N \frac{1}{\text{Tr} \rho \Pi_n} \sum_{\mu\nu} \text{Tr} \left( \frac{a_{\mu}}{2} (\mathcal{L}^{\mu} \rho + \rho \mathcal{L}^{\mu}) \Pi_n \right) \\ &\quad \times \text{Tr} \left( \frac{a_{\nu}}{2} (\mathcal{L}^{\nu} \rho + \rho \mathcal{L}^{\nu}) \Pi_n \right) \\ &= \sum_{\mu\nu} a_{\mu} \mathcal{F}_{\text{CFisher}}^{\mu\nu} a_{\nu}. \end{aligned} \quad (\text{I11})$$

First, we show the inequality

$$\begin{aligned} &\sum_{\mu\nu} a_{\mu} \mathcal{F}_{\text{CFisher}}^{\mu\nu} a_{\nu} \\ &= \sum_{n=1}^N \frac{1}{\text{Tr} \rho \Pi_n} \left( \text{Tr} \left( \frac{1}{2} (\tilde{\mathcal{L}} \rho + \rho \tilde{\mathcal{L}}) \Pi_n \right) \right)^2 \\ &= \sum_{n=1}^N \frac{1}{\text{Tr} \rho \Pi_n} \left( \text{Tr} \left( \text{Re} \tilde{\mathcal{L}} \rho \Pi_n \right) \right)^2 \\ &\leq \sum_{n=1}^N \frac{1}{\text{Tr} \rho \Pi_n} \left| \text{Tr} \left( \tilde{\mathcal{L}} \rho \Pi_n \right) \right|^2. \end{aligned} \quad (\text{I12})$$

Next, setting

$$A^{\dagger} = \frac{\sqrt{\rho} \sqrt{\Pi_n}}{\sqrt{\text{Tr} \rho \Pi_n}}, \quad B = \sqrt{\Pi_n} \tilde{\mathcal{L}} \sqrt{\rho}, \quad (\text{I13})$$

we use the Schwartz inequality

$$|\text{Tr} A^{\dagger} B|^2 \leq \text{Tr} A^{\dagger} A \text{Tr} B^{\dagger} B. \quad (\text{I14})$$

The left-hand side is

$$\begin{aligned} |\text{Tr} A^{\dagger} B|^2 &= \left| \text{Tr} \frac{\sqrt{\rho} \sqrt{\Pi_n}}{\sqrt{\text{Tr} \rho \Pi_n}} \sqrt{\Pi_n} \tilde{\mathcal{L}} \sqrt{\rho} \right|^2 \\ &= \left| \text{Tr} \frac{\sqrt{\rho} \Pi_n \tilde{\mathcal{L}} \sqrt{\rho}}{\sqrt{\text{Tr} \rho \Pi_n}} \right|^2 \\ &= \left| \text{Tr} \frac{\tilde{\mathcal{L}} \rho \Pi_n}{\sqrt{\text{Tr} \rho \Pi_n}} \right|^2, \end{aligned} \quad (\text{I15})$$

while the right-hand side is

$$\begin{aligned} &\sum_{n=1}^N \text{Tr} A^{\dagger} A \text{Tr} B^{\dagger} B \\ &= \sum_{n=1}^N \text{Tr} \frac{\sqrt{\rho} \sqrt{\Pi_n}}{\sqrt{\text{Tr} \rho \Pi_n}} \frac{\sqrt{\Pi_n} \sqrt{\rho}}{\sqrt{\text{Tr} \rho \Pi_n}} \text{Tr} \sqrt{\Pi_n} \tilde{\mathcal{L}} \sqrt{\rho} \sqrt{\rho} \tilde{\mathcal{L}} \sqrt{\Pi_n} \\ &= \sum_{n=1}^N \text{Tr} \frac{\sqrt{\rho} \Pi_n \sqrt{\rho}}{\text{Tr} \rho \Pi_n} \text{Tr} \sqrt{\Pi_n} \tilde{\mathcal{L}} \rho \tilde{\mathcal{L}} \sqrt{\Pi_n} \\ &= \sum_{n=1}^N \text{Tr} \frac{\rho \Pi_n}{\text{Tr} \rho \Pi_n} \text{Tr} \Pi_n \tilde{\mathcal{L}} \rho \tilde{\mathcal{L}} = \sum_{n=1}^N \text{Tr} \Pi_n \tilde{\mathcal{L}} \rho \tilde{\mathcal{L}} \\ &= \text{Tr} \tilde{\mathcal{L}} \rho \tilde{\mathcal{L}} = \text{Tr} \rho \tilde{\mathcal{L}}^2 = \frac{1}{2} \mathcal{F}_{\text{QFisher}}, \end{aligned} \quad (\text{I16})$$

where we have defined

$$\begin{aligned} \mathcal{F}_{\text{QFisher}}^{\mu\nu} &\equiv \frac{1}{2} \text{Tr} \rho \tilde{\mathcal{L}}^2 = \frac{1}{2} \text{Tr} \rho \left( \sum_{\mu} a_{\mu} \mathcal{L}^{\mu} \right)^2 \\ &= \frac{1}{2} \sum_{\mu\nu} a_{\mu} \text{Tr} [\rho \{ \mathcal{L}^{\mu}, \mathcal{L}^{\nu} \}] a_{\nu} \\ &= \sum_{\mu\nu} a_{\mu} \mathcal{F}_{\text{QFisher}}^{\mu\nu} a_{\nu}. \end{aligned} \quad (\text{I17})$$

Hence, the quantum Cramér-Rao inequality (282) is proved.

### 3. Quantum Fisher information for a pure state

By inserting

$$\rho = |\psi_n\rangle \langle \psi_n|, \quad (\text{I18})$$

to Eq.(290), we have

$$\begin{aligned} &\mathcal{F}_{\text{QFisher}}^{\mu\nu} \\ &= 2 \text{Tr} |\psi_n\rangle \langle \psi_n| \left( \frac{\partial |\psi_n\rangle \langle \psi_n|}{\partial k_{\mu}} \frac{\partial |\psi_n\rangle \langle \psi_n|}{\partial k_{\nu}} \right. \\ &\quad \left. + \frac{\partial |\psi_n\rangle \langle \psi_n|}{\partial k_{\nu}} \frac{\partial |\psi_n\rangle \langle \psi_n|}{\partial k_{\mu}} \right) \\ &= 2 \text{Tr} \langle \psi_n| \frac{\partial |\psi_n\rangle}{\partial k_{\mu}} \langle \psi_n| \frac{\partial |\psi_n\rangle}{\partial k_{\nu}} \\ &\quad + \langle \psi_n| \frac{\partial |\psi_n\rangle}{\partial k_{\mu}} \frac{\partial \langle \psi_n|}{\partial k_{\nu}} | \psi_n \rangle \\ &\quad + \frac{\partial \langle \psi_n|}{\partial k_{\mu}} \frac{\partial |\psi_n\rangle}{\partial k_{\nu}} + \frac{\partial \langle \psi_n|}{\partial k_{\mu}} | \psi_n \rangle \frac{\partial \langle \psi_n|}{\partial k_{\nu}} | \psi_n \rangle \\ &\quad + \langle \psi_n| \frac{\partial |\psi_n\rangle}{\partial k_{\nu}} \langle \psi_n| \frac{\partial |\psi_n\rangle}{\partial k_{\mu}} + \langle \psi_n| \frac{\partial |\psi_n\rangle}{\partial k_{\nu}} \frac{\partial \langle \psi_n|}{\partial k_{\mu}} | \psi_n \rangle \\ &\quad + \frac{\partial \langle \psi_n|}{\partial k_{\nu}} \frac{\partial |\psi_n\rangle}{\partial k_{\mu}} + \frac{\partial \langle \psi_n|}{\partial k_{\nu}} | \psi_n \rangle \frac{\partial \langle \psi_n|}{\partial k_{\mu}} | \psi_n \rangle. \end{aligned} \quad (\text{I19})$$

By using the relations

$$\begin{aligned} & \langle \psi_n | \frac{\partial |\psi_n\rangle}{\partial k_\mu} \langle \psi_n | \frac{\partial |\psi_n\rangle}{\partial k_\nu} + \langle \psi_n | \frac{\partial |\psi_n\rangle}{\partial k_\mu} \frac{\partial \langle \psi_n |}{\partial k_\nu} | \psi_n \rangle \\ &= \langle \psi_n | \frac{\partial |\psi_n\rangle}{\partial k_\mu} \frac{\partial \langle \psi_n | \psi_n \rangle}{\partial k_\nu} = 0, \end{aligned} \quad (I20)$$

$$\begin{aligned} & \langle \psi_n | \frac{\partial |\psi_n\rangle}{\partial k_\nu} \langle \psi_n | \frac{\partial |\psi_n\rangle}{\partial k_\mu} + \langle \psi_n | \frac{\partial |\psi_n\rangle}{\partial k_\nu} \frac{\partial \langle \psi_n |}{\partial k_\mu} | \psi_n \rangle \\ &= \langle \psi_n | \frac{\partial |\psi_n\rangle}{\partial k_\nu} \frac{\partial \langle \psi_n | \psi_n \rangle}{\partial k_\mu} = 0, \end{aligned} \quad (I21)$$

we have

$$\begin{aligned} \mathcal{F}_{\text{QFisher}}^{\mu\nu} &= 2\text{Tr} \frac{\partial \langle \psi_n | \partial |\psi_n\rangle}{\partial k_\mu \partial k_\nu} - \frac{\partial \langle \psi_n |}{\partial k_\mu} | \psi_n \rangle \langle \psi_n | \frac{\partial |\psi_n\rangle}{\partial k_\nu} \\ &+ \frac{\partial \langle \psi_n | \partial |\psi_n\rangle}{\partial k_\nu \partial k_\mu} - \frac{\partial \langle \psi_n |}{\partial k_\nu} | \psi_n \rangle \langle \psi_n | \frac{\partial |\psi_n\rangle}{\partial k_\mu} \\ &= 2(\mathcal{F}^{\mu\nu} + \mathcal{F}^{\nu\mu}) = 4g^{\mu\nu}. \end{aligned} \quad (I22)$$

This is Eq.(292) in the main text.

$$\begin{aligned} \mathcal{U}^{\mu\nu} &= -2i\text{Tr} | \psi_n \rangle \langle \psi_n | \left( \frac{\partial |\psi_n\rangle \langle \psi_n |}{\partial k_\mu} \frac{\partial |\psi_n\rangle \langle \psi_n |}{\partial k_\nu} \right. \\ &\quad \left. - \frac{\partial |\psi_n\rangle \langle \psi_n |}{\partial k_\nu} \frac{\partial |\psi_n\rangle \langle \psi_n |}{\partial k_\mu} \right) \\ &= -2i\text{Tr} \langle \psi_n | \frac{\partial |\psi_n\rangle}{\partial k_\mu} \langle \psi_n | \frac{\partial |\psi_n\rangle}{\partial k_\nu} \\ &\quad + \langle \psi_n | \frac{\partial |\psi_n\rangle}{\partial k_\mu} \frac{\partial \langle \psi_n |}{\partial k_\nu} | \psi_n \rangle \\ &\quad + \frac{\partial \langle \psi_n | \partial |\psi_n\rangle}{\partial k_\mu \partial k_\nu} + \frac{\partial \langle \psi_n |}{\partial k_\mu} | \psi_n \rangle \frac{\partial \langle \psi_n |}{\partial k_\nu} | \psi_n \rangle \\ &\quad - \langle \psi_n | \frac{\partial |\psi_n\rangle}{\partial k_\nu} \langle \psi_n | \frac{\partial |\psi_n\rangle}{\partial k_\mu} - \langle \psi_n | \frac{\partial |\psi_n\rangle}{\partial k_\nu} \frac{\partial \langle \psi_n |}{\partial k_\mu} | \psi_n \rangle \\ &\quad - \frac{\partial \langle \psi_n | \partial |\psi_n\rangle}{\partial k_\nu \partial k_\mu} - \frac{\partial \langle \psi_n |}{\partial k_\nu} | \psi_n \rangle \frac{\partial \langle \psi_n |}{\partial k_\mu} | \psi_n \rangle. \end{aligned} \quad (I23)$$

Using the relations Eqs.(I20) and (I21), we have

$$\begin{aligned} \mathcal{U}^{\mu\nu} &= -2i\text{Tr} \frac{\partial \langle \psi_n | \partial |\psi_n\rangle}{\partial k_\mu \partial k_\nu} - \frac{\partial \langle \psi_n |}{\partial k_\mu} | \psi_n \rangle \langle \psi_n | \frac{\partial |\psi_n\rangle}{\partial k_\nu} \\ &\quad - \frac{\partial \langle \psi_n | \partial |\psi_n\rangle}{\partial k_\nu \partial k_\mu} + \frac{\partial \langle \psi_n |}{\partial k_\nu} | \psi_n \rangle \langle \psi_n | \frac{\partial |\psi_n\rangle}{\partial k_\mu} \\ &= -2i(\mathcal{F}^{\mu\nu} - \mathcal{F}^{\nu\mu}) = -4\Omega^{\mu\nu}. \end{aligned} \quad (I24)$$

This is Eq.(293) in the main text.

- 
- [1] J. P. Provost and G. Vallee, Riemannian structure on manifolds of quantum states, *Comm. Math. Phys.* 76, 289 (1980).  
 [2] M. V. Berry, Quantal phase factors accompanying adiabatic changes, *Proc. R. Soc. A* 392, 45 (1984).  
 [3] Yu-Quan Ma, Shu Chen, Heng Fan, and Wu-Ming Liu, Abelian and non-Abelian quantum geometric tensor, *Phys. Rev. B* 81, 245129 (2010).  
 [4] D. J. Thouless, M. Kohmoto, M. P. Nightingale, and M. den Nijs, Quantized Hall Conductance in a Two-Dimensional Periodic Potential *Phys. Rev. Lett.* 49, 405 (1982)  
 [5] Qian Niu, D. J. Thouless, and Yong-Shi Wu, Quantized Hall conductance as a topological invariant, *Phys. Rev. B* 31, 3372 (1985)  
 [6] J. Ahn, G.-Y. Guo, N. Nagaosa, Low-Frequency Divergence and Quantum Geometry of the Bulk Photovoltaic Effect in

- Topological Semimetals, *Phys. Rev. X* 10, 041041 (2020).  
 [7] T. Holder, D. Kaplan, B. Yan, Consequences of time-reversal-symmetry breaking in the light-matter interaction: Berry curvature, quantum metric, and diabatic motion, *Phys. Rev. Res.* 2, 033100 (2020).  
 [8] P. Bhalla, K. Das, D. Culcer, A. Agarwal, Resonant Second-Harmonic Generation as a Probe of Quantum Geometry, *Phys. Rev. Lett.* 129, 227401 (2022)  
 [9] J. Ahn, G.-Y. Guo, N. Nagaosa, A. Vishwanath, Riemannian geometry of resonant optical responses, *Nature Physics* 18, 290 (2022)  
 [10] Ivo Souza, Tim Wilkens, and Richard M. Martin, Polarization and localization in insulators: Generating function approach, *Phys. Rev. B* 62, 1666 (2000)  
 [11] W. Chen and G. von Gersdorff, Measurement of interaction-

- dressed Berry curvature and quantum metric in solids by optical absorption, *SciPost Phys. Core* 5, 040 (2022).
- [12] Yugo Onishi and Liang Fu, Fundamental Bound on Topological Gap, *Phys. Rev. X* 14, 011052 (2024)
- [13] Matheus S. M. de Sousa, Antonio L. Cruz, and Wei Chen, Mapping quantum geometry and quantum phase transitions to real space by a fidelity marker, *Phys. Rev. B* 107, 205133 (2023)
- [14] Barun Ghosh, Yugo Onishi, Su-Yang Xu, Hsin Lin, Liang Fu and Arun Bansil, Probing quantum geometry through optical conductivity and magnetic circular dichroism, *Science Advances: sciadv.ado1761* (2024)
- [15] Wei Chen, Quantum geometrical properties of topological materials, *J. Phys.: Condens. Matter* 37 025605 (2025)
- [16] Wei Chen, Dielectric and optical markers originating from quantum geometry, *Phys. Rev. B* 111, 085202 (2025)
- [17] M. Ezawa, Analytic approach to quantum metric and optical conductivity in Dirac models with parabolic mass in arbitrary dimensions, *Phys. Rev. B* 110, 195437 (2024)
- [18] Chang-geun Oh, Sun-Woo Kim, Kun Woo Kim, Bartomeu Monserrat, and Jun-Won Rhim, Universal Optical Conductivity from Quantum Geometry in Quadratic Band-Touching Semimetals, arXiv:2503.18372
- [19] M. Ezawa, Quantum geometry and elliptic optical dichroism in p-wave magnets, *Phys. Rev. B* 112, 045302 (2025)
- [20] I. Sodemann and L. Fu, Quantum nonlinear Hall effect induced by Berry curvature dipole in time-reversal invariant materials, *Phys. Rev. Lett.* 115, 216806 (2015).
- [21] Q. Ma, et al., Observation of the nonlinear Hall effect under time-reversal-symmetric conditions, *Nature* 565, 337 (2019)
- [22] C. Wang, Y. Gao, and D. Xiao, Intrinsic nonlinear Hall effect in antiferromagnetic tetragonal cumnas, *Phys. Rev. Lett.* 127, 277201 (2021).
- [23] Y. Michishita and N. Nagaosa, Dissipation and geometry in nonlinear quantum transports of multiband electronic systems, *Phys. Rev. B* 106, 125114 (2022).
- [24] Kamal Das, Shibalik Lahiri, Rhonald Burgos Atencia, Dimitrie Culcer, and Amit Agarwal, Intrinsic nonlinear conductivities induced by the quantum metric, *Phys. Rev. B* 108, L201405 (2023)
- [25] A. Gao, Y.-F. Liu, J.-X. Qiu, B. Ghosh, T.V. Trevisan, Y. Onishi, C. Hu, T. Qian, H.-J. Tien, S.-W. Chen et al., Quantum metric nonlinear Hall effect in a topological antiferromagnetic heterostructure, *Science* 381, eadfl506 (2023).
- [26] N. Wang, D. Kaplan, Z. Zhang, T. Holder, N. Cao, A. Wang, X. Zhou, F. Zhou, Z. Jiang, C. Zhang et al., Quantum metric-induced nonlinear transport in a topological antiferromagnet, *Nature (London)* 621, 487 (2023).
- [27] Daniel Kaplan, Tobias Holder and Binghai Yan, Unification of Nonlinear Anomalous Hall Effect and Nonreciprocal Magnetoresistance in Metals by the Quantum Geometry, *Phys. Rev. Lett.* 132, 026301 (2024)
- [28] Giacomo Sala, et.al., The quantum metric of electrons with spin-momentum locking, *Science* 389, 822 (2025)
- [29] Yuan Fang, Jennifer Cano, and Sayed Ali Akbar Ghorashi, Quantum Geometry Induced Nonlinear Transport in Altermagnets, *Phys. Rev. Lett.* 133, 106701 (2024)
- [30] Zhen-Hao Gong, Z. Z. Du, Hai-Peng Sun, Hai-Zhou Lu, X. C. Xie, Nonlinear transport theory at the order of quantum metric, arXiv:2410.04995v2
- [31] M. Ezawa, Intrinsic nonlinear conductivity induced by quantum geometry in altermagnets and measurement of the in-plane Neel vector, *Phys. Rev. B* 110, L241405 (2024)
- [32] M. Ezawa, Purely electrical detection of the Neel vector of p-wave magnets based on linear and nonlinear conductivities, *Phys. Rev. B* 112, 125412 (2025)
- [33] Hikaru Watanabe and Youichi Yanase, Chiral Photocurrent in Parity-Violating Magnet and Enhanced Response in Topological Antiferromagnet, *Phys. Rev. X*, 11, 011001 (2021)
- [34] M. Ezawa, Higher-order bulk photovoltaic effects, quantum geometry and application to p-wave magnets, *Phys. Rev. B* 112, 155308 (2025)
- [35] M. Kang et al., Measurements of the quantum geometric tensor in solids, *Nature Physics* 21, 110 (2025)
- [36] S. Kim et al., Direct measurement of the quantum metric tensor in solids, *Science*. 388, 1050 (2025).
- [37] Makoto Naka, Satoru Hayami, Hiroaki Kusunose, Yuki Yanagi, Yukitoshi Motome and Hitoshi Seo, Spin current generation in organic antiferromagnets, *Nat. Com.* 10, 4305 (2019).
- [38] Rafael Gonzalez-Hernandez, Libor Šmejkal, Karel Vbourn, Yuta Yahagi, Jairo Sinova, Tomš Jungwirth, and Jakub Železn, Efficient electrical spin splitter based on nonrelativistic collinear antiferromagnetism, *Phys. Rev. Lett.*, 126:127701, (2021).
- [39] M Naka, Y Motome, and H Seo, Perovskite as a spin current generator. *Phys. Rev. B*, 103, 125114, (2021).
- [40] Arnab Bose, Nathaniel J. Schreiber, Rakshit Jain, Ding-Fu Shao, Hari P. Nair, Jiaxin Sun, Xiyue S. Zhang, David A. Muller, Evgeny Y. Tsymbal, Darrell G. Schlom & Daniel C. Ralph, Tilted spin current generated by the collinear antiferromagnet ruthenium dioxide, *Nature Electronics* 5, 267 (2022).
- [41] S. Hayami, Y. Yanagi, and H. Kusunose, Momentum-Dependent Spin Splitting by Collinear Antiferromagnetic Ordering, *J. Phys. Soc. Jpn.* 88, 123702 (2019).
- [42] L. Šmejkal, J. Sinova, and T. Jungwirth, Beyond Conventional Ferromagnetism and Antiferromagnetism: A Phase with Nonrelativistic Spin and Crystal Rotation Symmetry, *Phys. Rev. X*, 12, 031042 (2022).
- [43] Libor Šmejkal, Jairo Sinova, and Tomas Jungwirth, Emerging Research Landscape of Altermagnetism, *Phys. Rev. X* 12, 040501 (2022).
- [44] S. Hayami, Y. Yanagi, and H. Kusunose, Bottom-up design of spin-split and reshaped electronic band structures in antiferromagnets without spin-orbit coupling: Procedure on the basis of augmented multipoles, *Phys. Rev. B* 102, 144441 (2020)
- [45] Anna Birk Hellenes, Tomas Jungwirth, Jairo Sinova, Libor Šmejkal, Unconventional p-wave magnets, arXiv:2309.01607.
- [46] M. Ezawa, Planar Hall effects in X-wave magnets with  $X=p, d, f, g, i$  arXiv:2508.09472
- [47] M. Ezawa, Tunneling magnetoresistance in a junction made of X-wave magnets with  $X = p, d, f, g, i$ , arXiv:2509.16867
- [48] Paivi Torma, Essay: Where Can Quantum Geometry Lead Us? *Phys. Rev. Lett.* 131, 240001 (2023)
- [49] Tianyu Liu, Xiao-Bin Qiang, Hai-Zhou Lu, X. C. Xie, Quantum geometry in condensed matter, *National Science Review*, 12, nwae334 (2025)
- [50] Jiabin Yu, B. Andrei Bernevig, Raquel Queiroz, Enrico Rossi, Paivi Torma Bohm-Jung Yang, Quantum Geometry in Quantum Materials, arXiv:2501.00098
- [51] Yiyang Jiang, Tobias Holder, and Binghai Yan, Revealing Quantum Geometry in Nonlinear Quantum Materials, arXiv:2503.04943.
- [52] Ling Bai, Wanxiang Feng, Siyuan Liu, Libor Šmejkal, Yuriy Mokrousov, Yugui Yao, Altermagnetism: Exploring New Frontiers in Magnetism and Spintronics *Adv. Funct. Mater.*, 2409327 (2024).
- [53] T. Jungwirth, R. M. Fernandes, E. Fradkin, A. H. MacDonald,

- J. Sinova, L. Smejkal, From superfluid He3 to altermagnets, arXiv:2411.00717v1
- [54] Makoto Naka, Yukitoshi Motome and Hitoshi Seo, Altermagnetic Perovskites, *npj Spintronics* volume 3, 1 (2025)
- [55] Yuri Fukaya, Bo Lu, Keiji Yada, Yukio Tanaka, Jorge Cayao, Superconducting phenomena in systems with unconventional magnets, arXiv:2502.15400
- [56] Tomas Jungwirth, Jairo Sinova, Rafael M. Fernandes, Qihang Liu, Hikaru Watanabe, Shuichi Murakami, Satoru Nakatsuji and Libor Smejkal, Symmetry, microscopy and spectroscopy signatures of altermagnetism, arXiv:2506.22860
- [57] T. Jungwirth, J. Sinova, P. Wadley, D. Kriegner, H. Reichlova, F. Krizek, H. Ohno, and L. Smejkal, Altermagnetic spintronics, arXiv:2508.09748
- [58] Sayantika Bhowal, and Arnab Bose, Non-relativistic spin splitting: Features and Functionalities, arXiv:2510.20306
- [59] R. Resta, The insulating state of matter: a geometrical theory, *Eur. Phys. J. B* 79, 121 (2011)
- [60] G. Fubini, Sulle metriche definite da una forma Hermitiana, *Atti del Reale Istituto Veneto di Scienze, Lettere ed Arti*, 63 501 (1904)
- [61] E. Study, "Kurzeste Wege im komplexen Gebiet". *Mathematische Annalen* (in German). 60 (3). Springer Science and Business Media LLC: 321 (1905)
- [62] Frank Wilczek and A. Zee, Appearance of Gauge Structure in Simple Dynamical Systems, *Phys. Rev. Lett.* 52, 2111 (1984)
- [63] Mahito Kohmoto, Topological invariant and the quantization of the Hall conductance, *Annals of Physics*, 160, 343 (1985)
- [64] Nicola Marzari and David Vanderbilt, Maximally localized generalized Wannier functions for composite energy bands, *Phys. Rev. B* 56, 12847 (1997)
- [65] R. Roy, Band geometry of fractional topological insulators, *Physical Review B* 90, 165139 (2014).
- [66] S. Peotta and P. Torma, Superfluidity in topologically nontrivial flat bands, *Nat. Commun.* 6, 8944 (2015).
- [67] Tomoki Ozawa and Bruno Mera, Relations between topology and the quantum metric for Chern insulators, *Phys. Rev. B* 104, 045103 (2021)
- [68] Bruno Mera and Tomoki Ozawa, Kahler geometry and Chern insulators: Relations between topology and the quantum metric, *Phys. Rev. B* 104, 045104 (2021)
- [69] J. Bellissard, A. van Elst, and H. Schulz-Baldes, The noncommutative geometry of the quantum Hall effect, *J. Math. Phys.* 35, 5373–5451 (1994)
- [70] F. Combes, M. Trescher, F. Pichon, and J.-N. Fuchs, Statistical mechanics approach to the electric polarization and dielectric constant of band insulators, *Phys. Rev. B* 94, 155109 (2016).
- [71] Yugo Onishi, Liang Fu, Quantum weight: A fundamental property of quantum many-body systems, *Phys. Rev. Res.* 7, 023158 (2025)
- [72] Shunji Matsuura and Shinsei Ryu, Momentum space metric, nonlocal operator, and topological insulators, *Phys. Rev. B* 82, 245113 (2010).
- [73] O. Bleu, D. D. Solnyshkov, and G. Malpuech, Measuring the quantum geometric tensor in two-dimensional photonic and exciton-polariton systems, *Phys. Rev. B* 97, 195422 (2018)
- [74] G. von Gersdorff and W. Chen, Measurement of topological order based on metric-curvature correspondence, *Phys. Rev. B* 104, 195133 (2021).
- [75] Y.-M. Robin Hu, Elena A. Ostrovskaya, and Eliezer Estrecho, Generalized quantum geometric tensor in a non-Hermitian exciton-polariton system, *Optical Materials Express* 14, 664 (2024)
- [76] Balazs Hetenyi, Peter Levay, Fluctuations, uncertainty relations, and the geometry of quantum state manifolds, *Phys. Rev. A* 108 032218 (2023)
- [77] Wei Chen, Generating functions for quantum metric, Berry curvature, and quantum Fisher information matrix, arXiv:2511.05260
- [78] M. Ezawa, Monolayer Topological Insulators: Silicene, Germanene and Stanene, *J. Phys. Soc. Jpn.* 84, 121003 (2015)
- [79] W.-Y. Hsiang and D.-H. Lee, Chern-Simons invariant in the Berry phase of a  $2 \times 2$  Hamiltonians, *Phys. Rev. A* 64, 052101 (2001).
- [80] Doru Sticlet, Frederic Piechon, Jean-Noel Fuchs, Pavel Kalugin, and Pascal Simon, Geometrical engineering of a two-band Chern insulator in two dimensions with arbitrary topological index, *Phys. Rev. B* 85, 165456 (2012).
- [81] Chao-Ming Jian, Zheng-Cheng Gu, and Xiao-Liang Qi, Momentum-space instantons and maximally localized flat-band topological Hamiltonians, *Phys. Status Solidi RRL* 7, 154 (2013).
- [82] W. Yao, D. Xiao, and Q. Niu, *Phys. Rev. B* 77, 235406 (2008).
- [83] D. Xiao, G.-B. Liu, W. Feng, X. Xu, and W. Yao, Coupled Spin and Valley Physics in Monolayers of MoS<sub>2</sub> and Other Group-VI Dichalcogenides, *Phys. Rev. Lett.* **108**, 196802 (2012).
- [84] M. Ezawa, Spin-valley optical selection rule and strong circular dichroism in silicene, *Phys. Rev. B* 86, 161407(R) (2012)
- [85] M. Ezawa, Elliptic Dichroism and Valley-Selective Optical Pumping in the Surface of Topological Crystalline Insulator, *Phys. Rev. B* 89, 195413 (2014) 245306 (2024).
- [86] X. Li, T. Cao, Q. Niu, J. Shi, and J Feng, Coupling the valley degree of freedom to antiferromagnetic order, *PNAS* 110 (10) 3738 (2013)
- [87] V. I. Belinicher and B. I. Sturman, The photogalvanic effect in media lacking a center of symmetry, *Sov. Phys. Usp.* 23, 199 (1980).
- [88] W. Kraut and R. von Baltz, Anomalous bulk photo-voltaic effect in ferroelectrics: A quadratic response theory, *Phys. Rev. B* 19, 1548 (1979).
- [89] C. Aversa and J. E. Sipe, Nonlinear Optical Susceptibilities of Semiconductors: Results with a Length-Gauge Analysis, *Phys. Rev. B* 52, 14636 (1995)
- [90] J. E. Sipe and A. I. Shkrebtii, Second-order optical response in semiconductors, *Phys. Rev. B* 61, 5337 (2000).
- [91] V. M. Fridkin, Bulk photovoltaic effect in noncentrosymmetric crystals, *Crystallogr. Rep.* 46, 654 (2001).
- [92] F. de Juan, Y. Zhang, T. Morimoto, Y. Sun, J. E. Moore, and A.G. Grushin, Difference Frequency Generation in Topological Semimetals, *Phys. Rev. Research* 2, 012017 (2020).
- [93] Z. Dai and A. M. Rappe, Recent progress in the theory of bulk photovoltaic effect, *Chemical Physics Reviews* 4, 011303 (2023).
- [94] M. Ezawa, Bulk photovoltaic effects in altermagnets, *Phys. Rev. B* 111, L201405 (2025)
- [95] Fernando de Juan, Adolfo G. Grushin, Takahiro Morimoto, Joel E. Moore, Quantized circular photogalvanic effect in Weyl semimetals, *Nature Communications* 8, 15995 (2017).
- [96] S. M. Young and A. M. Rappe, First Principles Calculation of the Shift Current Photovoltaic Effect in Ferroelectrics, *Phys. Rev. Lett.* 109, 116601 (2012).
- [97] S. M. Young, F. Zheng, and A. M. Rappe, First-Principles Calculation of the Bulk Photovoltaic Effect in Bismuth Ferrite, *Phys. Rev. Lett.* 109, 236601 (2012).
- [98] T. Morimoto and N. Nagaosa, Topological nature of nonlinear optical effects in solids, *Science Advances* 2, e1501524 (2016)
- [99] Kun Woo Kim, Takahiro Morimoto, and Naoto Nagaosa, Shift

- charge and spin photocurrents in Dirac surface states of topological insulator, *Phys. Rev. B*, **95**, 035134 (2017)
- [100] T. Barik and J. D. Sau, Nonequilibrium nature of nonlinear optical response: Application to the bulk photovoltaic effect, *Phys. Rev. B* **101**, 045201 (2020).
- [101] Hiroki Yoshida and Shuichi Murakami, Diverging shift current responses in the gapless limit of two-dimensional systems, *Phys. Rev. B* **111**, 155402 (2025)
- [102] T. Ideue, K. Hamamoto, S. Koshikawa, M. Ezawa, S. Shimizu, Y. Kaneko, Y. Tokura, N. Nagaosa, and Y. Iwasa, Bulk rectification effect in a polar semiconductor, *Nat. Phys.* **13**, 578 (2017).
- [103] D. Kaplan, T. Holder, and B. Yan, Unifying semiclassics and quantum perturbation theory at nonlinear order, *SciPost Phys.* **14**, 082 (2023).
- [104] Xiao-Bin Qiang, Tianyu Liu, Zi-Xuan Gao, Hai-Zhou Lu, and X. C. Xie, A Clarification on Quantum-Metric-Induced Nonlinear Transport, arXiv:2508.02088
- [105] Zhichao Guo, Xing-Yuan Liu, Hua Wang, Li-kun Shi, and Kai Chang, Dissipation-Shaped Quantum Geometry in Nonlinear Transport, arXiv:2511.16422
- [106] H. Liu, J. Zhao, Y.-X. Huang, W. Wu, X.-L. Sheng, C. Xiao, and S. A. Yang, Intrinsic second-order anomalous Hall effect and its application in compensated antiferromagnets, *Phys. Rev. Lett.* **127**, 277202 (2021).
- [107] Y. Gao, S. A. Yang, and Q. Niu, Field induced positional shift of Bloch electrons and its dynamical implications, *Phys. Rev. Lett.* **112**, 166601 (2014).
- [108] Maria Teresa Mercaldo, Mario Cuoco, and Camine Ortix, Nonlinear planar magnetotransport as a probe of the quantum geometry of topological surface states, *Phys. Rev. B* **111**, 155442 (2025)
- [109] Yuan Dong Wang, Zhi Fan Zhang, Zhen-Gang Zhu, and Gang Su, Intrinsic nonlinear Ohmic current, *Phys. Rev. B* **109**, 085419 (2024).
- [110] Longjun Xiang, Hao Jin, and Jian Wang, Spin Transport Revealed by Spin Quantum Geometry, *Phys. Rev. Lett.* **135**, 146303 (2025).
- [111] Longjun Xiang, Jinxiong Jia, Fuming Xu, Zhenhua Qiao, and Jian Wang, Intrinsic Gyrotropic Magnetic Current from Zeeman Quantum Geometry, *Phys. Rev. Lett.* **134**, 116301 (2025)
- [112] Neelanjan Chakraborti, Sudeep Kumar Ghosh and Snehasish Nandy, Intrinsic Linear Response from Zeeman Quantum Geometry in 2D Unconventional Magnets, arXiv:2508.14745
- [113] Longjun Xiang, Jinxiong Jia, Fuming Xu, and Jian Wang, Classification of electromagnetic responses by quantum geometry, arXiv:2510.02661
- [114] Longjun Xiang, Bin Wang, Yadong Wei, Zhenhua Qiao, and Jian Wang, Linear displacement current solely driven by the quantum metric, *Phys. Rev. B* **109**, 115121 (2024).
- [115] Navot Silberstein, Jan Behrends, Moshe Goldstein, and Roni Ilan, Berry connection induced anomalous wave-packet dynamics in non-Hermitian systems, *Phys. Rev. B* **102**, 245147 (2020)
- [116] Weicen Dong, Qing-Dong Jiang, and Matteo Baggioli, Non-Hermitian wave-packet dynamics and its realization within a non-Hermitian chiral cavity, arXiv:2501.12163
- [117] Chao Chen Ye, W. L. Vleeshouwers, S. Heatley, V. Gritsev and C. Morais Smith, Quantum metric of non-Hermitian Su-Schrieffer-Heeger systems, *Phys. Rev. Res.* **6**, 023202 (2024)
- [118] Jan Behrends, Roni Ilan, and Moshe Goldstein, Quantum geometry of non-Hermitian systems, arXiv:2503.13604
- [119] Kunal Pal, Generalised state space geometry in Hermitian and non-Hermitian quantum systems, arXiv:2507.18486
- [120] Shi-Dong Liang, Guang-Yao Huang, Topological invariance and global Berry phase in non-Hermitian systems *Phys. Rev. A* **87**, 012118 (2013)
- [121] H. Jiang, C. Yang and S. Chen, Topological invariants and phase diagrams for one-dimensional two-band non-Hermitian systems without chiral symmetry, *Phys. Rev. A* **98**, 052116 (2018)
- [122] K. Esaki, M. Sato, K. Hasebe, and M. Kohmoto, Edge states and topological phases in non-Hermitian systems, *Phys. Rev. B* **84**, 205128 (2011).
- [123] B. Zhu, R. Lu and S. Chen, PT symmetry in the non-Hermitian Su-Schrieffer-Heeger model with complex boundary potentials, *Phys. Rev. A* **89**, 062102 (2014).
- [124] C. Yin, H. Jiang, L. Li, Rong Lu and S. Chen, Geometrical meaning of winding number and its characterization of topological phases in one-dimensional chiral non-Hermitian systems, *Phys. Rev. A* **97**, 052115 (2018).
- [125] H. Shen, B. Zhen and L. Fu, Topological Band Theory for Non-Hermitian Hamiltonians, *Phys. Rev. Lett.* **120**, 146402 (2018).
- [126] S. Lieu, Topological phases in the non-Hermitian Su-Schrieffer-Heeger model, *Phys. Rev. B* **97**, 045106 (2018).
- [127] M. Ezawa, Electric circuits for non-Hermitian Chern insulators, *Phys. Rev. B* **100**, 081401(R) (2019).
- [128] M. Ezawa, Electric circuit simulations of nth-Chern-number insulators in 2n-dimensional space and their non-Hermitian generalizations for arbitrary n *Phys. Rev. B* **100**, 075423 (2019).
- [129] A. Uhlmann, Parallel transport and “quantum holonomy” along density operators, *Reports on Mathematical Physics* **24**, 229 (1986)
- [130] A. Uhlmann, A gauge field governing parallel transport along mixed states, *Letters in Mathematical Physics* **21**, 229 (1991)
- [131] M. Hubner, Explicit computation of the Bures distance for density matrices, *Phys. Lett. A* **163**, 239 (1992).
- [132] A. Carollo, B. Spagnolo, and D. Valenti, Uhlmann curvature in dissipative phase transitions, *Scientific Reports* **8**, 9852 (2018)
- [133] L. Leonforte, D. Valenti, B. Spagnolo, and A. Carollo, Uhlmann number in translational invariant systems, *Scientific Reports* **9**, 9106 (2019)
- [134] Y. M. Zhang, X. W. Li, W. Yang and G. R. Jin Quantum Fisher information of entangled coherent states in the presence of photon loss, *Phys. Rev. A* **88** 043832 (2013)
- [135] Jing Liu, Xiao-Xing Jing, Wei Zhong, Xiaoguang Wang, Quantum Fisher information for density matrices with arbitrary ranks, *Communications in Theoretical Physics*, **61**(01), 45 (2014)
- [136] Jing Liu, Heng-Na Xiong, Fei Song, Xiaoguang Wang, Fidelity susceptibility and quantum Fisher information for density operators with arbitrary ranks, *Physica A* **410**, 167 (2014)
- [137] M. Hubner, Computation of Uhlmann’s parallel transport for density matrices and the Bures metric on three-dimensional Hilbert space, *Phys. Lett. A* **179**, 226 (1993)
- [138] A. Uhlmann, Geometric phases and related structures, *Rep. Math. Phys.* **36**, 461 (1995)
- [139] Donald Bures, An extension of Kakutani’s theorem on infinite product measures to the tensor product of semifinite  $\omega^*$ -algebras, *Transactions of the American Mathematical Society*. **135**. American Mathematical Society (AMS): 199 (1969)
- [140] Matteo G. A. Paris, Quantum estimation for quantum technology, *Int. J. Quant. Inf.* **7**, 125 (2009)
- [141] Xu-Yang Hou, Zheng Zhou, Xin Wang, Hao Guo, and Chih-Chun Chien, Local geometry and quantum geometric tensor of mixed states, *Phys. Rev. B* **110**, 035144 (2024)
- [142] Carl W. Helstrom, Quantum Detection and Estimation Theory,



- Journal of Statistical Physics, 1, 231 (1969)
- [143] Guanyue Ji, David E. Palomino, Nathan Goldman, Tomoki Ozawa, Peter Riseborough, Jie Wang, and Bruno Mera, Density Matrix Geometry and Sum Rules, arXiv:2507.14028
- [144] Wei Chen, Generating functions for quantum metric, Berry curvature, and quantum Fisher information matrix, arXiv:2511.05260
- [145] Samuel L. Braunstein and Carlton M. Caves, Statistical distance and the geometry of quantum states, Phys. Rev. Lett. 72, 3439 (1994)
- [146] Samuel L. Braunstein, Carlton M. Caves, G.J. Milburn, Generalized Uncertainty Relations: Theory, Examples, and Lorentz Invariance, Annals of Physics 247, 135 (1996)
- [147] M. Ezawa, Third-order and fifth-order nonlinear spin-current generation in g-wave and i-wave altermagnets and perfectly nonreciprocal spin current in f-wave magnets, Phys. Rev. B 111, 125420 (2025).
- [148] Merce Roig, Andreas Kreise, Yue Yu, Brian M. Andersen, and Danie F. Agterberg, Minimal models for altermagnetism, Phys. Rev. B 110, 144412 (2024)
- [149] L. Smejkal, A. H. MacDonald, J. Sinova, S. Nakatsuji and T. Jungwirth, Anomalous Hall antiferromagnets, Nat. Rev. Mater. 7, 482 (2022).
- [150] Di Zhu, Zheng-Yang Zhuang, Zhigang Wu, and Zhongbo Yan, Topological superconductivity in two-dimensional altermagnetic metals, Phys. Rev. B 108, 184505 (2023).
- [151] Sayed Ali Akbar Ghorashi, Taylor L. Hughes, Jennifer Cano, Altermagnetic Routes to Majorana Modes in Zero Net Magnetization, Phys. Rev. Lett. 133, 106601 (2024).
- [152] Yu-Xuan Li and Cheng-Cheng Liu, Majorana corner modes and tunable patterns in an altermagnet heterostructure, Phys. Rev. B 108, 205410 (2023).
- [153] M. Ezawa, Detecting the Neel vector of altermagnets in heterostructures with a topological insulator and a crystalline valley-edge insulator, Physical Review B 109 (24), 245306 (2024).
- [154] Shun Okumura, Takahiro Morimoto, Yasuyuki Kato, and Yukitoshi Motome, Quadratic optical responses in a chiral magnet, Phys. Rev. B 104, L180407 (2021)
- [155] Honglin Zhou, Muyu Wang, Xiaoyan Ma, Gang Li, Ding-Fu Shao, Bo Liu, Shiliang Li, Anisotropic resistivity of a p-wave magnet candidate CeNiAsO, rXiv:2509.07351
- [156] Rinsuke Yamada, Max T. Birch, Priya R. Baral, Shun Okumura, Ryota Nakano, Shang Gao, Yuki Ishihara, Kamil K. Kolincio, Ilya Belopolski, Hajime Sagayama, Hironori Nakao, Kazuki Ohishi, Taro Nakajima, Yoshinori Tokura, Taka-hisa Arima, Yukitoshi Motome, Moritz M. Hirschmann, and Max Hirschberger, Gapping the spin-nodal planes of an anisotropic p-wave magnet to induce a large anomalous Hall effect, arXiv:2502.10386
- [157] Qian Song, Srdjan Stavic, Paolo Barone, Andrea Droghetti, Daniil S. Antonenko, Jorn W. F. Venderbos, Connor A. Occhialini, Batyr Ilyas, Emre Ergecen, Nuh Gedik, Sang-Wook Cheong, Rafael M. Fernandes, Silvia Picozzi, and Riccardo Comin, Electrical switching of a p-wave magnet, Nature 642, 64 (2025)
- [158] Sanjib Kumar Das, Bitan Roy, From local spin nematicity to altermagnets: Footprints of band topology, Phys. Rev. B 111, L201102 (2025).
- [159] Yichen Liu, Junxi Yu, and Cheng-Cheng Liu, Twisted Magnetic Van der Waals Bilayers: An Ideal Platform for Altermagnetism, Phys. Rev. Lett. 133, 206702 (2024)
- [160] K.-H. Ahn, A. Hariki, K.-W. Lee, and J. Kunes, Antiferromagnetism in RuO<sub>2</sub> as d-wave Pomeranchuk instability, Phys. Rev. B 99, 184432 (2019).
- [161] L. Smejkal, R. Gonzalez-Hernandez, T. Jungwirth, and J. Sinova, Crystal time-reversal symmetry breaking and spontaneous Hall effect in collinear antiferromagnets. Science Advances 6, eaaz8809 (2020).
- [162] Teresa Tschirner, Philipp Keler, Ruben Dario Gonzalez Betancourt, Tommy Kotte, Dominik Kriegner, Bernd Buechner, Joseph Dufouleur, Martin Kamp, Vedran Jovic, Libor Smejkal, Jairo Sinova, Ralph Claessen, Tomas Jungwirth, Simon Moser, Helena Reichlova, Louis Veyrat, Saturation of the anomalous Hall effect at high magnetic fields in altermagnetic RuO<sub>2</sub>, APL Mater. 11, 101103 (2023)
- [163] O. Fedchenko, J. Minar, A. Akashdeep, S.W. D'Souza, D. Vasilyev, O. Tkach, L. Odenbreit, Q.L. Nguyen, D. Kutnyakhov, N. Wind, L. Wenthaus, M. Scholz, K. Rossnagel, M. Hoesch, M. Aeschlimann, B. Stadtmueller, M. Klauui, G. Schoenhense, G. Jakob, T. Jungwirth, L. Smejkal, J. Sinova, H. J. Elmers, Observation of time-reversal symmetry breaking in the band structure of altermagnetic RuO<sub>2</sub>, Science Advances 10,5 (2024) DOI: 10.1126/sciadv.adj4883.
- [164] Zihan Lin, Dong Chen, Wenlong Lu, Xin Liang, Shiyu Feng, Kohei Yamagami, Jacek Osiecki, Mats Leandersson, Balasubramanian Thiagarajan, Junwei Liu, Claudia Felser, Junzhang Ma, Observation of Giant Spin Splitting and d-wave Spin Texture in Room Temperature Altermagnet RuO<sub>2</sub>, arXiv:2402.04995.
- [165] Miina Leivisk Javier Rial, Anton Badura, Rafael Lopes Seeger, Ismaa Kounta, Sebastian Beckert, Dominik Kriegner, Isabelle Jourard, Eva Schmoranzarov Jairo Sinova, Olena Gomonay, Andy Thomas, Sebastian T. B. Goennenwein, Helena Reichlov Libor Smejkal, Lisa Michez, Tom Jungwirth, Vincent Baltz, Anisotropy of the anomalous Hall effect in the altermagnet candidate Mn<sub>5</sub>Si<sub>3</sub> films, Phys. Rev. B 109, 224430 (2024)
- [166] I. I. Mazin, K. Koepernik, M.D. Johannes, Rafael Gonzalez-Hernandez, Libor Šmejkal, Prediction of unconventional magnetism in doped FeSb<sub>2</sub>, Proceedings of the National Academy of Sciences 118, e2108924118 (2021)
- [167] Bei Jiang, Mingzhe Hu, Jianli Bai, Ziyin Song, Chao Mu, Gexing Qu, Wan Li, Wenliang Zhu, Hanqi Pi, Zhongxu Wei, Yu-Jie Sun, Yaobo Huang, Xiquan Zheng, Yingying Peng, Lunhua He, Shiliang Li, Jianlin Luo, Zheng Li, Genfu Chen, Hang Li, Hongming Weng and Tian Qian, A metallic room-temperature d-wave altermagnet KV<sub>2</sub>Se<sub>2</sub>O, Nature Physics 21, 754 (2025)
- [168] S. Hayami, Y. Yanagi, and H. Kusunose, Spontaneous antisymmetric spin splitting in noncollinear antiferromagnets without spin-orbit coupling, Phys. Rev. B 101, 220403 (2020)
- [169] J. Krempask, L. Šmejkal, S. W. D'Souza, M. Hajlaoui, G. Springholz, K. Uhlov F. Alarab, P. C. Constantinou, V. Strocov, D. Usanov, W. R. Pudelko, R. Gonzalez-Hernandez, A. Birk Hellenes, Z. Jansa, H. Reichlov Z. Šob, R. D. Gonzalez Betancourt, P. Wadley, J. Sinova, D. Kriegner, J. Min, J. H. Dil and T. Jungwirth, Altermagnetic lifting of Kramers spin degeneracy, Nature 626, 517 (2024).
- [170] Suyoung Lee, Sangjae Lee, Saegyool Jung, Jiwon Jung, Donghan Kim, Yeonjae Lee, Byeongjun Seok, Jaeyoung Kim, Byeong Gyu Park, Libor Šmejkal, Chang-Jong Kang, and Changyoung Kim, Broken Kramers Degeneracy in Altermagnetic MnTe, Phys. Rev. Lett. 132, 036702 (2024)
- [171] T. Osumi, S. Souma, T. Aoyama, K. Yamauchi, A. Honma, K. Nakayama, T. Takahashi, K. Ohgushi, and T. Sato, Observation of a giant band splitting in altermagnetic MnTe, Phys. Rev. B 109, 115102 (2024)

- [172] M. Hajlaoui, S.W. D'Souza, L. Šmejkal, D. Krieger, G. Krizman, T. Zakusylo, N. Olszowska, O. Caha, J. Michalička, A. Marmodoro, K. Vyborny, A. Ernst, M. Cinchetti, J. Minar, T. Jungwirth, G. Springholz, Temperature Dependence of Relativistic Valence Band Splitting Induced by an Altermagnetic Phase Transition, *Advanced Material* 36, 2314076 (2024)
- [173] Suyoung Lee, Sangjae Lee, Saegyeol Jung, Jiwon Jung, Donghan Kim, Yeonjae Lee, Byeongjun Seok, Jaeyoung Kim, Byeong Gyu Park, Libor Šmejkal, Chang-Jong Kang, Changyong Kim, Broken Kramers Degeneracy in Altermagnetic MnTe, *Phys. Rev. Lett.* 132, 036702 (2024).
- [174] Zheyuan Liu, Makoto Ozeki, Shinichiro Asai, Shinichi Itoh, and Takatsugu Masuda, Chiral Split Magnon in Altermagnetic MnTe *Phys. Rev. Lett.* 133, 156702 (2024).
- [175] Sonka Reimers, Lukas Odenbreit, Libor Šmejkal, Vladimir N. Strocov, Procopios Constantinou, Anna B. Hellenes, Rodrigo Jaeschke Ubiergo, Warlley H. Campos, Venkata K. Bharadwaj, Atasi Chakraborty, Thibaud Denneulin, Wen Shi, Rafal E. Dunin-Borkowski, Suvadip Das, Mathias Kli, Jairo Sinova & Martin Jourdan, Direct observation of altermagnetic band splitting in CrSb thin films, *Nat. Com.* 15, 2116 (2024)
- [176] Guowei Yang, Zhanghuan Li, Sai Yang, Jiyuan Li, Hao Zheng, Weifan Zhu, Ze Pan, Yifu Xu, Saizheng Cao, Wenxuan Zhao, Anupam Jana, Jiawen Zhang, Mao Ye, Yu Song, Lunhui Hu, Lexian Yang, Jun Fujii, Ivana Vobornik, Ming Shi, Huiqiu Yuan, Yongjun Zhang, Yuanfeng Xu, Yang Liu, Three-dimensional mapping and electronic origin of large altermagnetic splitting near Fermi level in CrSb, arXiv:2405.12575
- [177] Jianyang Ding, Zhicheng Jiang, Xiuhua Chen, Zicheng Tao, Zhengtai Liu, Jishan Liu, Tongrui Li, Jiayu Liu, Yichen Yang, Runfeng Zhang, Liwei Deng, Wenchuan Jing, Yu Huang, Yuming Shi, Shan Qiao, Yilin Wang, Yanfeng Guo, Donglai Feng, Dawei Shen, Large band-splitting in g-wave type altermagnet CrSb, arXiv:2405.12687
- [178] Cong Li, Mengli Hu, Zhilin Li, Yang Wang, Wanyu Chen, Balasubramanian Thiagarajan, Mats Leandersson, Craig Polley, Timur Kim, Hui Liu, Cosma Fulga, Maia G. Vergniory, Oleg Janson, Oscar Tjernberg, Jeroen van den Brink, Topological Weyl Altermagnetism in CrSb, arXiv:2405.14777
- [179] Wenlong Lu, Shiyu Feng, Yuzhi Wang, Dong Chen, Zihan Lin, Xin Liang, Siyuan Liu, Wanxiang Feng, Kohei Yamagami, Junwei Liu, Claudia Felser, Quansheng Wu, Junzhang Ma, Observation of surface Fermi arcs in altermagnetic Weyl semimetal CrSb, arXiv:2407.13497
- [180] Mayukh Kumar Ray, Mingxuan Fu, Youzhe Chen, Taishi Chen, Takuya Nomoto, Shiro Sakai, Motoharu Kitatani, Motoaki Hirayama, Shusaku Imajo, Takahiro Tomita, Akito Sakai, Daisuke Nishio-Hamane, Gregory T. McCandless, Michi-To Suzuki, Zhijun Xu, Yang Zhao, Tom Fennell, Yoshimitsu Kohama, Julia Y. Chan, Ryotaro Arita, Collin Broholm and Satoru Nakatsuji, Zero-field Hall effect emerging from a non-Fermi liquid in a collinear antiferromagnet  $V_{1/3}NbS_2$ , *Nature Communications* 16, 3532 (2025)
- [181] Rina Takagi, Ryosuke Hirakida, Yuki Settai, Rikuto Oiwa, Hirotaka Takagi, Aki Kitaori, Kensei Yamauchi, Hiroki Inoue, Jun-Ichi Yamaura, Daisuke Nishio-Hamane, Shinichi Itoh, Seno Aji, Hiraku Saito, Taro Nakajima, Takuya Nomoto, Ryotaro Arita, Shinichiro Seki, Spontaneous Hall effect induced by collinear antiferromagnetic order at room temperature, *Nat Mater.* 24, 63 (2025).
- [182] I. Mazin, R. Gonzalez-Hernandez, and L. Smejkal, Induced monolayer altermagnetism in  $mnp_3$  and  $fese$  arXiv:2309.02355
- [183] M. Julliere, Tunneling between ferromagnetic films, *Phys. Lett. A* 54, 225 (1975).
- [184] J. S. Moodera, L. R. Kinder, T. M. Wong, and R. Meservey, Large magnetoresistance at room temperature in ferromagnetic thin film tunnel junctions, *Phys. Rev. Lett.* 74, 3273 (1995).
- [185] F. Liu, Z. Zhang, X. Yuan, Y. Liu, S. Zhu, Z. Lu, and R. Xiong, Giant tunneling magnetoresistance in insulated altermagnet/ferromagnet junctions induced by spin-dependent tunneling effect, *Phys. Rev. B* 110, 134437 (2024).
- [186] Run-Wu Zhang, Chaoxi Cui, Runze Li, Jingyi Duan, Lei Li, Zhi-Ming Yu and Yugui Yao, Predictable Gate-Field Control of Spin in Altermagnets with Spin-Layer Coupling *Phys. Rev. Lett.* 133, 056401 (2024)
- [187] B. Chi, L. Jiang, Y. Zhu, G. Yu, C. Wan, J. Zhang, and X. Han, Crystal-facet-oriented altermagnets for detecting ferromagnetic and antiferromagnetic states by giant tunneling magnetoresistance, *Phys. Rev. Applied* 21, 034038 (2024).
- [188] Z. Yan, R. Yang, C. Fang, W. Lu, and X. Xu, Giant electrode effect on tunneling magnetoresistance and electroresistance in van der waals intrinsic multiferroic tunnel junctions using VS<sub>2</sub>, *Phys. Rev. B* 109, 205409 (2024).
- [189] Dmitrii L. Vorobev and Vladimir A. Zyuzin, d-wave Hall effect and linear magnetoconductivity in metallic collinear anti-ferromagnets, *Phys. Rev. B* 109, L180411 (2024)
- [190] Zongmeng Yang, Xingyue Yang, Jianhua Wang, Rui Peng, Lee Ching, Hua, Lay Kee Ang, Jing Lu, Yee Sin Ang, and Shibo fang, Unconventional tunnel magnetoresistance scaling with altermagnets, arXiv:2505.17192
- [191] Yu-Fei Sun, Yue Mao, Yu-Chen Zhuang, and Qing-Feng Sun, Tunneling Magnetoresistance Effect in Altermagnets, arXiv:2509.04015
- [192] Bjonulf Brekke, Pavlo Sukhachov, Hans Glokner Giil, Arne Brataas, Jacob Linder, Minimal models and transport properties of unconventional p-wave magnets, *Phys. Rev. Lett.* 133, 236703 (2024)
- [193] Amar Fakhredine, Raghottam M. Sattigeri, Giuseppe Cuono, and Carmine Autieri, Interplay between altermagnetism and nonsymmorphic symmetries generating large anomalous Hall conductivity by semi-Dirac points induced anticrossings, *Phys. Rev. B* 108, 115138 (2023).
- [194] Toshihiro Sato, Sonia Haddad, Ion Cosma Fulga, Fakher F. Assaad, Jeroen van den Brink, Altermagnetic anomalous Hall effect emerging from electronic correlations, *Phys. Rev. Lett.* 133, 086503 (2024)
- [195] H. X. Tang, R.K. Kawakami, D. D. Awschalom, and M. L. Rouk, Giant Planar Hall Effect in Epitaxial (Ga,Mn)As Devices, *Phys. Rev. Lett.* 90, 107201 (2003).
- [196] Xin Liu, Hsiu-Chuan Hsu, and Chao-Xing Liu, In-Plane Magnetization-Induced Quantum Anomalous Hall Effect, *Phys. Rev. Lett.* 111, 086802 (2013).
- [197] S. Nandy, Gargee Sharma, A. Taraphder, and Sumanta Tewari, Chiral Anomaly as the Origin of the Planar Hall Effect in Weyl Semimetals, *Phys. Rev. Lett.* 119, 176804 (2017).
- [198] A. A. Taskin, Henry F. Legg, Fan Yang, Satoshi Sasaki, Yasushi Kanai, Kazuhiko Matsumoto, Achim Rosch and Yoichi Ando, Planar Hall effect from the surface of topological insulators, *Nature Communications* 8, 1340 (2017).
- [199] A. A. Burkov, Giant planar Hall effect in topological metals, *Phys. Rev. B* 96, 041110(R) (2017).
- [200] Nitesh Kumar, Satya N. Guin, Claudia Felser, and Chandra Shekhar, Planar Hall effect in the Weyl semimetal GdPtBi, *Phys. Rev. B* 98, 041103(R) (2018).
- [201] Zhao Liu, Gan Zhao, Bing Liu, Z.F. Wang, Jinlong Yang, and Feng Liu, Intrinsic Quantum Anomalous Hall Effect with In-

- Plane Magnetization: Searching Rule and Material Prediction, *Phys. Rev. Lett.* 121, 246401 (2018).
- [202] Srimayi Korrapati, Snehasish Nandy, and Sumanta Tewari, Approximate half-integer quantization in anomalous planar transport in d-wave altermagnets, arXiv:2506.24122.
- [203] Bao-Feng Chen, Jie-Xiang Yu, and Gen Yin, Large anisotropic magnetoresistance in  $\alpha$ -MnTe induced by strain, arXiv:2507.16738.
- [204] Wang Chen, Xiaoying Zhou, Wen-Kai Lou, and Kai Chang, Magneto-optical conductivity and circular dichroism in d-wave altermagnets, *Phys. Rev. B* 111, 064428 (2025)
- [205] Zhi-Xia Li, Xiangang Wan, Wei Chen, Diagnosing Altermagnetic Phases through Quantum Oscillations, *Phys. Rev. B* 111, 125119 (2025)
- [206] T. Ando and Y. Uemura, Theory of quantum transport in a two-dimensional electron system under magnetic fields. I. Characteristics of level broadening and transport under strong fields, *J. Phys. Soc. Jpn.* 36, 959 (1974)
- [207] M. Koshino and T. Ando, Magneto-optical properties of multilayer graphene, *Phys. Rev. B* 77, 115313 (2008)
- [208] C. J. Tabert and E. J. Nicol, Valley-spin polarization in the magneto-optical response of silicene and other similar 2D crystals, *Phys. Rev. Lett.* 110, 197402 (2013).
- [209] Z. Li and J. P. Carbotte, Magneto-optical conductivity in a topological insulator, *Phys. Rev. B* 88, 045414 (2013).
- [210] Wang Chen, Xiaoying Zhou, Dong Zhang, Ying-Qiang Xu, and Wen-Kai Lou. Impurity scattering and Friedel oscillations in altermagnets, *Phys. Rev. B* 110, 165413 (2024)
- [211] Pavlo Sukhachov and Jacob Linder, Impurity-induced Friedel oscillations in altermagnets and p-wave magnets, *Phys. Rev. B* 110, 205114 (2024)
- [212] Libor Smejkal, Alberto Marmodoro, Kyo-Hoon Ahn, Rafael Gonzalez-Hernandez, Ilja Turek, Sergiy Mankovsky, Hubert Ebert, Sunil W. D'Souza, Ondrej Sipr, Jairo Sinova, and Tomas Jungwirth, Chiral Magnons in Altermagnetic RuO<sub>2</sub>, *Phys. Rev. Lett.* 131, 256703 (2023)
- [213] Qirui Cui, Bowen Zeng, Ping Cui, Tao Yu and Hongxin Yang, Efficient spin Seebeck and spin Nernst effects of magnons in altermagnets, *Phys. Rev. B* 108, L180401 (2023)
- [214] Zheyuan Liu, Makoto Ozeki, Shinichiro Asai, Shinichi Itoh, and Takatsugu Masuda, *Phys. Rev. Lett.* 133, 156702 (2024)
- [215] Rintaro Eto, Matthias Gohlke, Jairo Sinova, Masahito Mochizuki, Alexander L. Chernyshev, and Alexander Mook, Spontaneous Magnon Decays from Nonrelativistic Time-Reversal Symmetry Breaking in Altermagnets, *Phys. Rev. B* 112, 094442 (2025)
- [216] Libor Smejkal, Altermagnetic multiferroics and altermagneto-electric effect, arXiv:2411.19928
- [217] Mingqiang Gu, Yuntian Liu, Haiyuan Zhu, Kunihiro Yananose, Xiaobing Chen, Yongkang Hu, Alessandro Stroppa, Qihang Liu, Ferroelectric Switchable Altermagnetism, *Phys. Rev. Lett.* 134, 106802 (2025)
- [218] B. M. Fregoso, R. A. Muniz and J.E. Sipe, Jerk Current: A Novel Bulk Photovoltaic Effect, *Phys. Rev. Lett.* 121, 176604 (2018)
- [219] G. B. Ventura, D.J. Passos, J. M. Viana Parente Lopes, and J. M. B. Lopes dos Santos, Comment on "Jerk Current: A Novel Bulk Photovoltaic Effect" *Phys. Rev. Lett.* 126, 259701 (2021)
- [220] B. M. Fregoso, R. A. Muniz and J.E. Sipe, "Fregoso, Muniz, and Sipe Reply" *Phys. Rev. Lett.* 126, 259702 (2021)
- [221] Benjamin M. Fregoso, Bulk photovoltaic effects in the presence of a static electric field, *Phys. Rev. B* 100, 064301 (2019): Erratum, *Phys. Rev. B* 102, 059901(E) (2020)
- [222] A. S Holevo, Statistical decision theory for quantum systems, *Journal of Multivariate Analysis*, 3, 337 (1973)